A new diffusely infiltrating glioma mouse model reveals neuronal alterations in the brain tumor microenvironment

Daniela Torres

Submitted in partial fulfillment of the
requirements for the degree
of Doctor of Philosophy
in the Graduate School of Arts and Sciences

COLUMBIA UNIVERSITY

2018

Abstract

A new diffusely infiltrating glioma mouse model reveals neuronal alterations in the brain tumor microenvironment

Daniela Torres

Gliomas are brain tumors that present with neurological symptoms including seizures and cognitive deficits. Starting at early stages of tumor development glioma cells diffusely infiltrate brain tissue where they interact with non-neoplastic cells including neurons and can perturb normal brain function. While the clinical consequences of glioma induced cortical dysfunction are well established, the neuronal alterations that underlie cortical dysfunction in glioma are unknown. We hypothesize that glioma cells infiltrate surrounding brain tissue and induce alterations in neurons that may contribute to the neurological symptoms associated with gliomas. Due to intermingling of glioma cells and neurons it has been challenging to isolate and characterize neurons from glioma brain tissue while preserving complex neuronal morphology. To address this issue we developed a new mouse glioma model that allowed us to obtain a neuron specific gene expression profile, otherwise obscured by the predominantly large population of glioma cells within the tumor. In this thesis I use this model to test the hypothesis that infiltrating glioma cells induce phenotypic alterations in neurons that contribute to the neurological symptoms associated with glioma.

The Camk2a-Ribotag mouse glioma model enabled us to isolate neuron specific transcripts from glioma brain tissue. The Ribotag mouse has a conditional HA-tagged ribosomal protein (Rpl22) that can be expressed upon Cre-recombination. Camk2a is specifically expressed in excitatory neurons, the Camk2a-Cre mouse induces Cre-recombination in the Ribotag mouse so that

Camk2a+ neurons selectively express HA-tagged Rpl22. We used the Camk2a-Ribotag glioma model to isolate neuron specific ribosome bound transcripts to characterize neuronal alterations in glioma.

In chapter 2 of this thesis I describe how we developed and characterized the Camk2a-Ribotag mouse glioma model. We first obtained mouse glioma cells that have p53 deletion and overexpress PDGFRa, then we injected these cells in the Camk2a-Ribotag mouse and use this as our glioma model to extract neuron specific ribosome bound transcripts. This method is referred to as translating ribosome affinity purification (TRAP) which is used to obtain cell type specific translational profiles. Using this approach we identified alterations in neuronal gene expression, specifically we show that there is an upregulation of actin binding genes associated with dendritic spine morphology and a downregulation of synaptic genes associated synaptic regulation. We demonstrate that drebrin, an actin binding protein in dendritic spines, is upregulated in tumor brain synaptosomes, we also show a downregulation of dendritic spine density in HA-tagged neurons which suggests that these neuronal alterations contribute to synaptic dysfunction in our glioma model.

Dendritic spines are dynamic structures that regulate synaptic function in response to diverse stimuli. mTOR signaling can regulate brain specific functions such as synaptic plasticity. Alterations in mTOR signaling can result in cognitive deficits, epilepsy and brain abnormalities that are associated with neurological disease. We hypothesized that mTOR regulates the neuronal alterations we identified in our glioma model. In chapter 3 of this thesis I describe how we tested this hypothesis by acutely inhibiting mTOR signaling with the ATP competitive inhibitor AZD8055 in the Camk2a-Ribotag mouse glioma model. Using TRAP we show that acute mTOR inhibition reverses many neuron specific alterations that occurs in the glioma

infiltrated cortex, actin binding genes that were upregulated in tumor brains were downregulated after mTOR inhibition and synaptic genes that were downregulated in tumor brains were upregulated after mTOR inhibition. These results suggest that key neuron specific alterations are regulated by mTOR signaling in our glioma model.

In chapter 4 of this thesis I describe how we used ribosome profiling to identify translational alterations in our Camk2a-Ribotag mouse glioma model. Ribosome profiling in an RNA sequencing based method that is used to measure translation efficiency by calculating the number of ribosomes per transcript. Using this approach we identified an upregulation in the translation of DNA methylation and demethylation gene ontologies. These results suggest that alterations in specific DNA methylation and demethylation gene ontologies are regulated at the level of translation and warrant further analysis of cell type specific translational alterations using ribosome profiling.

The work described in this thesis demonstrates 1) use of the Camk2a-Ribotag mouse glioma model for the identification of neuron specific alterations, 2) neuron specific alterations include the upregulation of dendritic spine genes, downregulation of synaptic genes and downregulation of dendritic spine density, 3) acute mTOR inhibition reverses many of these neuronal alterations, 4) ribosome profiling revealed the translational upregulation of epigenetic genes in our mouse glioma model. The findings described in this thesis provide the first characterization of neuron specific transcriptional and translational alterations in glioma infiltrated cortex that and provide new insights into the mechanisms that underlie the devastating neurological symptoms in glioma patients.

TABLE OF CONTENTS

CHAPTER 6

LIST OF FIGURES AND TABLES

Acknowledgements

I would like to thank my mentor Dr. Peter Canoll for allowing me to join his lab and complete my thesis research there. I would also like to acknowledge the members of my thesis committee Dr. Peter Sims, Dr. Dave Sulzer and Dr. Jan Kitajewski for their valuable input on my thesis projects during the past 5 years. All of the work described in this thesis was made possible thanks to the support and guidance of my mentor Dr. Peter Canoll. Thank you for the time you invested in my training as a PhD student, because of this I have developed my critical thinking, writing, and presentation skills which will be invaluable to my career in the future. I really appreciated your help in planning experiments, analyzing data and generating new hypothesis to test, thanks for being a great mentor.

Several lab members also contributed to essential elements of my thesis projects, Dr. Angelina Mela developed the retroviral mouse glioma model from which I derived glioma cells used in the glioma mouse model described for my thesis, Dr. Thanassis Dovas performed the diolistic imaging experiments described in Chapter 2 of this thesis. Thanks to Dr. Mela for being my lab bay mate and for her plant that never dies which made our lab bay a lively place. Thank you to Dr. Dovas for your advice and infinite enthusiasm for science. Also, thanks to Dr. Frank Garcia, a former graduate student, for showing me how to perform immunostaining, western blots and mouse experiments when I first joined the lab. Special thanks to Dr. Matei Banu and Dr. Brian Gill for your suggestions and insightful discussions regarding my thesis research.

Thank you to lab members who joined the lab relatively recently, especially Nelson Humala and Aayushi Mahajan for keeping the lab organized and for your positive attitude, and to Dr. Markel Olabarria Larizgoitia for your contribution to the final experiments for our manuscript. Also, thanks to Dr. Edgar Gonzalez Buendia for your advice and taking the time to explain complex

DEDICATION

This thesis dissertation is dedicated to my parents, Marco and Mercedes, my siblings Santiago

and Carolina, and my dog, Brownie.

CHAPTER 1

Introduction

1.1 Glioma as a neurological disease and challenges associated with studying gliomas

Glioma classification, standard of care, and survival

Diffusely infiltrating gliomas are one of the most common primary brain tumors in adults (Weller, Wick et al. 2015). These types of brain tumors are classified based on histological and molecular features to guide treatment options (Louis, Perry et al. 2016, Masui, Mischel et al. 2016). Standard of care for patients with glioma include surgical resection, followed by chemotherapy and radiotherapy (Stupp , Mason et al. 2005, van den Bent, Snijders et al. 2012, Davis 2016). However, because these tumors diffusely infiltrate the brain, complete surgical resection is not possible and remaining tumor cells eventually result in recurrence.

Gliomas are classified based on histological and molecular features which determine the World Health Organization (WHO) grade and influence the course of treatment. Histological assessment of glioma tissue analyzes the degree of mitotic activity, nuclear atypia, vascular proliferation and necrosis as well as the astrocytic and oligodendroglial features. Lower grade gliomas consist of grade I and II tumors, which have none to one of the histological features described above. Low grade tumors include diffuse astrocytoma and oligodendroglioma. The presence of mitotic activity determines grade III anaplastic astrocytoma tumors, and the presence of necrosis and vascular proliferation determines grade IV glioblastoma diagnosis (Wesseling, Kros et al. 2011).

Glioblastoma (GBM) is characterized as a high-grade tumor (grade IV) that generally arises as a de novo lesion that progresses rapidly despite standard of care therapy with survival ranging from 12-18 months. GBMs are more common in the older population with an average age of 64 years. However, despite aggressive treatment, glioma recurrence is inevitable which is believed to be a result of the invasiveness of tumor cells throughout brain tissue that makes complete surgical removal impossible (Cuddapah, Robel et al. 2014). Gliomas that are characterized as lower-grade gliomas (grade II or III) are slower growing lesions for which survival ranges from 3-10 years and more often affect young adults (Delgado-López, Corrales-García et al. 2017). Despite the slower growing capacity of lower-grade glioma these tumors eventually progress to higher-grade tumors.

Patients with diffusely infiltrating glioma have neurological deficits

Symptoms prior to glioma diagnosis include headaches, seizures and cognitive deficits (Taphoorn and Klein 2004, Bosma, Vos et al. 2007, Miotto, Silva Junior et al. 2011, Bergo, Lombardi et al. 2016). After diagnosis, patients continue to present with these symptoms which generally get worse as a result of tumor growth and treatment effects resulting in a poor quality of life. Neurological symptoms include impaired working memory, decision making, verbal fluency and social cognition. Seizures and impaired neurological function are particularly debilitating in patients with lower-grade glioma that have a longer survival range and which are often refractory to anti-epileptic drugs (Vecht, Kerkhof et al. 2014).

Gliomas are mostly localized to the cerebral cortex (frontal and temporal lobes), which explains the impairment in executive function, memory, emotion or concentration. Worsening of seizures and cognitive function is usually a sign of tumor progression which is attributed to the

diffuse infiltration of tumor cells in these brain regions (Bergo, Lombardi et al. 2015). However, very little is known about how infiltrating glioma cells affect cortical function, and virtually nothing is known about the phenotypic or functional alterations in cortical neurons at the infiltrative margins of glioma.

Reactive plasticity as a response to slow growing glioma lesions

Patients with low grade glioma (LGG) often have a pre-symptomatic period when glioma growth is taking place with no observable symptoms. In fact, gliomas can occupy a remarkably large volume of brain before they manifest clinical symptoms. This could be explained by the glioma cell infiltration induced adaptions in brain tissue which enable the preservation of neural function despite glioma cell infiltration. This concept is referred to as reactive plasticity which is a response mechanism by which the brain adapts to pathological stimuli resulting in the reorganization of neural circuits to preserve remaining function (Kong, Gibb et al. 2016). This concept has been studied in various neurological diseases including traumatic brain injury, stroke and is more recently being explored in low grade glioma (Desmurget, Bonnetblanc et al. 2007).

Acute brain injuries include sudden insults such as stroke or traumatic brain injury which occur over the course of minutes. Progressive brain injuries slowly develop including neurodegenerative disease or low grade gliomas which develop over the course of years. One important difference between acute and progressive brain injuries is the functional recovery of the affected brain circuits and the associated cognitive process. Progressive brain injuries result in a much better recovery compared to acute brain injury, suggesting that slower developing lesions allow for reactive plasticity and the adaptive processes required to preserve function (Desmurget, Bonnetblanc et al. 2007).

Reactive plasticity in glioma has been studied primarily from a clinical perspective using intraoperative direct electrocortical stimulation (DES) which allows neurosurgeons to identify critical brain regions for specific functions by inhibiting the cortical area associated with a specific function (Kong, Gibb et al. 2016). These methods have identified cortical brain regions responsible for specific functions such as speech or movement (so called eloquent cortex). During subsequent surgical resections DES showed that the same brain region once responsible for a specific function is no longer critical for that function, providing compelling clinical evidence that reactive plasticity is continuously taking place at in glioma infiltrated cortex (Duffau 2014). Research on reactive plasticity has begun to study how acute and progressive brain injuries differentially influence plasticity (Kong, Gibb et al. 2016)

Neuroplasticity occurs during development and in adults during which guidance cues for axonal sprouting guide brain development and dendritic and synaptic morphology are altered for making appropriate synaptic connections (Nudo 2013). The mechanisms involved in synaptic plasticity during development have been widely characterized and point to mechanisms including the alterations in the regulation of glutamate receptors as well as alterations in the morphology and function of dendritic spines. The actin cytoskeleton plays an essential role in dendritic spines, it can be regulated by synaptic inputs and adapts to modulate the morphology and function of dendritic spines during synaptic plasticity (Yuste and Bonhoeffer 2001, Lai and Ip 2013, Maiti, Manna et al. 2015, Hlushchenko, Koskinen et al. 2016, Kong, Gibb et al. 2016). However, plasticity following brain injury is less well understood but motivates efforts to identify the molecular mechanisms of neuroplasticity in progressive lesions such as glioma

Molecular characterization of glioma reveals gene expression profiles that identifies distinct glioma subtypes

Molecular characterization of gliomas has identified genetic alterations found in brain tumor tissue that can predict patient prognosis, response to therapy and provide molecular markers for more accurate classification by clinicians (Masui, Mischel et al. 2016). Extensive characterization of GBM has contributed to the identification of distinct gene expression profiles including proneural, mesenchymal, neural, and classical subtypes (Nutt, Mani et al. 2003, Shai, Shi et al. 2003, Freije, Castro-Vargas et al. 2004, Phillips, Kharbanda et al. 2006, Parsons, Jones et al. 2008, The Cancer Genome Atlas Research 2008, Verhaak, Hoadley et al. 2010, Zong, Verhaak et al. 2012, Brennan, Verhaak et al. 2013). The proneural GBM subtype is characterized by genetic alterations that result in overexpression of PDGFRα, IDH1 mutations, and p53 mutation or loss of heterozygosity. Proneural tumors are also characterized by oligodendrocyte developmental genes such as Olig2 and PDGFRα (Verhaak, Hoadley et al. 2010). However, due to the cellular heterogeneity of gliomas, studies have detected different GBM subtypes from distinct biopsies from the same patient suggesting that this classification system is variable and depends on the cellular composition of the tissue sampled (Sottoriva, Spiteri et al. 2013, Gill, Pisapia et al. 2014, Patel, Tirosh et al. 2014)

Molecular characterization of the infiltrative margins of glioma

Most of the molecular characterization in glioma has come from analysis of the tissue taken from the tumor core, since this is generally what is removed during surgery. Our lab has shown that MRI-localized biopsies from the contrast enhancing tumor core have distinct gene expression profiles from MRI-localized biopsies from the non-enhancing infiltrative margins of glioma (Gill, Pisapia et al. 2014). This is likely influenced by the cellular composition of each

5

tissue sample which is reflected in the gene expression profile that defines a GBM subtype. Tissue from the infiltrative margins contains a mixture of glioma cells and non-neoplastic cells, including microglia, astrocytes, oligodendrocytes and neurons. Identifying the molecular and cellular alterations at the infiltrative margins is of great clinical importance since this tissue is what gets left behind after surgery and will eventually give rise to tumor recurrence.

Recent research has assessed microglia and astrocytes found in glioma brain tumor tissue since these cells can contribute to glioma cell proliferation and invasion and can potentially be targeted to inhibit tumor growth (O'Brien, Howarth et al. 2013, Gutmann 2015, Hambardzumyan, Gutmann et al. 2015, Placone, Quiñones-Hinojosa et al. 2016). As discussed below, neurons are implicated in many of the clinical manifestations of glioma (including seizures and cognitive dysfunction) and have also recently been implicated in regulating glioma cell proliferation (Venkatesh, Johung et al. 2015, Venkatesh, Tam et al. 2017). However, the transcriptional and translational alterations that occur in neurons in the glioma infiltrating cortex has not been well characterized.

Molecular alterations of neurons in glioma remain an understudied problem

Research on the interactions between glioma cells and neurons has focused on the effects of glutamate on neurotoxicity and seizure induction (Buckingham, Campbell et al. 2011, Campbell, Buckingham et al. 2012, Savaskan, Fan et al. 2015). This research has primarily focused on the levels of glutamate found in the glioma microenvironment which result in neuronal alterations that contribute to seizure activity. However, the alterations in neurons themselves within glioma have not been studied. As discussed below, neuronal activity has been implicated in regulating glioma cell proliferation which may contribute to glioma growth (Venkatesh, Johung et al. 2015,

Johung and Monje 2017, Venkatesh, Tam et al. 2017). Gliomas exhibit a histological feature referred to as perineuronal satellitosis, where tumor cells closely encircle neuronal cell bodies in brain tissue (figure 1) (Claes, Idema et al. 2007). The physical proximity of these distinct cell types suggests a close relationship between tumor cells and neurons that has not been explored.

The relationship between glial cells and neurons has been explored in normal brain where satellite cells, including astrocytes and oligodendrocytes, closely surround neuronal soma in the cerebral cortex and hippocampus (Sarnat and Flores-Sarnat 2013). This histologic feature occurs in normal brain, and has been shown to increase during neurologic disease. Satellite glial cells are generally adhered to normal neurons, but in epilepsy they are shown to surround dying neurons. It has been proposed that the function of satellite glial cells is to protect neurons during suboptimal conditions, such as dysregulated neuronal activity in epilepsy. One way satellite glial cells can do this is through adhesion molecules on glia (β2 subunit of Na/K ATPase pump) which helps mediate ion homeostasis to maintain a resting membrane potential (Sarnat and Flores-Sarnat 2013). Alternatively, satellite glial cells can contribute to dysregulated neuronal activity, one way they could do this is by dysregulating ion homeostasis which can result in neuronal membranes to become more easily depolarized.

Further characterization of the effects of glioma cells on neurons is essential as this may underlie the neurological deficits associated with glioma and can provide therapeutic alternatives for these symptoms. However, to identify alterations in neurons within glioma infiltrated cortex, we must develop methods to overcome the challenges imposed by the complex cellular composition of this tissue.

1.2 Identification of distinct cell types in brain tissue

Complex cellular composition contributes to challenges in dissociating specific cell types in brain tissue

Brain tissue is composed of multiple cell types including neurons, astrocytes, oligodendrocytes, microglia and progenitor cells. These different cell types are physiologically and structurally entangled. Neurons have processes that allow them to send and receive signals for proper functional connections in neural circuits across brain regions. Neurons rely on other cell types in brain tissue to form intricate neural circuits (Pekna and Pekny 2012). For example, oligodendrocytes are closely positioned on the axonal processes of neurons for facilitating signal transmission, astrocytic endfeet form part of the neuronal synapse and work to regulate synaptic transmission, microglia help to clear pathogens and toxic cell debris when needed (Allen and Barres 2009, Pfrieger 2010). Astrocytes can respond to neurotransmitter release by modulating calcium signals that influence neuronal excitability and ultimately modulate synaptic plasticity (Ota, Zanetti et al. 2013, Haydon and Nedergaard 2015, Verkhratsky and Nedergaard 2017). Together, these cell types function to respond to internal and external signals such as brain injury and learning and memory (Pekna and Pekny 2012).

Distinct cell types in brain tissue are intermingled among one another making it difficult to technically separate cells for further characterization. Neurons are particularly subject to this constraint due to their intricate morphology. Neuronal processes have been shown to contain ribosomes and mRNAs that are transported via RNA granules which contribute to localized protein synthesis during development and plasticity (Kiebler and Bassell 2006). Selective mRNAs are enriched in neuronal dendrites and their expression is thought to be locally regulated as a result of synaptic activity (Doyle and Kiebler 2011). Due to the information contained

within neuronal processes it is essential to use methods that preserve rather than disturb neuronal processes as a result of physically separating neurons for molecular characterization.

Methods used to study specific cell types in brain tissue

Characterization of distinct cell types in brain tissue generally begins by immunohistochemical staining and morphological assessment. Isolation of specific cell types from brain tissue has allowed for further molecular characterization. However, due to the limited number of genes that can be assessed at one time, next generation sequencing has emerged as a prominent tool that can be used to characterize specific brain cell types based on their gene expression profile (Lein, Hawrylycz et al. 2007, Cahoy, Emery et al. 2008, Hawrylycz, Lein et al. 2012, Zhang, Chen et al. 2014, Tasic, Menon et al. 2016).

Recently, single cell sequencing has enabled the characterization of individual cells from brain tissue (Zeisel, Muñoz-Manchado et al. 2015, Földy, Darmanis et al. 2016, La Manno, Gyllborg et al. 2016, Poulin, Tasic et al. 2016, Cuevas-Diaz Duran, Wei et al. 2017, Picardi, Horner et al. 2017). Methods used to isolate specific cell types include enzymatic dissociation which incubates brain tissue with a proteolytic enzyme that releases individual cells from bulk tissue. Further isolation of specific cell types can be performed by fluorescence-activated cell sorting (FACS) which relies on the cell type of interest expressing a marker for which an antibody against that marker is used to sort cells via a flow cytometer. Additionally, mechanical dissociation and laser capture microdissection discreetly dissect tissue from a brain region of interest and further purify the tissue to remove other cell types typically by immunopanning (Garrido-Gil, Fernandez-Rodríguez et al. 2017, Olah, Patrick et al. 2018). These methods are effective in isolating cell types that well circumscribed without long processes intertwined within

brain tissue. However the physical disruption that the tissue undergoes during these procedures has the risk of damaging neuronal axons and dendrites and potentially losing the critical information contained within them.

Challenges associated with studying specific cell types in brain tissue

Bulk tissue is subject to enzymatic digestion and mechanical isolation when isolating individual cells or a population of cell types. There are multiple caveats associated with these types of methods that should be considered when assessing results from this field of research including 1) enzymatic dissociation induces mechanical stress that influences gene expression, 2) gene expression from cell types that are less abundant, or harder to isolate, in the tissue may not be well represented, 3) microdissection and enzymatic dissociation can damage neuronal processes and deplete RNAs that are found in these compartments (Poulin, Tasic et al. 2016).

Molecular profiling of less abundant cell types in glioma make it difficult to isolate cells such as neurons, and obtain gene expression profiles that reflect their alterations in brain tumor tissue were tumor cells are the predominant cell type. Our laboratory has contributed to an effort that implemented a computational algorithm that can predict cellular composition based on cell type specific markers (Gill, Pisapia et al. 2014, Gonzalez, Sims et al. 2014).

Single cell sequencing has been applied in glioma and confirms the cellular heterogeneity observed between and within different glioma tumors (Darmanis, Sloan et al. 2017, Tirosh and Suvà 2017). This paper compared gene expression profiles peritumoral cells between tumor core and peripheral regions and did not find a difference among neuronal gene expression (Darmanis, Sloan et al. 2017). This finding could be confounded by the fact that both regions where neurons were taken from were affected by the tumor resulting in transcriptionally similar profiles and

10

thus a significant change in gene expression wouldn't be detected. Additionally, the enzymatic dissociation method used to assess neuronal alterations could have damaged neuronal process and resulted in a loss of critical information contained within these structures. Thus, there is a need for better methods that carefully characterize neurons from glioma brain tissue without damaging neuronal cell morphology.

The Ribotag system as a tool to profile cell type specific translation in brain tissue

Transgenic mouse models have been developed to enable the isolation and extraction of cell type specific signatures from brain tissue (Heiman, Schaefer et al. 2008, Heiman, Kulicke et al. 2014). For example, the Ribotag mouse harbors a floxed ribosomal protein (Rpl22) followed by an identical HA-tagged version of Rpl22 (Sanz, Yang et al. 2009). Expression of the HA-tagged version of Rpl22 depends on Cre recombination, in the absence of Cre expression only endogenous Rpl22 is expressed. This system allows for the immunoprecipitation of HA-tagged ribosomes using an anti-HA antibody and isolating their associated translating mRNAs in the cell type of interest. It also allows for the identification of specific cell types from immunohistochemical staining using an anti-HA antibody.

The Ribotag mouse has been crossed with multiple cell type specific Cre transgenic mice resulting in expression of the HA-tagged ribosomes in a cell type of interest, this method is referred to as translational ribosome affinity profiling (TRAP) (Doyle, Dougherty et al. 2008, Heiman, Schaefer et al. 2008, Sanz, Evanoff et al. 2013, Soden, Miller et al. 2016). This methodology has also been used with bacterial artificial chromosome (BAC) transgenic mice which express an EGFP-L10a ribosomal transgene that enables immunoprecipitation of GFP-tagged ribosomes and identification of the translating mRNAs in a cell type of interest. The

difference between the Ribotag and the BAC transgenic mice is that the EGFP-tagged ribosomal protein L10a is driven by an exogenous promoter that can result in different levels of EGFP-L10a and wildtype L10a which can affect the enrichment of cell type specific mRNAs (Kapeli and Yeo 2012). Instead, the Ribotag allele (Rpl22-HA) is expressed under the control of the endogenous promoter which results in cell type specific expression of the HA-tag.

In particular, the Ribotag mouse has been used to identify transcriptional and translational alterations in glioma cells using one of our glioma mouse models (Gonzalez, Sims et al. 2014). We have also shown that the Ribotag mouse when crossed with Camk2a-cre mouse can be used to label and isolate Camk2a+ neuronal transcripts for molecular characterization in non-tumor bearing brain (Hornstein, Torres et al. 2016). Camk2a is a calcium binding protein, primarily expressed in brain and enriched in principal neurons which are found throughout the cortex (Tsien, Chen et al. 1996, Dragatsis and Zeitlin 2000). The Camk2acre mouse allows us to selectively target cre-mediated recombination specifically to principal neurons which are excitatory neurons located in the cortex. In combination with the Ribotag mouse, our model can be used for the extraction of neuron derived ribosomes and the transcripts that are bound to them. Molecular characterization of these transcripts by RNA sequencing then provides a translational profile of neuron specific ribosome bound transcripts which can be used for the analysis of neuronal alterations in neurological disease.

Mouse models used to study glioma

Many different types of mouse glioma models have been developed to aid in the identification of genetic alterations and molecular mechanisms underlying tumor growth. These models are also used for testing potential therapeutic drugs. Genetically engineered mouse

models are useful for understanding the mechanisms that drive tumor growth. Xenograft models are derived from human glioma cells and transplanted to immune compromised mice (Huszthy, Daphu et al. 2012). Both transgenic and xenograft models can be useful in studying glioma growth and identifying potential therapeutic targets, however tumors from xenograft models tend to grow as a well circumscribed balls rather than diffusely invading surrounding brain tissue. In order to study the effects of glioma cells on neighboring cells such as neurons it would be essential that the glioma model being used to study these effects replicated the infiltrative patterns seen in human gliomas.

Retrovirally induced glioma mouse model driven by PDGF overexpression and p53 deletion

Our laboratory has developed several different mouse glioma models that recapitulate the histological and molecular hallmarks of human glioma. Our glioma models rely on the stereotactic delivery of a retrovirus expressing platelet derived growth factor (PDGF) and Cre-recombinase to the subcortical white matter of p53 or PTEN floxed mice. This leads to retrovirally infected cells expanding to develop high grade glioma driven by PDGFB overexpression and p53 or PTEN deletion in retrovirally infected oligodendrocyte progenitors (OPCs) (Lei, Sonabend et al. 2011, Gonzalez, Sims et al. 2014, Sonabend, Bansal et al. 2014, Lu, Chen et al. 2016). These glioma models also harbor a cherry luciferase floxed allele that upon Cre expression in transformed OPCs expresses the luciferase reporter enabling bioluminescent imaging of tumor growth.

We have also delivered a retrovirus expressing PDGFA and Cre-recombinase to p53 floxed mice which result in the formation of low grade glioma tumors. Retrovirally infected cells overexpress PDGFA and expand to form a diffusely infiltrating tumor (unpublished).

Histological characterization of our PDGFA driven tumor model show diffuse infiltration of glioma cells into surrounding brain tissue and perineuronal satellitosis in cortical regions. Our model shows a high degree of infiltrating tumor cells into cortical brain tissue were neurons are intermingled with tumor cells, making this model ideal for us to use to study the effects of glioma cells on neurons. Furthermore, we isolated tumor cells from our PDGFA driven tumor model and injected them into Camk2a-Ribotag mice which enabled us to isolate Camk2a+ neuron derived ribosome bound transcripts from brain tissue during glioma growth (unpublished). These mice develop diffusely infiltrating gliomas that closely resemble human low grade glioma. Thus, our glioma mouse model serves as a tool for us to study the effects of glioma cells on neurons.

Our Camk2a-Ribotag mouse glioma model enables us to determine alterations in ribosome bound RNAs, but it is not able to tell us alterations in non-ribosome bound messages. In our model we calculate the enrichment of neuron-specific genes by taking the ratio of neuron specific ribosome bound RNAs over homogenate RNAs. The homogenate contains ribosome bound and non-ribosome bound RNAs, taking the ratio of IP/homogenate could be considered a limitation in our model since the IP only includes ribosome bound RNAs. Additionally, by taking the right frontal lobe of tumor-bearing brain tissue we could be losing the spatial distribution of alterations. Neurons could regulate their expression patterns in a distinct form depending on their location relative to the location of the tumor. Despite these limitations, our model has provided evidence for the first time about the molecular alterations in neurons within the glioma infiltrated cortex.

Current research on non-neoplastic cells found in glioma brain tissue

It is now recognized that similar to other types of cancer, brain tumors have microenvironments containing non-neoplastic cells that can contribute to tumor progression and response to treatment. This has motivated researchers to focus on the role of microglia and astrocytes in glioma progression. Microglia have been investigated for their role in producing paracrine factors and chemokines that stimulate tumor cell growth and migration (Coniglio and Segall 2013, Wei, Gabrusiewicz et al. 2013, Hambardzumyan, Gutmann et al. 2015). In glioma, astrocytes can promote proliferation and invasion of tumor cells by releasing cytokines and chemokines that activate an inflammatory response (Guan, Hasan et al. 2018). Astrocytes within glioma are also involved in the response to brain injury or neurological disease (Liddelow and Barres). As a result of injury or disease, astrocytes become reactive, meaning their morphology is altered and they can proliferate around the site of injury (Buffo, Rite et al. 2008). In glioma, astrocytes are also being considered for their contribution to tumor progression which can shed light on novel therapeutic targets (Katz, Amankulor et al. 2012).

Much of the research on neurons within glioma has focused on the effects of excess glutamate on neurotoxicity and seizure induction (de Groot and Sontheimer 2011, Huberfeld and Vecht 2016). Tumor cells release excess glutamate that binds NMDA receptors and induces an influx of calcium in neurons that results in cell death. The loss of neurons then presumably allows tumor cells to move into the empty space to propagate their growth (Sontheimer 2008). High glutamate levels have also been attributed to seizure induction, since seizures are generally characterized by an imbalance of excitatory and inhibitory transmission (Buckingham, Campbell et al. 2011, Campbell, Buckingham et al. 2012).

The effects of neuronal activity on other cell types in the brain has been explored through optogenetic approaches which showed that neuronal activation can induce progenitor cell and glioma cell proliferation suggesting that neuronal activity may contribute to glioma growth (Venkatesh, Johung et al. 2015, Venkatesh, Tam et al. 2017). Together these studies highlight multiple interactions between neurons and glioma cells but these studies have not taken a comprehensive approach to characterizing the alterations in neurons within the glioma microenvironment. To begin to investigate the effects of proliferating progenitor cells on neurons in vivo we assessed neuronal gene expression profiles at the level of transcription and translation.

1.3 Transcriptional and translational analysis in brain tissue

Translational regulation through mTOR signaling plays a key role in determining gene expression

Early findings that cancer cells have increased numbers of ribosomes and require increased protein synthesis has prompted researchers to identify the molecular mechanisms underlying translational regulation in cancer. Translation of mRNAs controls multiple cellular processes including metabolism, cell growth and proliferation (Ruggero 2013). Translational regulation serves as a cell's immediate response to alterations in its environment by providing adaptive changes in gene expression (Bhat, Robichaud et al. 2015). Translation is an energetically costly process in cells, as a result translation is tightly controlled to preserve cell resources.

mTOR signaling is known to regulate translation by controlling the expression of genes involved in various steps of protein synthesis (Ruggero 2013). Upregulation of the mTOR pathway can modulate protein synthesis while enabling cancer cells to grow and proliferate

(Silvera, Formenti et al. 2010). There are multiple pharmacological inhibitors that target mTOR signaling and have been used to investigate translation regulation, one study revealed that translationally regulated genes are associated with cell invasion, proliferation, and metabolism in pancreatic cancer cells while another study identified the mTOR regulated genes to be mainly components of the translational machinery in mouse embryonic fibroblasts (Hsieh, Liu et al. 2012, Thoreen, Chantranupong et al. 2012, Ruggero 2013). mTOR signaling has also been implicated in neuronal translation during synaptic plasticity in learning and memory processes (Takei and Nawa 2014). Additionally, dysregulation of mTOR in neurological disease is thought to contribute to brain dysfunction via alterations in translational regulation (Gal-Ben-Ari, Kenney et al. 2012).

Ribosome profiling as a tool for studying translation

Transcriptional analysis has provided information about the abundance of mRNAs available for translation. However, it has been shown that mRNA levels are not concordant with protein levels, suggesting that there is further regulation of protein synthesis (Maier, Güell et al. 2009). This has prompted researchers to focus on translational regulation which can be determined from the number of actively translated transcripts measured by the ribosome density per transcript. The translation of a specific mRNA can be obtained by polysome profiling which is a technique that isolates ribosome bound transcripts (polysomes) through sucrose gradient centrifugation under the assumption that a shift in translational status is determined by a shift of an mRNA in the polysomal gradient. These sucrose fractions were then analyzed by northern blot or qPCR (Mašek, Valášek et al. 2011, King and Gerber 2016).

Ribosome profiling has emerged as a technique in which short ribosome protected mRNA fragments are isolated and sequenced. Ribosome density is then used as a proxy for the rate of

translation (Brar and Weissman 2015). Translation rate can then be used to measure translation efficiency from individual genes from the entire genome (Ingolia, Ghaemmaghami et al. 2009). Translation efficiency is referred to as the ratio of the translation rate (ribosome density per transcript) to the abundance of a specific transcript. Ribosome profiling serves as a method to obtain the rate of translation and position of a ribosome on a transcript, providing information about the location of ribosomes which can tell us if ribosome bound transcripts are being translated or if ribosomes are stalled.

Translational regulation in neurological disease and glioma

Translation has been studied in neurons particularly during synaptic plasticity for cognitive processes. Dysregulation of mTOR signaling in neurological diseases such as Tuberous Sclerosis Complex (TSC), fragile X syndrome, Retts syndrome, and neurodegenerative diseases suggest that mTOR plays a role in translational regulation (Gal-Ben-Ari, Kenney et al. 2012). Neurons implement translational regulation mechanisms for specialized compartments such as axons and dendrites. Local translational regulation is essential for neurons because in some cases proteins can be harmful if found at other cellular compartments and also because it is required for rapid and localized responses to synaptic stimuli (Di Liegro, Schiera et al. 2014).

A study that analyzed translation in a glioma mouse model identified that there is increased translation efficiency for genes that promote cell proliferation while genes associated with synaptic proteins had decreased translation efficiency (Helmy, Halliday et al. 2012). This study claimed that the decreased translation of synaptic proteins was likely a result of the lack of neuronal differentiation of Olig2+ glioma cells. To assess translation this study used a BAC transgenic mouse that expresses the large ribosome unit protein L10a with GFP under the control of the Olig2 BAC promoter and using TRAP methodology calculated translation efficiency by

taking the ratio of the immunoprecipitated (for GFP) transcripts over the total transcripts (determined from FACS cell sorting for GFP). The methodology used in this study has a few limitations 1) Olig2 is expressed in untransformed glial progenitors 2) the number of transcripts determined from immunoprecipitation does not yield the density of ribosomes per transcript, which is required to calculate translation efficiency.

Our laboratory recently contributed to a study that assessed translational regulation using a different approach. We delivered a PDGFB-cre expressing retrovirus to Ribotag mice which induces expression of the ribosomal protein (Rpl22) tagged with HA selectively in retrovirally infected glial progenitors. We then performed RNA sequencing and ribosome profiling on homogenate and HA-immunoprecipitated mRNAs to measure total transcript levels across cell types and transformed glial progenitor transcript levels, respectively. This study determined that while the translation rate for genes enriched in transformed glial progenitors had increased, the translation efficiency of these genes is decreased (Gonzalez, Sims et al. 2014). These findings suggest that glioma cells are likely saturated with transcripts that they can no longer efficiently translate, suggesting that glioma cells are under a high degree of translational regulation.

Our lab also characterized translational regulation in normal brain tissue using the Ribotag mouse to isolate neuron specific transcripts. We assessed the efficiency of a new ribosome profiling strategy to detect changes in gene expression when pharmacologically inhibiting mTOR signaling. We determined that the novel ribosome profiling strategy is efficient and that canonical mTOR targets are promptly downregulated after mTOR inhibition in normal brain (Hornstein, Torres et al. 2016). Translational regulation plays an important role in glioma, which merits further characterization of the mechanisms involved in translation control. mTOR

signaling is often involved in driving glioma growth and its role in translation may provide a mechanistic understanding of how mTOR contributes to tumor growth.

1.4 mTOR signaling in neurological disease

Upstream and downstream of mTOR signaling

mTOR is a protein kinase and a component of a complex signaling cascade that integrates signals from growth factors and nutrients to regulate essential cell functions including cell growth, proliferation, differentiation and translation (figure 1.2)(Takei and Nawa 2014). mTOR activity is regulated through the PI3K/AKT pathway which is negatively regulated by PTEN and TSC1/2. mTOR exists in two multi-protein complexes, mTORC1 and mTORC2. mTORC1 can be activated by growth factors, amino acids, neurotransmitters, hormones and generally responds to cell energy status, hypoxia, and other types of stressors (Takei and Nawa 2014). mTORC2 can be activated by growth factors as well, however this seems to be context dependent (Oh and Jacinto 2011).

mTORC1 regulates the activity of S6 kinase and elongation binding proteins (4EBPs), resulting in the phosphorylation S6K1 and 4EBP1. Upon mTOR activation S6K1 is activated and phosphorylates ribosomal protein S6 (pS6), 4EBP is phosphorylated (p4EBP1) and 4EBP1 is disinhibited thereby enabling translation (Guertin and Sabatini 2009). Recent evidence has shown that the translation of TOP mRNAs, which contain a 5'-terminal oligopyrimidine sequence (TOP) and are specific for components of the translational machinery, is regulated through 4EBP phosphorylation (Thoreen, Chantranupong et al. 2012). The mTOR signaling pathway has feedback loops that are in place to maintain homeostatic regulation. mTOR is negatively regulated by suppressing PI3K through S6K (Guertin and Sabatini 2009). mTORC2 regulates Akt phosphorylation (Ser473) which is needed for maximal Akt activity, which places

mTOR both upstream and downstream of Akt (Efeyan and Sabatini 2010). Disruption of the mTOR pathway can have detrimental effects during development and in neurological disease which make mTOR essential for normal brain function.

mTOR signaling is required for normal brain function

mTOR is involved in brain development including dendritic development, axon guidance, learning and memory, and in neuronal repair after injury (Curatolo and Moavero 2013). mTOR activation is dependent upon neuron receptor and channel activation that regulate neuronal translation(Takei and Nawa 2014). Because of the role of mTOR in regulating translation, mTOR activity can modulate synaptic plasticity and has become a signaling pathway of interest for developmental processes and in many neurological diseases (Hoeffer and Klann 2010).

Dysregulated mTOR signaling is an underlying cause for several neurological disorders

Dysregulation of the mTOR pathway generally results in the upregulation of mTOR activity that is seen tuberous sclerosis complex disease (TSC), focal cortical dysplasia, and epilepsy (Lipton and Sahin 2014, Citraro, Leo et al. 2016). Upregulated mTOR activity results in enlarged neurons and abnormal cortical organization which is thought to contribute to the pathology of some neurological diseases. Several mouse studies have shown that seizures resulting from dysregulated mTOR activity can be prevented and inhibited with the mTOR inhibitor rapamycin, suggesting the potential use of mTOR inhibitors for seizures in other neurological disorders (Meikle, Talos et al. 2007, Zeng, Xu et al. 2008) (Huang, Zhang et al. 2010, Guo, Zeng et al. 2013).

In TSC, either TSC1 or TSC2 function is compromised resulting in direct upregulation of mTOR activity (Crino 2011). TSC results in seizures, benign brain tumors and other neurological deficits. The mTOR inhibitor everolimus is clinically approved to treat brain tumors and seizures

in TSC (Krueger, Care et al. 2010, Krueger Darcy, Wilfong Angus et al. 2013, French, Lawson et al. 2016). Because dysregulated mTOR signaling is seen in glioma and in seizures, inhibiting mTOR signaling in glioma would be an efficient way of targeting one pathway that affect both glioma growth and seizures associated with tumor growth (Huberfeld and Vecht 2016). Together, these studies show that targeting mTOR upregulation in neurological disease can inhibit neurological deficits.

Alterations in PTEN also result in upregulated mTOR activity that has been shown in in autism. Autism results in impaired social and restrictive behaviors that appear during development. These symptoms have been associated with abnormal synapses including increased dendritic spine density (Sato 2016). mTOR inhibition in mouse models of autism have shown to ameliorate some of the synaptic alterations including decreasing dendritic spine density (Tang, Gudsnuk et al. 2014). Fragile X syndrome (FXS) is caused by loss of function mutations in the RNA binding protein fragile X mental retardation protein (FMRP) which result in mental retardation, cognitive impairment, seizures and autism (Sharma, Hoeffer et al. 2010). FMRP selectively binds mRNAs, specifically during transport to synapses, and inhibits their translation, therefore loss of FMRP function results in increased translation (Zalfa, Adinolfi et al. 2005). Since FXS is characterized by excessive translation, and increased mTOR activity is seen in FXS brains, mTOR has become a plausible mechanism driving increased translation. mTOR inhibitors have been shown to target some of the symptoms in FXS mouse models which is thought to occur via inhibition of translation (Sharma, Hoeffer et al. 2010, Sato 2016). Overall mTOR inhibition in neurological disease has shown promising results and motivates future studies to identify the mechanisms underlying these effects as well as the effects of mTOR inhibition in other neurological diseases.

Inhibiting mTOR signaling in glioma as an anti-tumor therapy has had limited effects

Upregulated mTOR signaling is a frequent event in glioma that results from dysregulation in one or more upstream modulators of downstream effectors of mTOR (Akhavan, Cloughesy et al. 2010, Fan and Weiss 2012). Upregulated mTOR activity contributes to glioma cell proliferation and survival which has driven research to test the potential of mTOR inhibitors to inhibit glioma growth. Unfortunately mTOR inhibitors in glioma have had limited success which is most likely due to the fact that that mTOR inhibition is usually overcome since mTOR signaling is such a central component in maintaining cell survival. Alternatively, mTOR inhibitors that have been tested may not fully target all mTOR functions that drive tumor growth resulting in modest effects. This has driven the development of novel mTOR inhibitors that better target mTOR functions.

Rapamycin is a macrocyclic antibiotic produced by soil bacteria. Rapamycin is an allosteric inhibitor of mTOR that targets mTORC1, it does so by binding to FKBP12, a cytosolic protein which then binds to mTOR in a region that is adjacent to the catalytic site (Efeyan and Sabatini 2010). However, studies have shown that rapamycin partially targets mTORC1 functions, mainly affecting S6 kinase activity without affecting 4EBP (Feldman, Apsel et al. 2009, Thoreen, Kang et al. 2009). mTORC2 regulates Akt phosphorylation (Ser473) and is insensitive to rapamycin. To target more downstream mTOR effectors than allosteric mTOR inhibitors, novel ATP-competitive mTOR inhibitors have been developed. ATP-competitive inhibitors bind to the active site of the mTOR kinase and inhibit the activity of both mTOR complexes. ATP-competitive inhibitors have been shown to target both S6 and 4EBP making

them more suitable compounds for analyzing complete inhibition of mTOR activity (Chresta, Davies et al. 2010).

The innate cellular complexity in glioma has made it difficult to identify gene expression profiles in less abundant cell populations that are intermingled among tumor cells. The Camk2a-Ribotag approach described in chapter 2 allowed us to reveal translational alterations in neurons from the glioma infiltrated cortex that have not been identified before. In chapter 3 I describe how inhibiting mTOR signaling for 6 hours reversed several of the glioma induced translational alterations in neurons. In chapter 4 I used ribosome profiling to identify translational alterations in homogenate glioma tissue. The work described in this thesis provides evidence for how a novel glioma mouse model can be used to identify otherwise undetected neuronal signatures and hopefully serve as a tool for further characterization of the neuronal alterations in glioma that may contribute to the molecular mechanisms associated with neurological symptoms in glioma.
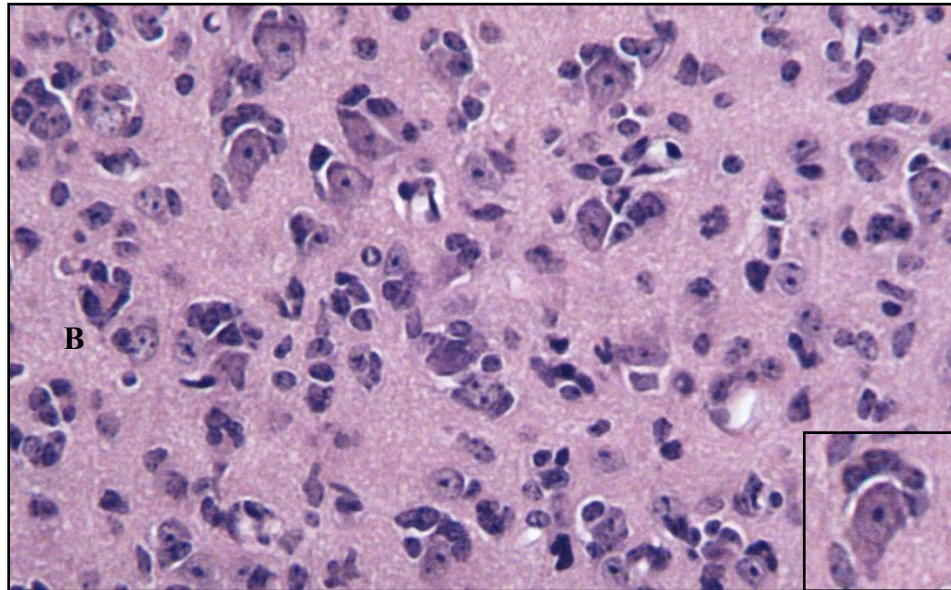
Figure 1.1: Mouse diffusely infiltrative glioma. HE from mouse tumor cortex, close up image shows neuronal soma surrounded by tumor cells (perineuronal satellitosis).
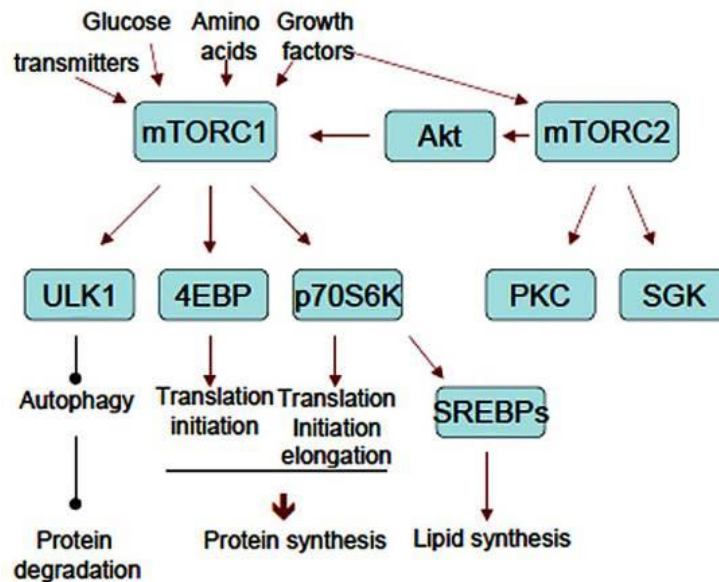
Figure 1.2: mTOR signaling pathway. Upstream and downstream components of the mTOR signaling pathway.

CHAPTER 2

A new diffusely infiltrating glioma mouse model reveals neuronal alterations in the brain tumor microenvironment

2.1 Introduction

Gliomas are debilitating brain tumors for which patients present with neurological impairments during the course of the disease. Neurological impairments can be a result of tumor progression and can lead to a poor quality of life for patients with glioma. Gliomas are diffusely infiltrating brain tumors in which tumor cells invade surrounding brain tissue and intermingle with non-neoplastic cells including neurons. Patients with glioma often present with seizures and impaired cognitive function that worsen as tumor infiltration increases (Taphoorn and Klein 2004, Miotto, Silva Junior et al. 2011, Bergo, Lombardi et al. 2015). Dysregulated neuronal activity has been demonstrated to contribute to seizures and impaired cognitive function in patients with glioma (Meyers 2002, Bosma, Vos et al. 2007, Buckingham, Campbell et al. 2011). However, molecular characterization of neurons within the glioma infiltrated cortex has been understudied.

Human gliomas have been extensively characterized by gene expression profiles (Verhaak, Hoadley et al. 2010, Brennan, Verhaak et al. 2013), however most of this work has focused on the core of the tumor which is predominately composed of glioma cells. As a result, these studies have not been able to assess the gene expression profiles of less abundant cell types in gliomas such as neurons. Our laboratory characterized the glioma infiltrative margins using

RNA sequencing and determined that it is mainly composed of non-neoplastic cells such as neurons and oligodendrocytes (Gill, Pisapia et al. 2014), providing further evidence for the intermingling of tumor cells and non-neoplastic cells in the brain tumor microenvironment. Recently, the development of single cell sequencing has been able to isolate individual cells and generate single cell gene expression profiles from glioma brain tissue. A recent study used single cell RNA sequencing from human glioblastoma tissue but found no difference between neurons from the tumor core compared to those from the peritumoral area (Darmanis, Sloan et al. 2017). However, these findings may be confounded by the harsh methods used to dissociate glioma tissue in order to isolate neurons which results in mechanical damage that can induce transcriptional alterations or it can damage neuronal processes and deplete information that is enriched in these subcellular compartments (Poulin, Tasic et al. 2016).

Previous studies have also used cell sorting or enzymatic dissociation methods to isolate cells and generate cell type specific gene expression profiles from normal brain (Cahoy, Emery et al. 2008, Doyle, Dougherty et al. 2008, Zhang, Chen et al. 2014, Tasic, Menon et al. 2016). Enzymatic dissociation and cell sorting introduce mechanical stress that can induce transcriptional alterations and damage cells with complex cellular morphology (Poulin, Tasic et al. 2016, Tirosh and Suvà 2017) . Neurons have complex cellular morphologies that are sensitive to currently used dissociation methods and thus information encoded in neuronal processes may have gone undetected in a recent study (Darmanis, Sloan et al. 2017). Neuronal processes contain ribosomes and mRNAs that are transported via RNA granules specialized for localized protein synthesis during neuronal plasticity (Kiebler and Bassell 2006). These transcripts can get lost during tissue dissociation resulting in a loss of the information encoded in these subcellular compartments. Therefore, there is a need to develop methods that can dissociate glioma brain

tissue while preserving complex neuronal morphology so as to isolate neuronal transcripts from subcellular compartments such as axons and dendrites.

Due to the intermingling of different cell types in brain tissue it has been difficult to physically isolate and assess the molecular characteristics of specific cell types. To address this issue, our laboratory has shown that the Ribotag mouse can be used to selectively label and identify Camk2a+ neuronal transcripts for transcriptomic and translational analysis (Hornstein, Torres et al. 2016). Camk2a is selectively expressed in excitatory principal neurons within the cortex (Tsien, Chen et al. 1996). The Ribotag mouse harbors an HA-tagged ribosomal protein (Rpl22) that is expressed upon crossing with a Cre-recombinase expressing mouse line (Sanz, Yang et al. 2009). We crossed the Ribotag mouse with the Camk2a-Cre mouse which results in HA-tagged ribosomes specifically in Camk2a+ neurons. The Camk2a-Ribotag mouse then allows for the isolation of HA-tagged ribosomes and the associated transcripts specifically from a subset of neurons from mouse brain tissue (Hornstein, Torres et al. 2016). This approach is also referred to as translating ribosome affinity purification (TRAP) in which purification of tagged ribosomes from a specific cell type can be used to obtain profiles of the ribosome bound mRNAs (Doyle, Dougherty et al. 2008, Heiman, Schaefer et al. 2008, Dougherty, Schmidt et al. 2010, Heiman, Kulicke et al. 2014, Shigeoka, Jung et al. 2018). Since all translated mRNAs are at one point associated with ribosomes, we can use the TRAP approach to identify which mRNAs are being translated (Kapeli and Yeo 2012).

We leveraged the Ribotag system to overcome the technical challenges of isolating specific cell types from glioma infiltrated brain tissue. We developed a diffusely infiltrating glioma mouse model that allows for studying neuron specific alterations. Our glioma model most closely resembles human low grade gliomas. We induce glioma growth by injecting mouse

glioma cells that have p53 deletion and overexpress PDGFA in Camk2a-Ribotag mice, which will be referred to as our Camk2a-Ribotag mouse glioma model. This enables the isolation of HA-tagged ribosomes from Camk2a+ neurons from glioma-infiltrated cortex. Using the Camk2a-Ribotag mouse glioma model, we found that genes associated with synapses were downregulated while genes associated with dendritic spines were upregulated in glioma-infiltrated cortex compared to normal cortex. The genes associated with synapses included synaptophysin, snap25, and synaptotagmin among others. The genes associated with dendritic spines are enriched for genes encoding actin-binding proteins that play a role in dendritic spine dynamics (Lin and Webb 2009). We further showed an upregulation in the expression of drebrin (an actin binding protein expressed in dendritic spines) in the synaptosomal fraction of glioma infiltrated cortex. Finally, diolistic imaging revealed a decrease in dendritic spines density in Camk2a+ neurons from glioma infiltrated cortex compared to those found in control brains. Taken together these findings suggest that there is a degree of reactive plasticity occurring in glioma in which the downregulation of synaptic genes and dendritic spines results in the upregulation of dendritic spine genes so as to preserve brain function during glioma cell infiltration. Our methodology enabled us to identify changes in the translating mRNA profile of Camk2a+ neurons in glioma infiltrated cortex and enabled the histological, molecular and morphological characterization of Camk2a+ neurons in the brain tumor microenvironment.

2.2 Results

Development of diffusely infiltrating glioma mouse model for the isolation of neuron derived ribosomes and their associated transcripts

Diffuse infiltration of tumor cells into surrounding brain tissue is a major histological feature in glioma (Claes, Idema et al. 2007). We developed a glioma mouse model that recapitulates the histological features of human glioma (Wesseling, Kros et al. 2011). In our model, glioma growth is driven by transformed glial progenitor cells that have p53 deletion and overexpress PDGFA resulting in a diffusely infiltrating tumor (figure 2.1a). Transformed glial progenitor cells were obtained from a retrovirally induced glioma using methods that have been previously established in our lab (Lei, Sonabend et al. 2011, Sonabend, Bansal et al. 2014). Retrovirally induced gliomas were initiated by stereotactic injection of PDGFA-IRES-CRE retrovirus to the subcortical white matter of p53 floxed neonates (unpublished). These mice also harbor a floxed cherry-luciferase reporter allele, upon retroviral delivery glial progenitor cells are infected and begin to overexpress PDGFA, have exon 5 of the p53 gene deleted, and express the cherry-luciferase reporter allele. The luciferase reporter allows for monitoring tumor growth by bioluminescence as demonstrated in other glioma mouse models from our lab (Lei, Sonabend et al. 2011, Sonabend, Bansal et al. 2014). We isolated transformed glial progenitor cells from this model for stereotactic injection in Camk2a-Ribotag mice. The transformed glial progenitors with p53 deletion, PDGFA overexpression, cherry-luciferase reporter expression will be referred to as glioma cells in this thesis. We chose to use glioma cells to induce glioma growth rather than the retrovirus to induce glioma growth since we were interested in using the Camk2a-Cre mouse to induce Cre-recombination in neurons to study neuronal alterations in glioma. I could not have used the retrovirus to induce glioma growth in Camk2a-Cre mice because the retrovirus (PDGFA-Cre) already expressed Cre-recombinase. The retrovirally induced glioma model is currently being characterized by other lab members. Both the glioma cell model and the

retroviral model share similar histological and molecular characteristics, which I compared and described in chapter 1.

Glioma cells were injected into Camk2a-Ribotag in adult mice to induce glioma growth. These mice develop gliomas that diffusely invade surrounding brain tissue. Histologically, these tumors show glioma cells infiltrating the cortex in the right frontal lobe (figure 2.1a). This histological feature is referred to as perineuronal satellitosis, which shows neurons often surrounded by glioma cells (Claes, Idema et al. 2007). Staining for the pan-neuronal marker (NeuN), glial progenitor marker (Olig2) and the proliferation marker (Ki67) showed close intermingling of proliferating glioma cells and neurons throughout the cortex (figure 2.1a). The Ribotag mouse expresses an HA-tagged ribosomal protein (Rpl22) that is activated upon expression of Cre-recombinase in Camk2a+ neurons (Sanz, Yang et al. 2009). This system allows for the identification of Camk2a+ neurons by immunohistochemistry and the isolation of neuron specific ribosome bound transcripts from glioma brain tissue (figure 2.1a-b). Since tumor cells express the luciferase reporter allele, we used this feature to track tumor growth by bioluminescent imaging (figure 2.1c).

We performed immunofluorescence to identify the relative neuron, Camk2a+ neuron, and glioma cell populations within the glioma infiltrated cortex. We quantified the number of cells expressing NeuN, HA, Olig2, DAPI and the percentage of NeuN positive cells that are HA positive from the ipsilateral side of tumor and non-tumor bearing sections. These results showed an increase in the number of Olig2 positive cells, indicative of tumor cells, and a decrease in the number of neurons (determined by HA and NeuN) which shows that neurons are a minor cell population relative to tumor cells within the glioma infiltrated cortex (figure 2.2).

Neuron derived ribosome bound transcripts are enriched for neuronal genes in the Camk2a-Ribotag glioma mouse

We previously showed that the Camk2-Ribotag mouse can be used to isolate ribosome bound transcripts from neurons in normal brain for transcriptional and translational analysis (Hornstein, Torres et al. 2016). Our new Camk2a-Ribotag mouse glioma model allowed us to isolate neuron specific ribosome bound transcripts from glioma infiltrated cortex for molecular analysis. We obtained brain tissue from the right frontal lobe of tumor-bearing mice and non-tumor bearing mice and performed RNA sequencing on homogenate lysate (total) which includes HA-tagged and non-tagged ribosomes and on immunoprecipitated HA-tagged ribosome bound transcripts (IP). We calculated the enrichment score (ES) of each gene by dividing normalized counts from the IP over the normalized counts from the homogenate (IP/total). By calculating the enrichment score of a specific gene we can determine which transcripts were enriched in Camk2a+ neurons relative to homogenate brain tissue (Hornstein, Torres et al. 2016).

We conducted GSEA analysis on the IP from normal and tumor bearing brains to assess the enrichment of a set of neuronal genes identified in a previous study (Zhang, Chen et al. 2014). GSEA analysis showed that both normal brains and tumor brains are enriched for a published set of neuronal genes, demonstrating that the isolated transcripts are neuron specific (figure2.3a). To verify that neuronal gene enrichment was primarily a contribution from neurons rather than glioma cells, we compared the top ranked neuronal genes from the GSEA analysis (figure 2.3a) to the highly upregulated tumor cell genes (figure 2.3b). Tumor cell genes were defined as the top ranked genes with a positive fold change (calculated from normalized counts of homogenate tumor/homogenate normal) which suggests that they are expressed in the predominant cell type in the tumor, glioma cells. We calculated the ES for these genes and show

that neuronal genes are enriched while tumor cell genes are depleted from the neuron specific ribosome bound transcripts. These data show that we can effectively obtain neuron specific bound ribosomes from glioma brain tissue in our mouse model.

Neurons from glioma infiltrated cortex show a downregulation of synaptic genes and an upregulation of actin binding transcripts associated with dendritic spines

We performed gene ontology (GO) analysis using DAVID and identified highly significant and enriched GO terms for genes that were downregulated or upregulated based on differential gene expression calculated by DESeq. We performed differential gene expression between tumor IP and normal IP and considered upregulated genes as those with a log2 fold change greater than 0 and downregulated genes as those with a fold change less than 0, the fold change was obtained from DESeq output. Based on these criteria, we identified 1110 downregulated genes with an ES greater than 1.5, these genes were associated with many GO terms, including synapse and postsynaptic membrane (figure 2.4a). We identified 304 upregulated genes with an ES greater than 1.5, several of those genes were associated with actin binding and cytoskeleton GO terms (figure 2.4b). The ES to determine downregulated genes was obtained from normal brain while the ES to determine upregulated genes was obtained from tumor. We performed our analysis this way because if we use the ES from tumor to identify downregulated genes then we would not detect all genes that are enriched in neurons since the presence of glioma cells among neurons can affect the number of ribosomes per transcript thereby affecting the ES derived from tumor. We focused on actin binding genes since these were the most highly enriched and upregulated genes determined by GO and because they are associated with neuron specific functions. The actin cytoskeleton plays a fundamental role in

33

regulating dendritic spine morphology and ultimately synaptic activity (Lin and Webb 2009, Maiti, Manna et al. 2015).

Actin binding proteins are highly enriched in dendritic spines and some have been shown to be transported to dendritic spines via RNA granules for local translation (El Fatimy, Davidovic et al. 2016). We queried our differential gene expression analysis for actin binding genes enriched in RNA granules and important for dendritic spine dynamics (El Fatimy, Davidovic et al. 2016). We identified that several of these dendritic spine genes were upregulated and enriched in tumor IP (table 1), we show their p-value and log2 fold change obtained from differential expression of tumor IP vs normal brain IP in table 1. Several of these genes were also in the list of genes that were enriched in the actin binding GO term.

To further assess the enrichment of actin binding genes enriched in RNA granules important for dendritic spines we performed GSEA analysis to determine the enrichment of dendritic spine genes in normal vs tumor brain IP (El Fatimy, Davidovic et al. 2016). We obtained a positive and significant GSEA enrichment score for the expression of genes enriched in RNA granules (figure 2.4c) which shows that actin binding genes enriched in RNA granules and important for dendritic spines are enriched and upregulated in our glioma mouse model.

We performed the same GSEA analysis to determine the enrichment of actin binding genes enriched in RNA granules important for dendritic spines in normal vs tumor brain total homogenate. We obtained a negative GSEA enrichment score which shows that actin binding genes are not enriched in the total homogenate of glioma brain tissue (figure 2.4d). These results show that the enrichment of actin binding genes is only detectable by analyzing genes from tumor IP samples not tumor homogenate samples. These results show how neuron specific

alterations are undetected when profiling homogenate (bulk) tumor tissue which is likely due to 1) the low abundance of neurons within the tumor 2) alterations in cellular composition obscure cell type specific alterations in bulk tumor 3) the harsh methods used to dissociate glioma brain tissue make it difficult to preserve complex neuron morphology. These results provide evidence for how the Ribotag system serves as a means to identify an otherwise obscured gene expression signature.

Drebrin, an actin binding protein enriched in dendritic spines, is upregulated in the synaptic fraction of glioma infiltrated cortex

We queried the RNA granule gene list (El Fatimy, Davidovic et al. 2016) for the upregulated and enriched actin binding genes in our neuron specific ribosome bound gene signature, we identified drebrin, an actin binding gene specific to dendritic spines which had a tumor ES of 3.25. We focus on drebrin because it was one of the genes with a high enrichment and known function in dendritic spines (Ivanov, Esclapez et al. 2009). We examined whether drebrin was also upregulated at the protein level. Given the dendritic spine localization and function of drebrin, we decided to biochemically isolate synaptic fractions and test drebrin expression there. Synaptic fractions consist of pre and post-synaptic components (synaptosome) which are obtained through subcellular fractionation and differential centrifugation (figure 2.5a) (Bai and Witzmann 2007, Smalheiser and Lugli 2014). Following synaptosome isolation we probed for post-synaptic density protein (PSD95) across the different sub-cellular fractions (total, cytosolic, synaptic) in tumor and non-tumor brain lysate. We found PSD95 to be enriched in the synaptic fraction (relative to actin loading), suggesting that the synaptosome isolation protocol is effectively enriching for post-synaptic proteins (Hunt, Schenker et al. 1996). We also probed for HA expression in synaptic fractions and determined that HA expression is enriched in both

normal and tumor brain which suggest that HA-tagged ribosomes are localized to the synaptic component of dendritic spines and possibly be involved in RNA granule transport for local protein synthesis (figure 2.5b).

Drebrin is an actin binding protein primarily expressed in brain tissue and enriched in dendritic spines (Ivanov, Esclapez et al. 2009, Koganezawa, Hanamura et al. 2017). Drebrin was one of the highly enriched and upregulated genes in our neuron-specific data, thus we investigated the expression of drebrin in the synaptic fraction. We isolated total homogenate and synaptic fractions from normal and tumor bearing brains and found a significant increase in drebrin expression in the tumor synaptic fraction compared to total homogenate (One way ANOVA p=0.0070, p=0.0131 Tukey's multiple comparison test) (figure 2.5c). Drebrin expression in the tumor brain synaptic fraction was also significantly higher compared to normal brain synaptic fractions (One way ANOVA p=0.0070, p=0.0333 Tukey's multiple comparison test) (figure 2.5c). Our results are marginally significant, which is likely due to the high degree of variability in drebrin expression in tumor synaptic fractions. I suspect that this may be due to the heterogeneous cellular composition that is inevitable in glioma brain tissue. The variability in drebrin expression as a result of cellular composition may also account for the fact that drebrin, although highly enriched in neuron specific ribosome bound transcripts, did not come up in our list of differentially expressed genes. The normalized counts for drebrin show that one tumor sample is an outlier compared to the other two samples and could have been excluded by the algorithm that DESeq uses to calculate differential gene expression analysis, hence the NA p-value for drebrin. Despite the variability in drebrin expression, our results collectively show that in addition to the upregulation of ribosome bound drebrin mRNA, drebrin protein levels are also upregulated. These data point to alterations in genes that regulate dendritic spines in the glioma

infiltrated cortex and suggest that there may be resulting alterations in dendritic spines in our Camk2a-Ribotag glioma model.

Decreased dendritic spine density in glioma infiltrated cortex suggests that there are alterations at the synaptic level

We hypothesized that the upregulation of actin binding genes involved in dendritic spine dynamics would result in alterations in the density and morphology of dendritic spines in glioma associated neurons. In order to visualize such changes in situ, we used diolistic labelling in brain tissue sections which label neuronal processes with a fluorescent dye (Staffend and Meisel 2011). Sections were co-stained with the HA antibody to identify Diolistic-labelled Camk2a+ neurons (figure 2.6a). Overall, the Camk2a+ neurons within glioma infiltrated cortex demonstrated decreased complexity, with fewer dendritic projections and arborizations. We determined that Camk2a+ neurons within the glioma infiltrated cortex had significantly fewer dendritic spines compared to normal brains (*P*<0.0001; figure 2.6b). Further analysis of the morphology of these dendritic spines will enable a better understanding of dendritic spine dynamics in our glioma model.

The decrease in dendritic spine density and the downregulation of synaptic genes identified by ribosome bound mRNA levels suggests that there is decreased synaptic function in neurons within the glioma infiltrated cortex. The simultaneous upregulation of actin binding genes enriched in dendritic spines suggests that neurons are trying to compensate for the loss of dendritic spines and synapses within the glioma infiltrated cortex. This compensatory mechanism could explain that the upregulation of dendritic spine genes is induced by the loss of dendritic

spines and synaptic genes as a way to compensate for the loss of functional synapses induced by infiltrating glioma cells.

This compensatory mechanism could underlie a form of reactive plasticity that occurs during tumor growth in the glioma infiltrated brain. Reactive plasticity occurs in response to injury or pathology as a way to preserve neuronal function by reorganization of neural circuits (Kong, Gibb et al. 2016). Reactive plasticity has been studied in glioma primarily from a clinical perspective, research shows that low grade gliomas that have a slower growth rate allow for a higher degree of plasticity, compared to high grade gliomas that generally grow at a faster rate, that enables the reorganization of neural circuits in order to preserve cognitive functions (Duffau 2014). Reactive plasticity could explain our results that show a decrease in dendritic spine density and synaptic genes while simultaneously upregulating actin binding genes enriched in dendritic spines, however further characterization of the functional consequences of these synaptic alterations is needed to provide a better understanding of the neuronal alterations in glioma infiltrated cortex.

2.3 Discussion

The purpose of our study was to develop a model that allows us to specifically assess neuronal alterations from glioma infiltrated brain tissue. We developed the Camk2a-Ribotag mouse glioma model to be able to isolate neuron specific ribosome bound mRNAs from the glioma infiltrated cortex. Using this mouse model and TRAP methods we identified a decrease in the translation of ribosome bound synaptic mRNAs and a decrease in dendritic spine density from Camk2a+ neurons. We also identified an upregulation in the translation of ribosome bound actin binding mRNAs enriched in dendritic spines and an upregulation of drebrin protein levels in the

synaptic fraction of glioma infiltrated cortex. These results suggest that there is a compensatory mechanism underlying the neuronal alterations in glioma infiltrated cortex. We propose that this compensatory mechanism might underlie a form of reactive plasticity that occurs during glioma growth.

The effects of diffusely infiltrating glioma cells on neurons have been studied in the context of glioma associated seizures where it has been shown that glioma cells contribute to neuronal hyperexcitability resulting in seizure activity (Takano, Lin et al. 2001, Buckingham, Campbell et al. 2011, Campbell, Buckingham et al. 2012, Huberfeld and Vecht 2016). Seizure activity is often considered an imbalance of excitatory and inhibitory transmission which can lead to alterations in synaptic function (Lepeta, Lourenco et al. 2016). Mouse models of epilepsy have shown decreased dendritic spine density that may contribute to impaired synaptic function in seizures (Noebels 2015). These findings suggest that the decreased dendritic spine density in our glioma model may also induce alterations in synaptic function. In a kainic acid induced rat model of epilepsy seizures resulted in a decrease in Snap25, synaptophysin, and Syt1 that correlated with impaired cognitive functions (Zhang, Sun et al. 2014). These genes were also downregulated in our glioma model and suggest that the downregulation of synaptic proteins may be associated with impaired cognitive functions or seizures during glioma growth.

We discovered that neurons within the brain tumor microenvironment show an upregulation in the translation of ribosome bound actin binding mRNAs enriched in dendritic spines. The actin cytoskeleton plays an essential role in the formation and dynamics of dendritic spines (Goellner 2011). Several of these upregulated acting binding mRNAs are highly enriched in neuronal RNA granules (figure 2.4b). RNA granules can transport specific mRNAs to distal compartments in neurons including dendritic spines for local translation (El Fatimy, Davidovic et al. 2016). The

39

fact that there is an increase in the translation of actin binding mRNAs enriched in RNA granules suggests that these mRNAs are being transported in RNA granules for local translation in our glioma model. We show that the HA-tag is enriched in normal and tumor brain synaptic fractions from synaptosome western blot analysis, which suggest that there are more HA-bound ribosomes at or near synapses and that transport via RNA granules for local translation of ribosome bound transcripts is a plausible mechanism in our glioma model. This could be addressed using ribosome profiling, a method used to measure translation by quantifying the number or ribosomes per mRNA and the location of ribosomes on that mRNA (Ingolia, Ghaemmaghami et al. 2009). This differs from the TRAP approach used in this chapter since TRAP can only tell us whether an mRNA is ribosome bound, not the number of ribosomes per mRNA. Experiments using ribosome profiling of synaptic fractions from our glioma model could tell us how efficiently actin binding mRNAs are being translated and whether they are being translated or if the ribosomes bound to them are stalled.

We acknowledge that while synaptosome isolation is efficient to enrich for pre and post-synaptic membrane components, differential centrifugation may also enrich for endoplasmic reticulum (ER), mitochondrial or lysosome membranes (Levitan, Mushynski et al. 1972). To assess the purity of synaptosomes we blotted for PSD95 which is highly abundant in synaptic membranes. We observed an enrichment of PSD95 expression in the synaptic fraction and interpreted these results as showing an enrichment for synaptic proteins in the synaptosome fraction. We could also blot for markers specific to other subcellular compartments that may get enriched in the synaptic fraction. To obtain a more pure synaptosome preparation we could also use fluorescent activated cell sorting (FACS) for specific post-synaptic proteins to selectively enrich for synaptic membranes (H., A. et al. 2000).

We queried the list of RNA granule mRNAs enriched in dendritic spines and our list of neuron derived mRNAs and selected drebrin because it is a neuron specific actin binding protein whose role in regulating dendritic spines is well established (Ivanov, Esclapez et al. 2009). We identified an upregulation of drebrin protein levels in the synaptic fraction of glioma brain tissue which shows that one of the actin binding mRNAs is being translated and upregulated at the protein level. Overexpression of drebrin in rat neurons was shown to induce long protrusions along dendrites, similar to filopodia shaped protrusions which is indicative of immature spines (Mizui, Takahashi et al. 2005, Ivanov, Esclapez et al. 2009). Drebrin expression has also been shown to regulate synaptic transmission which may contribute to neuronal hyperexcitability in seizure models (Sbai, Khrestchatisky et al. 2012, Kreis, Hendricusdottir et al. 2013). These studies demonstrate that overexpression of drebrin induces alterations in dendritic morphology and neuronal excitability which suggest that the upregulation in drebrin expression in our glioma model may contribute to immature spine formation and neuronal hyperexcitability. Future experiments that assess neuronal excitability by electrophysiological recordings could address our hypothesis, experiments that assess dendritic spine morphology to identify immature and mature spines would also be able to assess dendritic spine alterations in our glioma model.

We discovered a decrease in the number of dendritic spines per length of dendritic segment in Camk2a+ neurons which suggests that there is a decrease in excitatory synapses that could result in impaired synaptic function in glioma brain tissue. We found one study that identified decreased dendritic spine density in human glioma (Špaček and Hartmann 1983) while a more recent study identified alterations in dendritic morphology and disrupted cortical structure in the peritumoral region in human astrocytomas (Goel, Wharton et al. 2003). Decreased dendritic spine density has been observed in other neurological disorders including epilepsy and focal

cortical dysplasia which are associated with impaired synaptic function (Lin and Webb 2009, Herms and Dorostkar 2016). The alterations in dendritic spine density seen in our glioma model suggest that there is impaired synaptic function which we suggest may contribute to the cognitive deficits observed in glioma.

We propose that the decrease in dendritic spines and translation of synaptic mRNAs results in a compensatory mechanism that increases the translation of actin binding mRNAs as an attempt to compensate for the loss of synaptic function. This type of compensatory mechanism could explain a form of reactive plasticity that occurs during low grade glioma growth. Reactive plasticity is thought of as the reorganization of synapses in response to injury or pathology as a way to preserve neuronal function (Nudo 2013, Kong, Gibb et al. 2016). During low grade glioma growth glioma cells diffusely invade a large amount of surrounding brain tissue before any neurological impairment can be detected. It has been suggested that the slow growing nature of low grade gliomas enables reactive plasticity to occur. Reactive plasticity occurs more often in low grade gliomas which are slow growing tumors rather than in high grade gliomas which grow faster, the high degree of reactive plasticity in low grade glioma is attributed to the longer time frame (years) available for the reorganization of neural circuits (Desmurget, Bonnetblanc et al. 2007). The high degree of reactive plasticity in low grade glioma has also been show in contrast to reactive plasticity in acute brain injuries such as stroke which have a rapid onset (minutes) and frequently result in detrimental neurological impairment (Desmurget, Bonnetblanc et al. 2007, Kong, Gibb et al. 2016). The mechanisms underlying reactive plasticity after brain injury are currently being investigated (Nudo 2013) and motivate future research to identify the molecular mechanisms underlying reactive plasticity in glioma.

The work described in Chapter 2 of this thesis shows the development of the Camk2a-Ribotag mouse glioma model and how we used TRAP methodology to identify translational alterations from neurons in glioma infiltrated cortex. The neuronal alterations we identified point to impaired synaptic function which motivates future studies to assess the consequences of these alterations on neuronal synapses in glioma. Ultimately the evaluation of this and future studies that focus on characterizing neuronal alterations in the brain tumor microenvironment will hopefully contribute to a better understanding of the neurological symptoms associated with glioma.
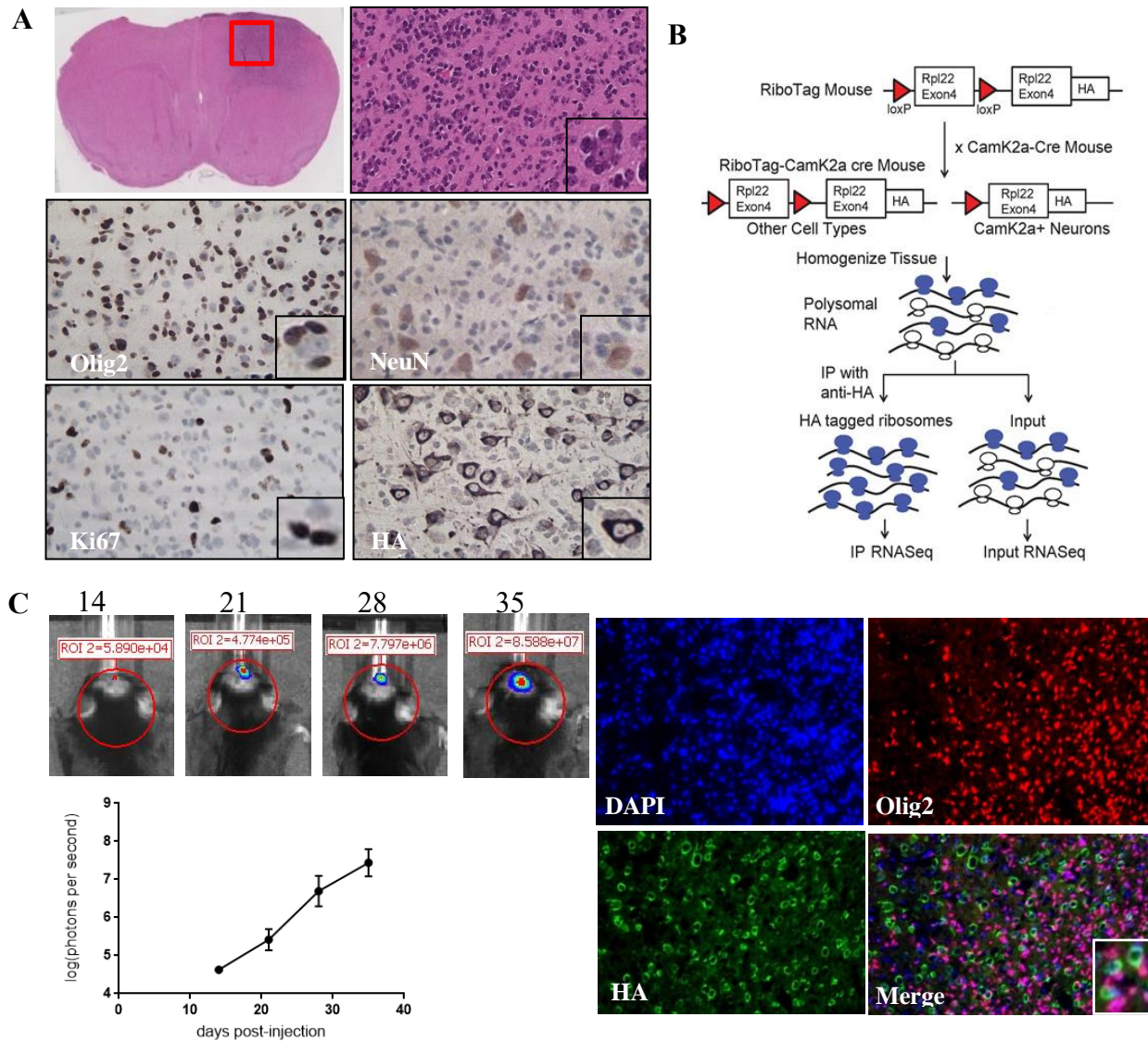
Figure 2.1: Diffusely infiltrating Camk2a-Ribotag mouse glioma model. A, Stereotactic injection of PDGFA/p53 deleted/mCherry-luciferase expressing cells in subcortical white mater of Camk2a-Ribotag mice result in diffusely infiltrating glioma with features of human glioma such as perineuronal satellitosis. B, In the Ribotag system the Ribotag mouse is crossed to a Camk2a-Cre mouse resulting in Camk2a-Ribotag mice in which Camk2a+ neurons express the HA-tag. Immunofluorescence shows neurons (HA+) and tumor cells (olig2+) intermingled in mouse tumor cortex. C, Bioluminescent images show the presence of a tumor at 14 days post glioma cell injection (dpi) and continued growth over time, quantification graph is the average of 3 mice per time point.
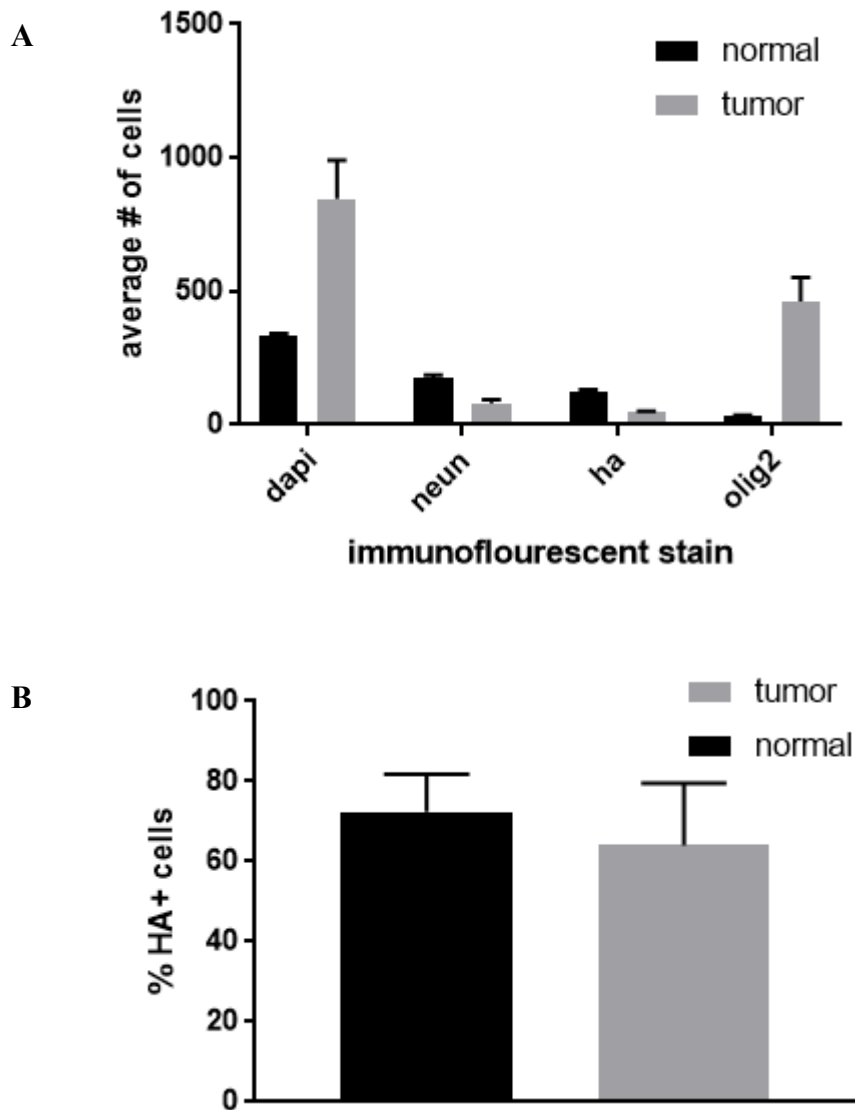
Figure 2.2. Immunofluorescent stain quantification from normal and Camk2a-Ribotag glioma infiltrated cortex. A) Average number of cells was determined from 3 adjacent fields per brain section for 3 normal brains and 3 tumor brains. Error bars show standard error. Dapi p=0.0235, NeuN p=0.0043, HA p=0.0002, Olig2 p=0.0091. B) Percent of HA+ cells relative to NeuN+ cells in normal and tumor brain. Average percentages were calculated from 3 adjacent fields per brain section p=0.4664.
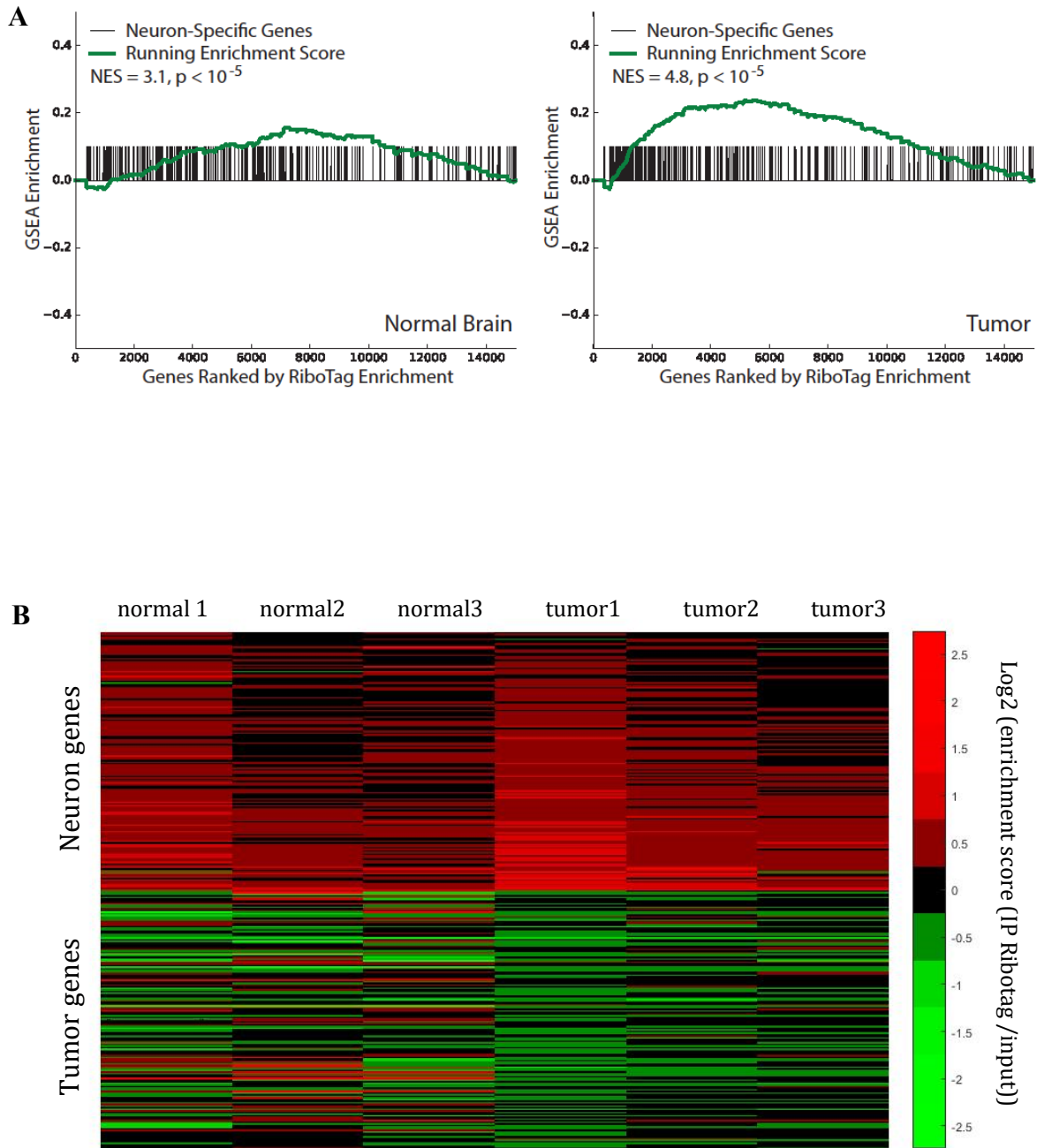
Figure 2.3: Enrichment of neuronal genes in Camk2a-Ribotag tumor IP. A, GSEA enrichment of neuronal genes in normal and tumor brain IP. B, Heatmap of highly enriched neuronal genes and tumor genes in normal and tumor brain IP.

A	GO term	# of genes from our list annotated with the term	Fold enrichment	p-value
	Actin binding GO: 0003779	20	4.32	2.1E-7
	Cytoskeleton GO: 0005856	26	1.72	9.1E-3
	Calcium ion binding GO: 0005509	16	1.67	5.6E-2

B	GO term	# of genes from our list annotated with the term	Fold enrichment	p-value
	Synapse GO:0045202	75	3.49	7.1E-17
	Postsynaptic membrane GO:0045211	83	2.94	8.3E-8
	Protein transport GO: 0015031	58	1.95	1.9E-6
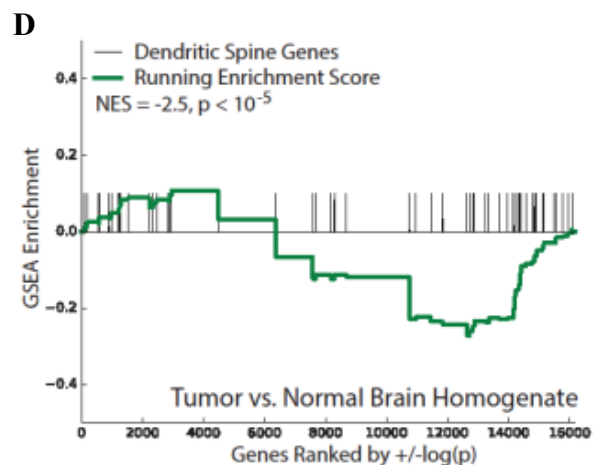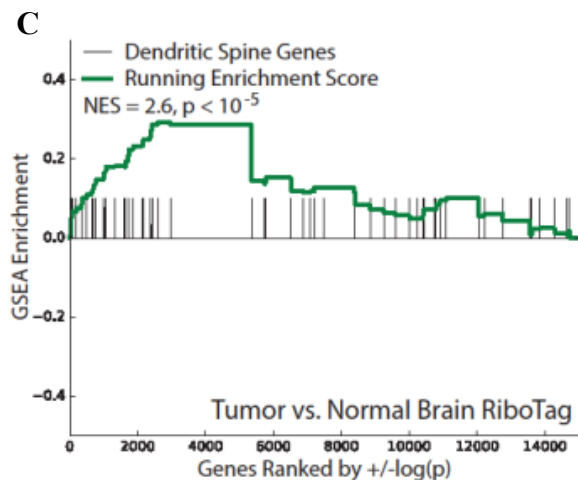
Figure 2.4: Camk2a+ neurons from glioma infiltrated cortex have alterations in synaptic and dendritic spine genes. A, Gene ontology terms for genes upregulated in tumor IP B) Gene ontology terms for downregulated genes in tumor IP. C) GSEA enrichment for dendritic spine genes in tumor vs. normal brain IP (Ribotag). D) GSEA enrichment for dendritic spine genes in tumor vs. normal brain homogenate.

gene	ES (tumor IP/tumor input)	Log2 fold change (tumor IP vs normal IP)	p-value
MYH10	4.04	1.12	1.43E-04
LIMCH1	3.97	1.52	5.48E-15
MYH9	3.72	2.70	5.30E-147
SPTBN1	3.26	0.93	3.48E-04
DBN1	3.25	0.89	NA
DST	2.99	1.30	8.71E-37
MYH14	2.74	1.59	5.16E-33
SPTAN1	2.53	1.03	4.29E-05
MYO5A	2.46	0.99	3.04E-09
SYNE2	2.44	1.71	1.35E-61
MPRIP	2.29	0.29	1.07E-03
TES	2.07	1.47	1.48E-08
MICAL1	1.98	3.01	2.34E-89
MYO6	1.84	0.60	4.46E-04
SVIL	1.58	2.83	2.50E-131
GSN	1.52	1.32	4.29E-24

Table 1. Actin binding genes enriched in dendritic spines and upregulated in Camk2a+ neurons from glioma infiltrated cortex. Table shows actin binding genes enriched in RNA granules and important for dendritic spine dynamics, ES was obtained from the ratio of normalized counts in tumor IP/normal brain IP., log2 fold change and p-value were obtained from differential gene expression analysis by DESeq.
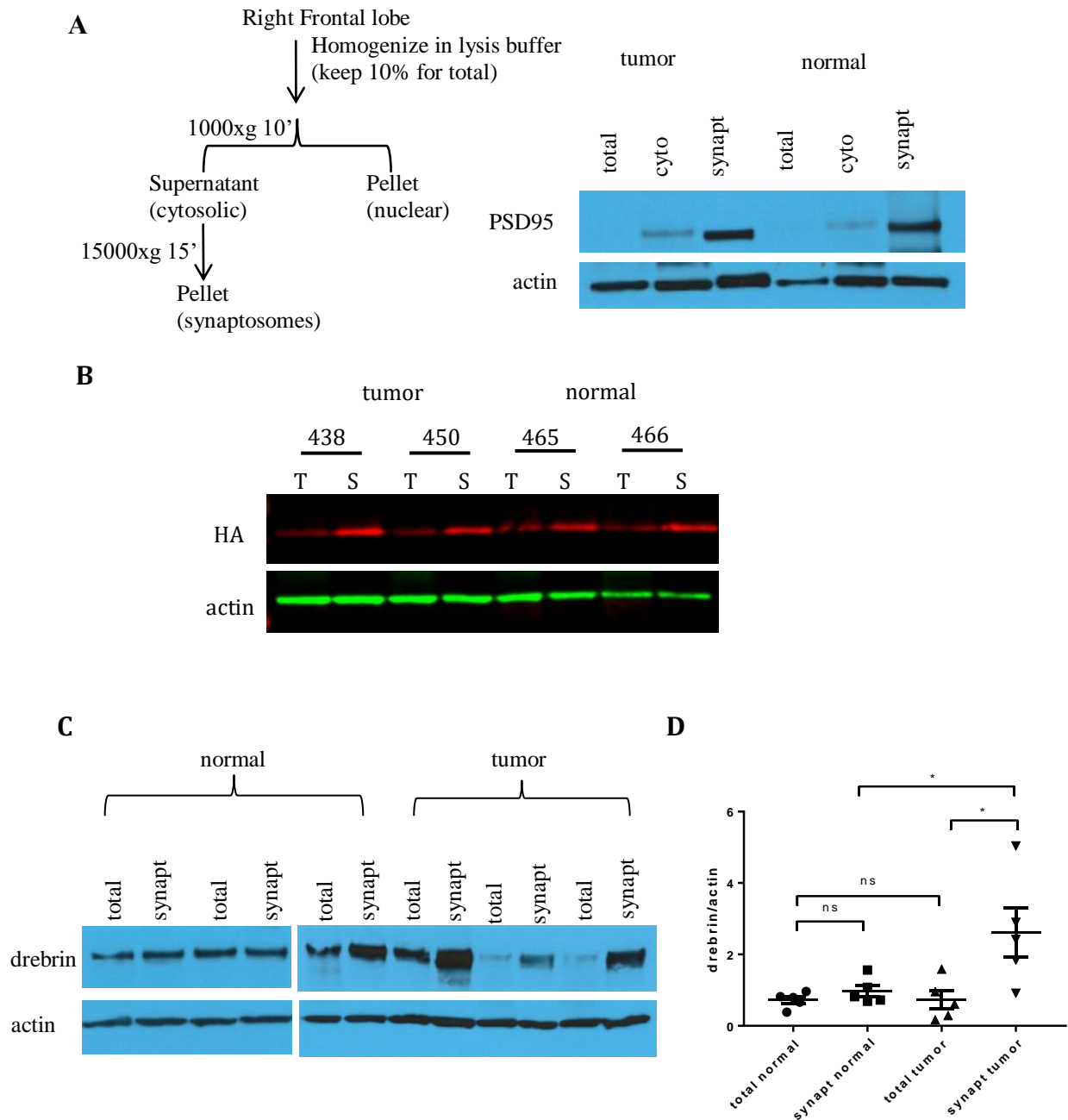
Figure 2.5: Dendritic spine gene drebrin has increased levels in Camk2a+ neurons. A, Total, cytosolic, and synaptic fractions were isolated from right frontal lobe in normal and tumor brains of 16 week old mice, PSD95 is a post-synaptic marker, actin was used as a loading control. B, HA expression of tumor and normal brain total (T) and synaptosome (S) fractions, 2 normal and 2 tumor brains were used. C, Drebrin expression in total and synaptic fractions in normal and tumor brains. D, Quantification of drebrin expression from 5 different normal brains and 5 different tumor brains. Drebrin signal intensity was normalized to actin. One way ANOVA p=0.0070, *p<0.05 Tukey's multiple comparison test.
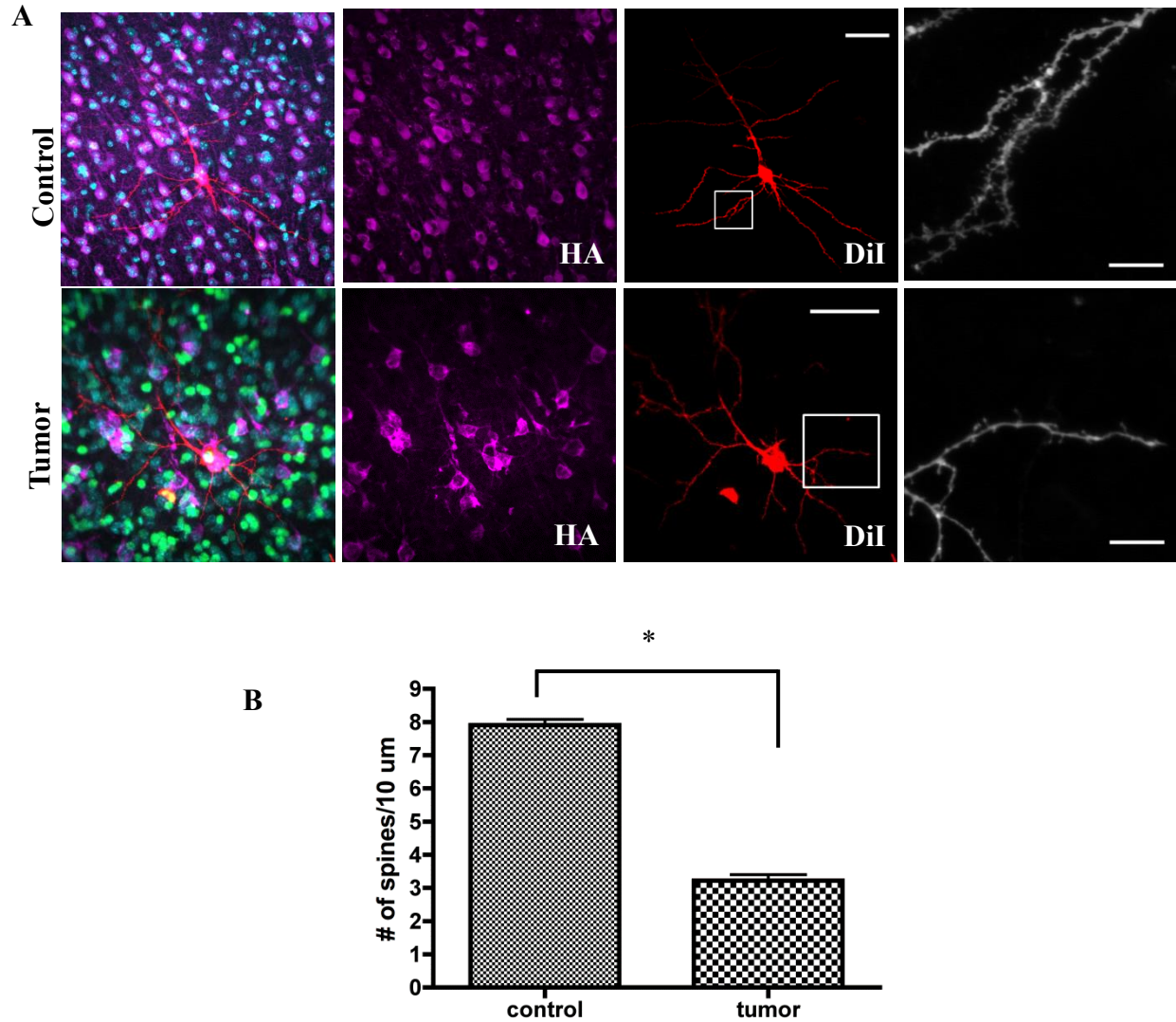
Figure 2.6: Decrease in dendritic spine number in Camk2a+ neurons in glioma infiltrated cortex. A, Camk2a+ neurons in glioma infiltrated cortex are identified by HA staining (magenta) from control (top) and tumor (bottom) Camk2a-Ribotag tumors.. DAPI (blue), Olig2 (green), DiI (red) and HA (magenta), (Bars,50 μm). The images at the right are magnifications of the insets which show the number of dendritic spines (Bars, 10 μm). B, quantitation of the number of dendritic spines per 10 μm of dendrite length in Camk2a+ neurons. *P<0.0001

CHAPTER 3

mTOR inhibition with AZD induces transcriptional and translational alterations in the Camk2a-Ribotag mouse glioma model

3.1 Introduction

mTOR signaling has the ability to regulate cell survival, growth, and proliferation in many cell types (Laplante and Sabatini 2009). In addition, mTOR regulates neuron specific functions such as neuronal excitability and synaptic plasticity (Bockaert and Marin 2015). mTOR regulates these processes in response to growth factors, amino acids, neurotransmitters, and neural activity (Takei and Nawa 2014). mTOR has been shown to regulate translation initiation through 4EBP and cell growth and size through S6K. mTOR activation results in the phosphorylation S6K1 and 4EBP1 (Guertin and Sabatini 2009), the former has been associated with synaptic plasticity (Bockaert and Marin 2015).

Alterations in mTOR signaling have been implicated in many neurological diseases (Hoeffer and Klann 2010, Wong 2013). Dysregulation of the mTOR pathway generally results in the upregulation of mTOR activity that is seen tuberous sclerosis complex disease (TSC), focal cortical dysplasia, and epilepsy (Lipton and Sahin 2014, Citraro, Leo et al. 2016). Upregulated mTOR activity results in enlarged neurons and abnormal cortical organization which is thought to contribute to the pathology of some neurological diseases. Several mouse studies have shown that seizures resulting from dysregulated mTOR activity can be prevented and inhibited with the mTOR inhibitor rapamycin, suggesting the potential use of mTOR inhibitors for seizures in other

neurological disorders (Meikle, Talos et al. 2007, Zeng, Xu et al. 2008) (Huang, Zhang et al. 2010, Guo, Zeng et al. 2013). Due to the neurological symptoms associated with glioma and the dysregulation of mTOR that contributes to neurological disease, we hypothesize that mTOR signaling is involved in regulating neuronal alterations in glioma infiltrated cortex in our Camk2a-Ribotag mouse glioma model.

To identify neuron specific ribosome bound transcripts from our Camk2a-Ribotag mouse glioma model we used translating ribosome affinity purification (TRAP) which has been previously described (Doyle, Dougherty et al. 2008, Heiman, Schaefer et al. 2008). Applying TRAP methods we immunoprecipitated HA-tagged ribosomes from tumor brain tissue, isolate the associated mRNAs and identify them by RNA sequencing. All translated mRNAs are at one point associated with ribosomes, which allows us to use the TRAP approach to determine which transcripts are being translated (Kapeli and Yeo 2012). Using this approach we identified alterations in the translation of ribosome bound mRNAs in response to mTOR inhibition with the ATP competitive mTOR inhibitor AZD8055 (AZD). Additionally, we extracted mRNAs from homogenate brain tumor tissue, which includes ribosome bound and non-ribosome bound mRNAs, and refer to any alterations identified from this analysis as transcriptional alterations.

In this chapter I describe how treating Camk2a-Ribotag glioma mice with AZD for 6 hours can reverse some of the transcriptional alterations in cell type specific mRNAs including those for glioma cells and neurons. We also show that mTOR inhibition reversed the neuron specific translational alterations after a 6 hour treatment with AZD. AZD treatment resulted in the upregulation of many neuron specific mRNAs including genes associated with synapses. We also determined that AZD treatment downregulated the translation of actin binding genes

enriched in dendritic spines. Overall, these data suggest that mTOR can regulate several of the transcriptional and translational alterations of many cell type specific genes in our glioma model.

3.2 Results

AZD8055 inhibits mTOR signaling in normal mouse brain tissue

The effects of delivering AZD in vivo have been shown to be safe and effective in a different mouse glioma model (Chresta, Davies et al. 2010). We decided to characterize the effects of AZD in vivo to validate these findings. We treated non-tumor bearing mice with AZD (20mg/kg) and sacrificed mice 1 and 8 hours after a single treatment. We also delivered a second dose of AZD (20mg/kg) after 24 hours in one mouse and sacrificed 1 hour after the second dose (25 hours, figure 3.1a). mTOR activation results in the phosphorylation S6K1 and 4EBP1. Activated S6K1 phosphorylates ribosomal protein S6 (pS6) which can regulate the translation of TOP mRNAs (Guertin and Sabatini 2009). 4EBP inhibits translation, upon mTOR activation 4EBP is phosphorylated (p4EBP1) and the inhibitory effect of 4EBP1on translation is reduced. Non-phosphorylated 4EBP is often increased as translation in inhibited via mTOR inhibition (Moschetta, Reale et al. 2014). We observed a marked decrease in pS6 and p4EBP expression after 1 hour AZD treatment (figure 3.1a). There also appears to be an increase in non-phosphorylated 4EBP after 1 hour treatment, suggesting that there is inhibition of translation (figure 3.1a). The effects of AZD on pS6 appear to be transient, since after 8 hours of AZD treatment pS6 levels returned to basal non-treated levels (figure 3.1a). A second dose of AZD 24 hours after the first dose inhibited pS6 levels as was seen 1 hour after the first dose suggesting that AZD has transient effects on pS6 and p4EBP expression (figure 3.1a). The transient effects of AZD on mTOR targets can be attributed to the short half-life of AZD (few hours), despite the

kinetics of AZD continued doses have shown to have long term effects on mTOR regulated processes (Chresta, Davies et al. 2010, Naing, Aghajanian et al. 2012, Rosborough, Raïch-Regué et al. 2014). To test if the transient effects of AZD are dose dependent we performed a dose-response study in vivo.

We treated non-tumor bearing mice with AZD and sacrificed mice 1, 2, 4, 6, 8, 16, 24 hours after AZD treatment. We used 20mg/kg AZD and 100mg/kg AZD to see if the effects of mTOR inhibition were dose dependent. We observed a marked decrease in pS6 levels after 1 hour of AZD (20mg/kg) treatment and a subsequent increase in pS6 expression back to control levels after 2 hours of treatment (figure 3.1b). Using a higher dose of AZD (100mg/kg) we saw a sustained decrease in pS6 levels up to 6 hours after treatment (figure 3.1b). These results suggest that the effects of AZD are prolonged (up to 6 hours) with a higher dose in vivo. We did not observe any side effects as a result of oral gavage administration of 20mg/kg or 100mg/kg AZD within 24 hours of treatment. Based on these findings we chose to use 6 hours of 100 mg/kg for our experiments in vivo.

AZD8055 alters the transcription of some cell type specific genes in our Camk2a-Ribotag mouse glioma model

We assessed mTOR activity in our Camk2a-Ribotag mouse glioma model and observed pS6 expression throughout glioma infiltrated cortex (figure 3.2). Although we did not quantify or perform double staining to determine cell type specificity of mTOR activity, we show that there is mTOR activation in neurons (determined by morphology) in glioma infiltrated cortex (figure 3.2). We treated mice with 100 mg/kg AZD and sacrificed them 6 hours after treatment. Our immunohistochemistry results show that mTOR activity is decreased after 6 hour AZD

treatment throughout glioma infiltrated cortex and appears to be decreased in neurons in both the ipsilateral and contralateral cortex (figure 3.2).

To determine the effects of mTOR inhibition with AZD treatment we performed RNA sequencing on treated and non-treated tumor brains. We obtained differential gene expression analysis in homogenate tumor vs normal brain. Homogenate brain lysate contains ribosome bound and non-ribosome bound mRNAs (figure 3.4a) which means that by assessing homogenate tissue mRNA levels from we can only determine the total abundance of transcripts, not whether they are being translated, and thus the alterations identified from homogenate brain tissue are referred to as transcriptional. Differential gene expression analysis identified 6054 differentially expressed genes in tumor brains (p-value <0.05). Highly upregulated genes in the tumor (log2foldchange>0) have been shown to be expressed in many glioma cells from retrovirally induced glioma models (Assanah, Lochhead et al. 2006). These genes are likely among the most upregulated genes because glioma cells compose the majority of cells in brain tumor tissue, thus marked transcriptional alterations in these cells will conceal alterations in minor cell populations in brain tumor tissue, an issue we address in chapter 2 of this thesis. We plotted differential gene expression output measures (adjusted p-value and log2foldchange) and show that Ki67, Olig2 and PDGFRa are among the most highly differentially expressed genes in our glioma model (figure 3.3a) which shows that there is an increase in the transcription of glioma cell mRNAs in brain tumor homogenate.

We performed RNA sequencing of treated tumor homogenate treated with AZD for 6 hours. We performed differential gene expression analysis between treated tumor and untreated tumor homogenate. We plotted differential gene expression output measures (adjusted p-value and log2foldchange) and show that Olig2 and PDGFRa are downregulated after mTOR

inhibition with AZD (figure 3.3b) which shows there is a decrease in the transcription of glioma cell mRNAs in brain tumor homogenate. We used Panther to determine the GOs that differentially expressed genes are associated with. We identified 1601 differentially expressed genes (p-value<0.05) that were upregulated after mTOR inhibition (log2 fold change>0), these genes were associated with ion transport GO terms (figure 3.4b). These genes included several excitatory ion channel genes which show that mTOR inhibition in our glioma model results in an upregulation of the transcription of excitatory ion channel mRNAs.

There were 1573 differentially expressed genes (p-value<0.05) that were downregulated after mTOR inhibition with AZD (log2 fold change<0) and associated with transcription and DNA replication GO terms (figure 3.4c). mTOR has been shown to regulate several genes associated with transcription which suggests that mTOR inhibition will result in alterations of transcriptional regulation (Mayer and Grummt 2006). Our results that mTOR inhibition induces a decrease in mRNAs associated with transcriptional activity which suggests that mTOR regulates transcription in our glioma model.

The fact that mTOR inhibition with AZD transcriptionally downregulated tumor cell mRNAs suggested that mTOR inhibition affects mRNAs specific to other brain cell types. This finding motivated us to assess the transcription of cell type specific mRNAs from neurons and OPCs since glioma cells in our tumor model are mainly OPCs. To do this we used published mRNA cell type specific expression profiles (Zhang, Chen et al. 2014). We queried the top 500 cell type specific genes for neurons and OPCs and compared each list to our list of significantly upregulated and downregulated genes after AZD treatment and show a heatmap of normalized counts in normal, tumor and AZD treated tumor brains (figure 3.5). From the top 500 neuron specific genes we identified 70 genes were upregulated after AZD and 11 were downregulated

after AZD. From the top 500 OPC specific genes we identified 11 genes were upregulated after AZD and 144 were downregulated after AZD.

We show that mTOR inhibition with AZD reversed many of the transcriptional alterations in tumor tissue. Some of the neuron specific genes that were downregulated in tumor homogenate were upregulated after mTOR inhibition (figure 3.5). Our data also show that many OPC specific genes which are also expressed in glioma cells that were upregulated in tumor tissue were downregulated after mTOR inhibition. These results show the effects of mTOR inhibition on the transcription of some cell type specific mRNAs in homogenate glioma tissue, and suggest that mTOR inhibition with AZD treatment for 6 hours reverses many of the cell type specific transcriptional alterations induced by diffusely infiltrating glioma cells.

We can attribute many of the transcriptional alterations in non-treated tumor to the changes in cellular composition that have occurred at this late stage of tumor growth. The glioma tissue samples used for RNA sequencing were obtained from a late stage in tumor growth when there is a large diffusely infiltrating tumor present. As I describe in Chapter 2 of this thesis, cellular composition at this stage of tumor growth is altered, brain tissue is mainly composed of glioma cells and there are fewer neurons within this tissue. Based on these results we can attribute the transcriptional downregulation of many neuron specific mRNAs to the low density of neurons in homogenate tumor tissue, while the upregulation of OPC specific mRNAs is likely a result of a high density of glioma cells present in homogenate tumor tissue.

We believe that the marked effects of mTOR inhibition on cell type specific mRNAs is not due to changes in cellular composition, since mTOR inhibition only lasted for 6 hours. We hypothesize that the marked effects of mTOR inhibition on cell type specific mRNAs precede

the translational effects of mTOR inhibition in brain tissue. To assess the translational effects of mTOR inhibition in neurons, we used TRAP methods to identify neuron specific ribosome bound mRNAs in our glioma mouse model.

AZD8055 alters the translation of neuron specific mRNAs in our glioma mouse model

To identify the effects of mTOR inhibition with AZD we used TRAP to identify neuron specific ribosome bound mRNAs. We immunoprecipitated HA-tagged ribosome bound transcripts (IP) from tumor brains treated with AZD for 6 hours and performed RNA sequencing. We performed differential gene expression analysis (DESeq) on IP treated tumor vs IP tumor. We obtained the enrichment score (ES) from the ratio of treated tumor IP counts (determined from TRAP) over treated tumor homogenate counts (determined from RNA seq of homogenate) and refer to this as the treated ES. From our differential gene expression analysis we searched among significantly expressed genes (p value<0.05) and found 738 genes that were upregulated (log2fold change>0) and had an ES>1.5 (figure 3.6b). Gene ontology analysis revealed that these genes are associated with synaptic GO terms (figure 3.6b). Synaptic GO terms included genes such as Syt1, snap25 and synaptophysin. These genes are associated with synaptic vesicle exocytosis suggesting that mTOR inhibition with AZD treatment upregulated the translation of these mRNAs in our glioma model. These synaptic mRNAs were translationally decreased in tumor brains which suggest that a 6 hour treatment with AZD reverses the translational alterations observed in tumor brains.

We performed gene ontology analysis for genes that were downregulated after mTOR inhibition with AZD. From our differential gene expression analysis we searched among significantly expressed genes (p value<0.05) that were downregulated (log2fold change<0) and

had an ES>1.5 and identified 163 genes (figure 3.6c). We used the ES from tumor brains to determine genes enriched in neurons from tumor brains and downregulated by AZD treatment. Gene ontology analysis revealed that these genes are associated with actin binding GO terms (figure 3.6b). These GO terms include several actin binding genes enriched in dendritic spines such as mical1, drebrin, limch1. These results show that mTOR inhibition with AZD downregulated the translation of actin binding genes enriched in dendritic spines suggesting that mTOR can regulate the translation of these mRNAs. Several of the actin binding mRNAs were translationally upregulated in non-treated tumors (Chapter 2) which suggests that mTOR inhibition with AZD for 6 hours reversed these translational alterations.

To visualize the magnitude of the translational alterations induced by mTOR inhibition we queried genes that were significantly upregulated in AZD treated tumor IP ($p<0.05$, log2foldchange>0) and enriched in AZD treated tumor IP (ES>1.5) which resulted in a list of 738 genes (figure 3.7a). From the list of 738 genes, we generated a heatmap that shows the normalized counts from normal, tumor and AZD treated IP of upregulated genes in AZD treated tumor IP (figure 3.7b). Our data show that these genes were downregulated in tumor IP, interestingly several of these genes are synaptic proteins which suggests that mTOR inhibition reversed the translational alterations of synaptic proteins. Similarly we queried genes that were significantly downregulated in AZD treated tumor IP ($p<0.05$, log2foldchange>0) and enriched in tumor IP (ES>1.5) which resulted in a list of 163 genes (figure 3.7c). From the list of 163 genes, we generated a heatmap that shows the normalized counts from normal, tumor and AZD treated IP of downregulated genes in AZD treated tumor IP (figure 3.7d). Our data show that actin binding genes were upregulated in tumor IP, several of these genes included actin binding genes and conversely several neuron specific mRNAs that are translationally downregulated in

tumor brains are upregulated by AZD treatment (synaptic mRNAs). These results highlight how mTOR inhibition with AZD for 6 hours can reverse several of the neuron specific translational alterations in our glioma model.

3.3 Discussion

In this chapter we demonstrated that mTOR activity is detectable in brain tissue and can be inhibited by the mTOR inhibitor AZD. We show that mTOR inhibition with AZD for 6 hours results in transcriptional alterations in many cell type specific transcripts as determined by mRNA levels in homogenate AZD treated tumor tissue. We also show that mTOR inhibition with AZD results in translational alterations in several neuron specific transcripts as determined by TRAP profiling of neuron specific ribosome bound mRNAs. Our findings suggest that mTOR signaling regulates the translation of several neuron specific transcripts as evidenced by the reversal of these alterations after a 6 hour treatment with AZD and motivate future studies to assess the effects mTOR inhibition with AZD on synaptic function.

We showed that delivering AZD by oral gavage crosses the blood brain barrier and inhibits mTOR activity. mTOR inhibition with AZD occurred 1 hour after administration which shows that the effects of AZD occur shortly after drug administration. We also show that AZD transiently inhibits mTOR activity as demonstrated by pS6 returning to basal levels 8 hours after treatment. The transient effects of AZD have been reported, despite this, these studies have shown that daily AZD treatment induced robust effects on cell proliferation and tumor growth (Chresta, Davies et al. 2010, Rosborough, Raïch-Regué et al. 2014). These studies suggest that despite the short half-life of AZD, daily mTOR inhibition with AZD is able to induce changes in cell function. In our experiments, we used a 6 hour treatment with AZD to assess the immediate

effects of mTOR inhibition on transcriptional and translational alterations, however daily treatment with AZD might be required to observe changes in cell function in brain tissue.

We show that mTOR activity is detectable in glioma infiltrated cortex and point out the expression of pS6 in neurons. We show that a 6 hour treatment with AZD inhibits mTOR activity in glioma infiltrated cortex and that neurons are particularly sensitive to mTOR inhibition. We assessed the effects of mTOR inhibition with AZD on the transcription of mRNAs from homogenate tumor tissue. These results showed that AZD reversed several of the cell type specific transcriptional alterations induced by diffusely infiltrating glioma cells, such as the downregulation of glioma cell genes PDGFRa and Olig2 after AZD treatment. Using published gene cell type specific expression profile data we show that several neuron specific mRNAs that were downregulated in homogenate tumor tissue were upregulated after AZD treatment. The reversal of these transcriptional alterations after only 6 hours of mTOR inhibition with AZD suggest that these effects are mediated by mTOR inhibition rather than by changes in cellular composition.

To identify the effects of mTOR inhibition with AZD on the translation of neuron specific ribosome bound mRNAs we used TRAP methods to isolate neuron specific transcripts. mTOR inhibition with AZD induced an upregulation in the translation of neuron specific mRNAs that were associated with synaptic genes including Snap25, synaptophysin and Syt1. These synaptic genes were translationally downregulated in tumor brains, which suggests that their upregulation after AZD treatment is an attempt to restore synaptic function. mTOR inhibition with AZD also induced a downregulation in the translation of neuron specific mRNAs that were associated with actin binding genes enriched in dendritic spines. These genes included mical1, drebrin, and limch1 among others. Several of the translationally downregulated actin

binding genes after AZD treatment were among those that were translationally upregulated in tumor brains. These results show that AZD reversed the translational alterations identified in tumor brains and suggest that the translation of actin binding genes enriched in dendritic spines is regulated by mTOR signaling in our glioma model. mTOR signaling has been associated with regulating dendritic spine morphology and synaptic plasticity (Hoeffer and Klann 2010). Increased mTOR activation resulted in increased dendritic spine density in a mouse model of autism (Tang, Gudsnuk et al. 2014) while mTOR inhibition resulted in decreased dendrite branching and arborization (Jaworski, Spangler et al. 2005). Future experiments that assess the effects of mTOR inhibition with AZD on dendritic spine dynamics would be informative to understand how mTOR inhibition affects dendritic spine alterations in our glioma model.

The work described in this chapter shows that mTOR inhibition with a 6 hour AZD treatment is achieved in normal and tumor brains. We show that AZD induced alterations in the transcription of several cell type specific mRNAs found in homogenate lysate. Lastly, we demonstrate that AZD induced alterations in the translation of several neuron specific ribosome bound mRNAs including the upregulation of synaptic genes and downregulation of dendritic spine genes. These findings suggest that mTOR inhibitors can reverse neuronal alterations at the level of translation which might contribute to prevent some of the neuronal alterations associated with neurological impairment seen in glioma.
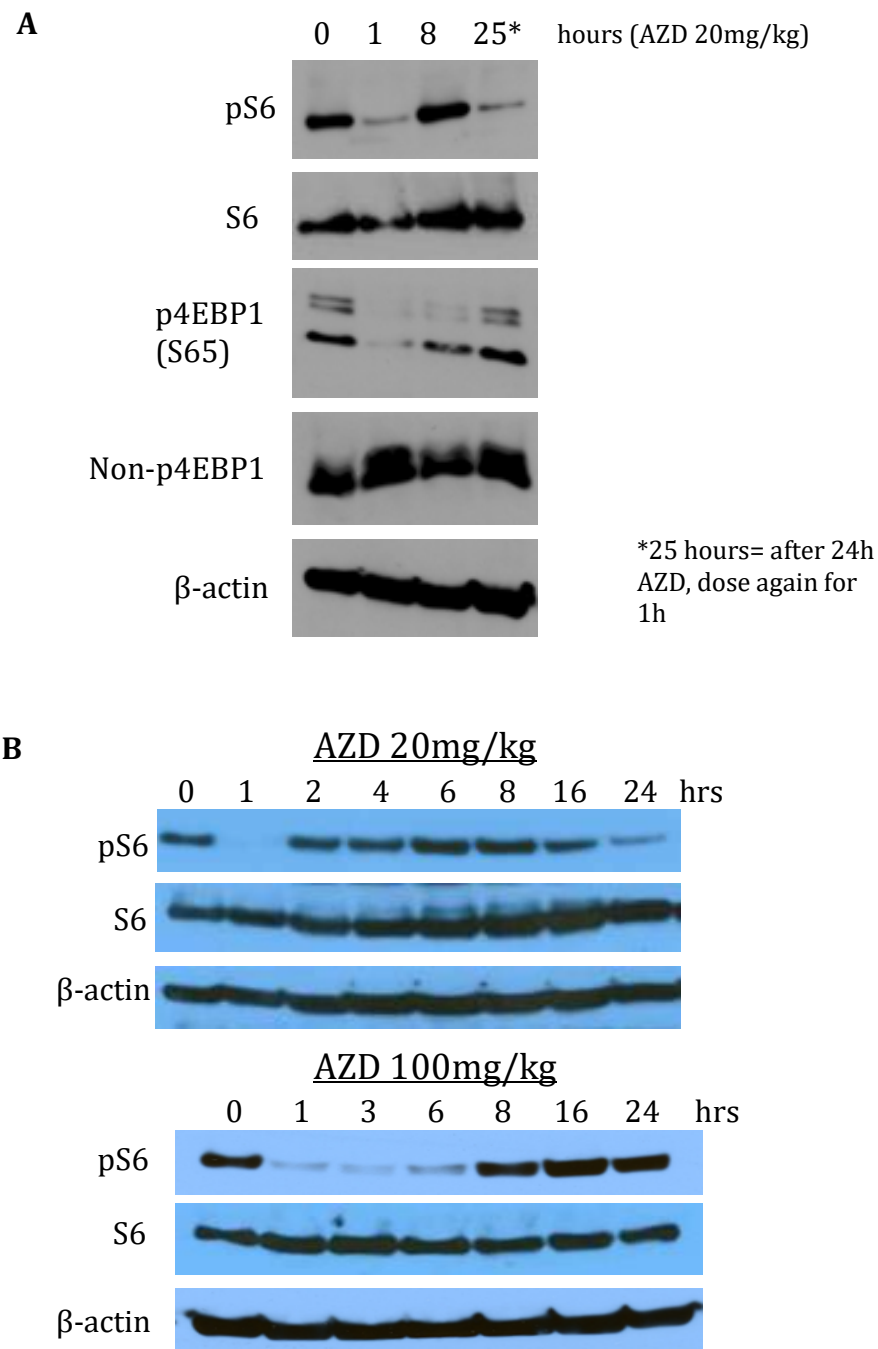
Figure 3.1: mTOR activity in response to AZD in normal mouse brains. A, normal mice were treated with AZD (20mg/kg by oral gavage) once and sacrificed 1 and 8 hours after treatment for western blot analysis of the right frontal brain lobe. The mouse treated with AZD for 25 hours was treated twice (once at time 0 and 1 hour before sacrificing). B, normal mice were treated with 20 mg/kg and 100 mg/kg AZD for the time specified. Brain tissue from 0 hours was collected from untreated mice.

pS6 staining

Vehicle

AZD

Ipsilateral
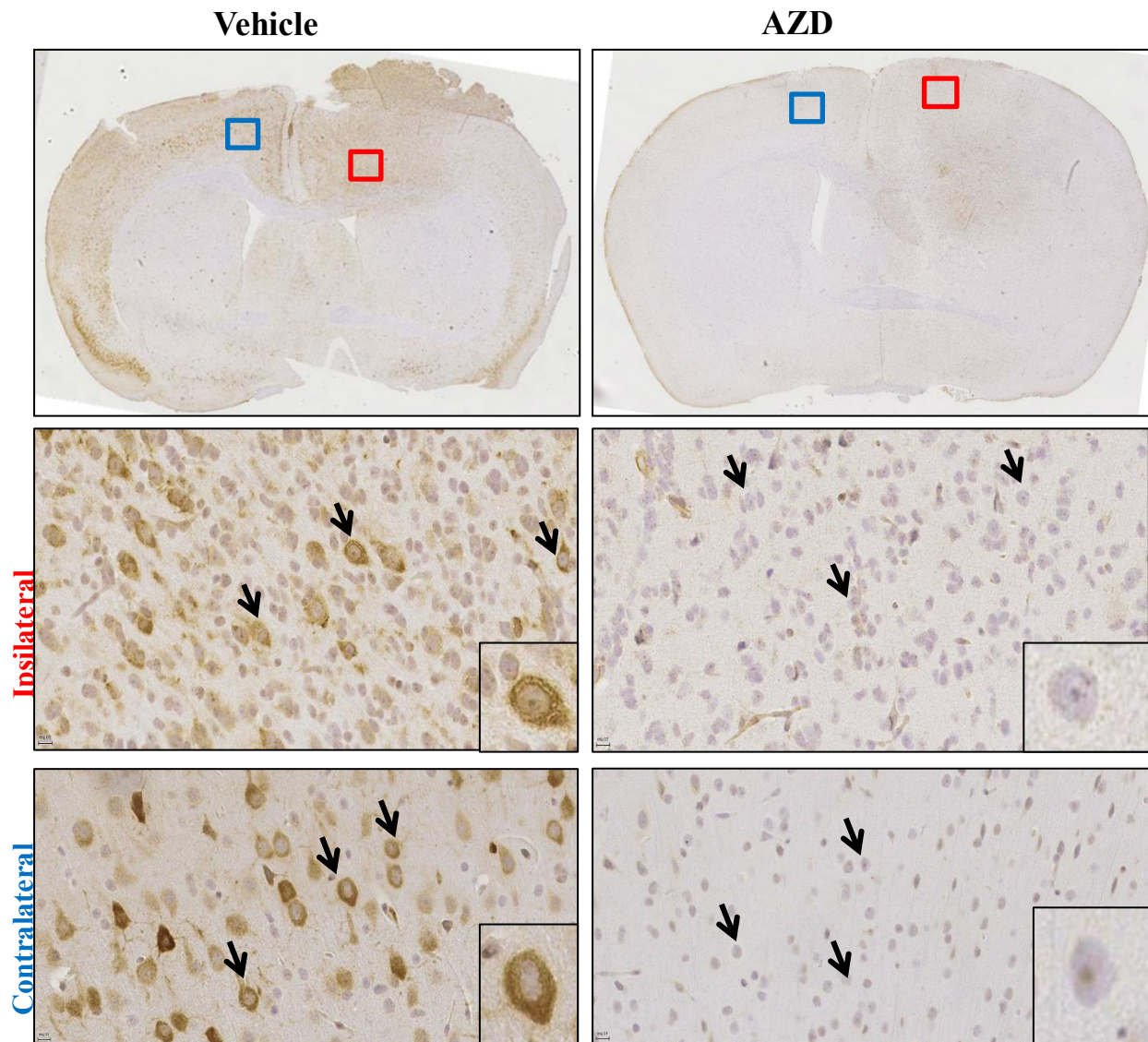
Contralateral

Figure 3.2: pS6 immunostaining in vehicle and AZD treated glioma mouse brain. Top row shows a 4x image of vehicle and AZD treated brain sections (AZD 100 mg/kg). Red square show ipsilateral tumor cortex, blue square show contralateral cortex. Second rows show 40x image of ipsilateral glioma infiltrated cortex, black arrows point to what is morphologically characterized as a neuron, bottom right corner shows one neuron as an example. Third row shows a 40x image of contralateral non-infiltrated cortex, black arrows point to neurons in non-infiltrated cortex. mTOR inhibition with AZD shoes decreased mTOR activity in neurons from both ipsilateral and contralateral cortex, black arrows point to what is morphologically characterized as a neuron.

A RNAseq of homogenate

B RNAseq of AZD treated tumor homogenate
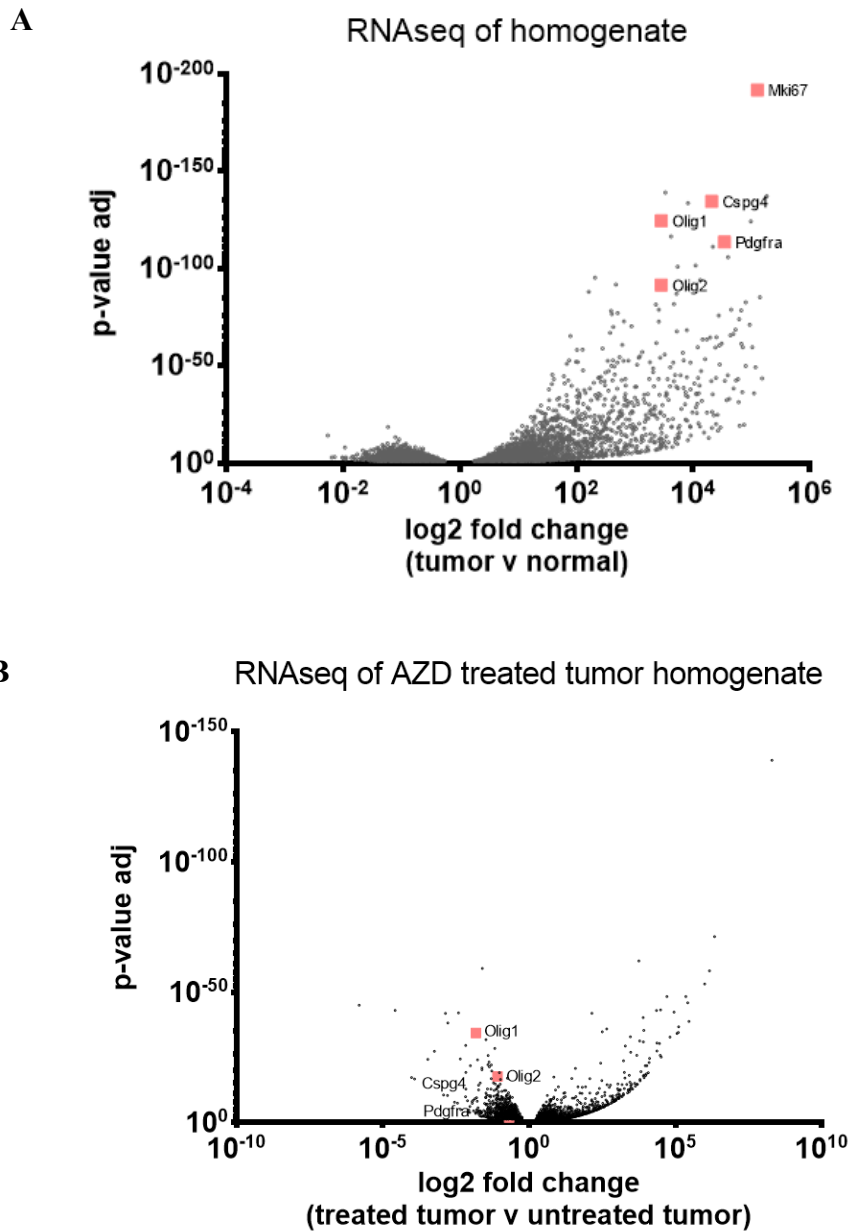
Figure 3.3: mTOR inhibition with AZD targets glioma cell genes in our glioma mouse model. A, Plot of all differentially upregulated (log2 fold change>0) and downregulated (log2 fold change<0) genes in tumor homogenate RNA sequencing data compared to normal brain. Genes labeled in pink include those expressed in OPCs (Olig1, Olig2, PDGFRa, Cspg4) and a proliferation marker (Ki67), among the most significantly expressed genes. B, Plot of differentially upregulated and downregulated genes in tumor homogenate treated with AZD for 6 hours @100 mg/kg.

65

A

Homogenate

Homogenate RNASeq

B
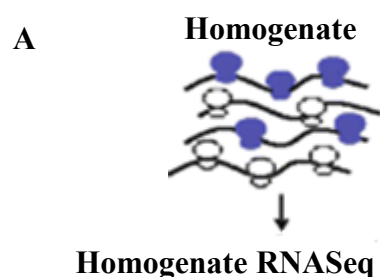
GO term	# of genes from our list annotated with the term	Fold enrichment	p-value
Transport GO: 0006810	158	1.49	2.2E-7
Ion transport GO:0006811	62	1.82	6.3E-6
Mitochondrial outer membrane GO:0005741	19	2.12	3.8E-3

C

GO term	# of genes from our list annotated with the term	Fold enrichment	p-value
Transcription, DNA templated GO:0006351	224	1.62	7.2E-14
DNA binding GO:0003677	217	1.62	
Regulation of transcription, DNA-templated GO: 0006355	254	1.52	1.5E-12

Figure 3.4: Gene ontologies for homogenate mRNAs affected by mTOR inhibition with AZD in our glioma mouse model. A, Homogenate mRNAs include those with HA tagged (blue) ribosomes, non HA-tagged ribosomes (white). B, Gene ontology terms of significantly (p<0.05) upregulated genes (1601 genes) in tumor homogenate from AZD treated brains . Upregulated genes were determined as having a log2 fold change (FC) greater than 0. C, Gene ontology terms of significantly (p<0.05) downregulated genes (1573 genes) in tumor homogenate from AZD treated brains. Downregulated genes had a FC less than 0. FC and p-values were obtained from differential gene expression analysis with DESeq2. Gene ontology terms for the most enriched gene clusters are shown, these were identified using DAVID gene ontology analysis.
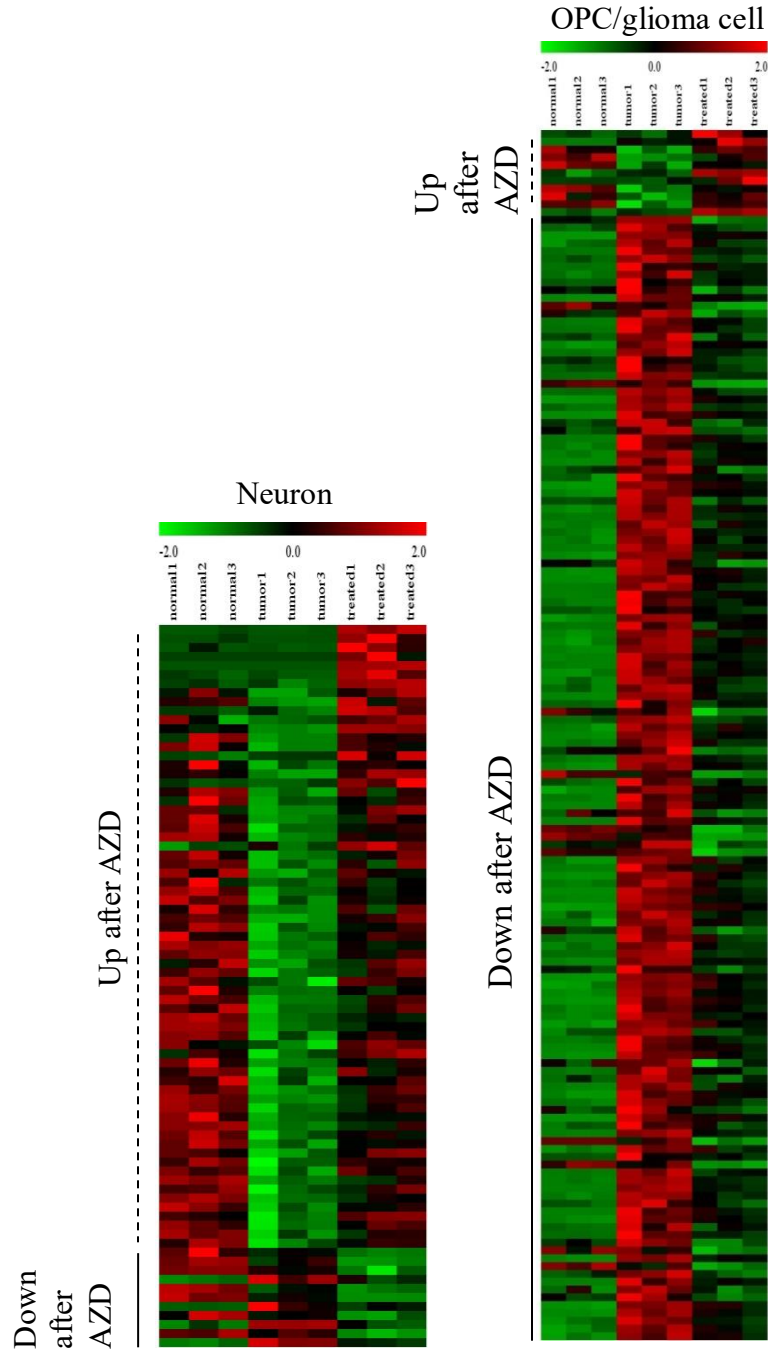
Figure 3.5: Neuron and OPC specific genes from homogenate affected by mTOR inhibition with AZD in our glioma mouse model. Heatmaps of normalized counts for cell type specific genes (obtained from Zhang et al 2014) for neuron and OPC specific genes. The first 3 columns are normalized counts for normal brain, the next 3 are tumor brain, and the last 3 are AZD treated tumor brains. Top 500 genes from Zhang et al 2014 were queried for significantly expressed genes in AZD treated tumor homogenate. Up after AZD refers to significantly upregulated genes (dashed line), and Down after AZD refers to significantly downregulated genes (solid line). Up regulation was determined by a positive log2 fold change and downregulation was determined by a negative log2 fold change from differential gene expression analysis.
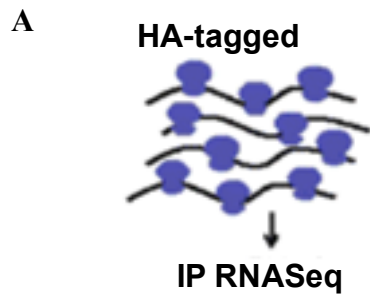
HA-tagged

IP RNASeq

B

GO term	# of genes from our list annotated with the term	Fold enrichment	p-value
Synapse GO:0045202	47	2.87	2.9E-10
Cell junction GO:0030054	49	2.10	1.8E-6
Postsynaptic membrane GO: 0045211	18	2.5	9.5E-4

C

GO term	# of genes from our list annotated with the term	Fold enrichment	p-value
Actin binding GO: 0003779	19	7.21	1.3-10
Actin cytoskeleton GO:0015629	10	6.61	2.1E-5
Cytoskeleton GO: 0005856	20	2.39	6.5E-4

Figure 3.6: Gene ontologies for Camk2a+ HA-tagged mRNAs affected by mTOR inhibition with AZD in our glioma mouse model. A, HA-tagged ribosomes and their associated mRNAs. B, Gene ontology terms of significantly (p<0.05) upregulated and enriched (ES>1.5) genes in tumor IP from AZD treated brains (738 genes). Upregulated genes were determined as having a log2 fold change (FC) greater than 0. C, Gene ontology terms of significantly (p<0.05) downregulated and enriched (ES>1.5) genes in tumor IP from AZD treated brains (163 genes). Downregulated genes had a FC less than 0. FC and p-values were obtained from differential gene expression analysis with DESeq2. ES from treated tumor brains was used to identify enriched genes that were upregulated, ES for non-treated tumor brains was used to identify enriched genes that were downregulated. Gene ontology terms for the most enriched gene cluster are shown, these were identified using DAVID gene ontology analysis.

B **Genes upregulated in AZD treated tumor IP**

A

Upregulated in AZD
treated tumor IP

Enriched in
treated tumor IP

C

Downregulated in AZD
treated tumor IP

D **Genes downregulated in AZD treated tumor IP**

Enriched in tumor IP
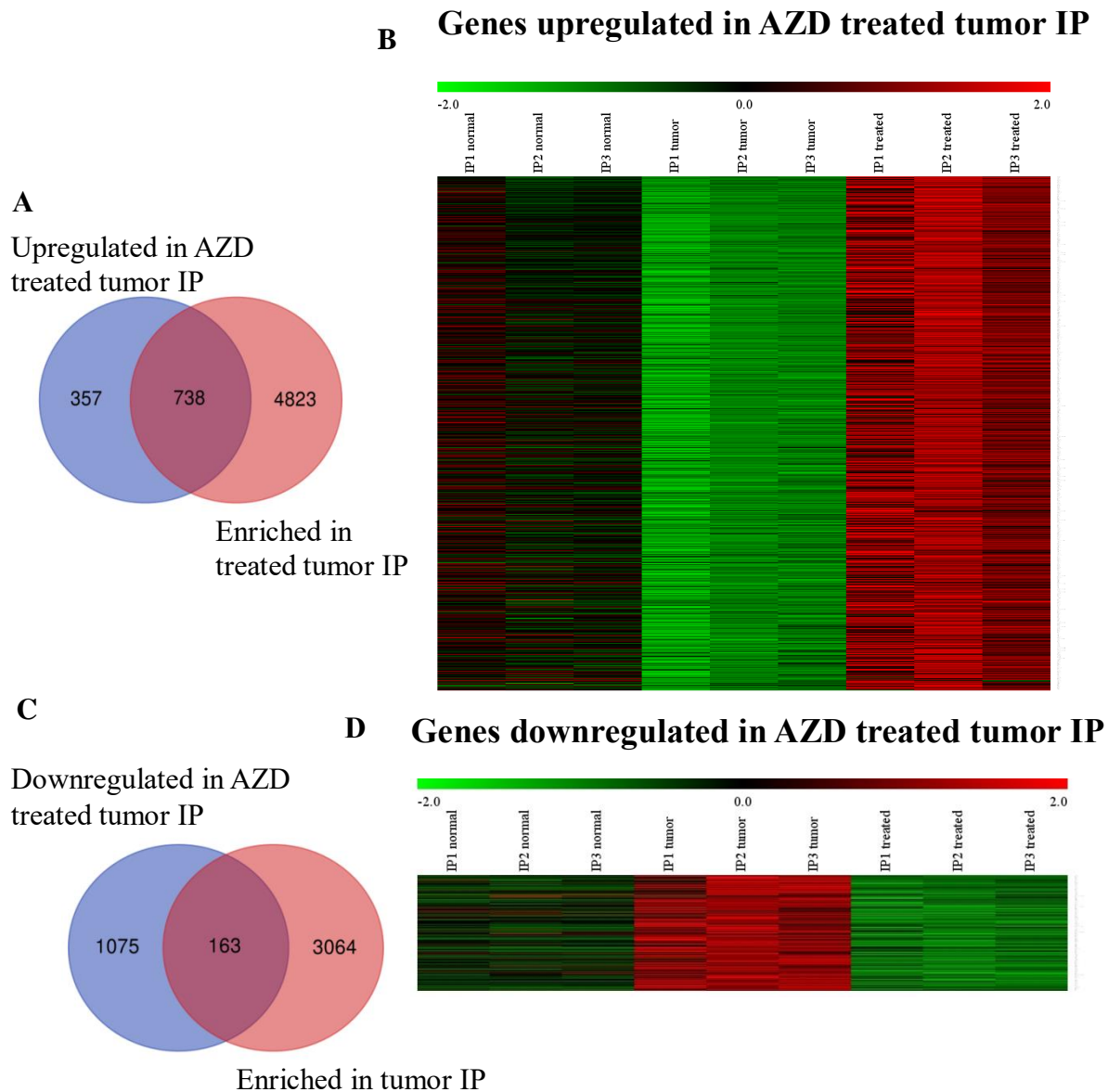
Figure 3.7: mTOR inhibition with AZD reverses some of the translational alterations in neuron specific genes. A) Venn diagram of genes that were upregulated in AZD treated tumor IP (blue) and genes that were enriched in treated tumor IP (pink), the 738 genes that are upregulated and enriched in AZD treated tumor IP are shown in panel B. B) Normalized counts for genes that were upregulated in AZD treated tumor IP and enriched in AZD treated IP. C) Venn diagram of genes that were downregulated in AZD treated tumor IP (blue) and genes that were enriched in tumor IP (pink), the 163 genes that are downregulated in AZD treated tumor IP and enriched in tumor IP are shown in panel D. D) Normalized counts for genes that were downregulated in AZD treated tumor IP and enriched in tumor IP. Upregulated (log2foldchange>0) and downregulated genes (log2foldchange<0) were determined from differential gene expression with DESeq2. ES from treated tumor brains was used to identify enriched genes that were upregulated, ES for non-treated tumor brains was used to identify enriched genes that were downregulated.

CHAPTER 4

Ribosome profiling reveals translational alterations in the Camk2a-Ribotag mouse glioma model

4.1 Introduction

Regulating the translation of mRNA into protein is essential for cells to modulate gene expression in response to endogenous and exogenous signals. Translational regulation is critical for maintaining a homeostatic balance during cell processes such as cell growth, proliferation and development. Protein synthesis is an energetically costly process for cells and is therefore under tight regulation (Hershey, Sonenberg et al. 2012). Translational regulation has been shown to play a critical role during pathological and non-pathological conditions thus identifying the mechanisms underlying translational control are needed for understanding regulation of gene expression in normal and disease conditions (Sonenberg and Hinnebusch 2009).

Dysregulation of translation occurs in cancer since some of the same pathways that contribute to cancer cell growth and proliferation also regulate translation. This is supported by the increased number of ribosomes and increased expression of components of the translational machinery seen in cancer (Silvera, Formenti et al. 2010). Recent analysis of translation regulation in tumor cells in one of our retrovirally induced mouse glioma models showed that tumor cells have lower translational efficiencies relative to other cell types in glioma, suggesting that there is a cell type specific mechanism of translational regulation in glioma (Gonzalez, Sims et al. 2014).

To study translation, ribosome profiling has emerged as a method to measure the translation efficiency per gene and has also been shown to be more correlated with protein synthesis compared to RNA sequencing (Maier, Güell et al. 2009, Ingolia 2016). Ribosome profiling tells us the number of ribosomes (ribosome footprint density) per transcript and the location of ribosomes on a transcript (Ingolia, Ghaemmaghami et al. 2009). Ribosome footprints are obtained by nuclease digestion of RNA that is not ribosome bound, which leaves ribosome protected RNA fragments (footprints). Ribosome footprints are then released from ribosomes and undergo size selection by gel electrophoresis followed by library generation for sequencing. Ribosome footprints are then sequenced to determine the ribosome footprint density which is used to calculate the translation efficiency (TE) per transcript. TE is obtained by taking the ratio of ribosome footprint density over the total mRNA per gene (Ingolia, Ghaemmaghami et al. 2009, Hornstein, Torres et al. 2016).

The mTOR pathway is involved in regulating protein synthesis and is also frequently dysregulated in cancer (Akhavan, Cloughesy et al. 2010). Alterations in mTOR signaling have been associated with alterations in translational regulation both in neurological disease and cancer (Hoeffer and Klann 2010, Showkat, Beigh et al. 2014). In this chapter I describe published work where we used the Ribotag and Camk2aCre mouse to obtain neuron specific ribosome bound transcripts from normal brains treated with the mTOR inhibitor AZD. When crossing Ribotag and Camk2aCre mice the resulting strain expresses the HA-tagged ribosomal protein (Rpl22) in Camk2a+ neurons (figure 4.1c). This model then allows for the immunoprecipitation of neuron specific HA-tagged ribosomes and their associated transcripts which we characterized by RNA sequencing and ribosome profiling (Hornstein, Torres et al. 2016). I also describe how we identified translational alterations using ribosome profiling in

homogenate tissue from our Camk2a-Ribotag mouse glioma model. We discovered that these translational alterations include the upregulation of specific DNA methylation and demethylation genes suggesting that epigenetic modifications in glioma may be regulated at the level of translation.

This chapter described the use of ribosome profiling to identify translational alterations in our Camk2a-Ribotag mouse glioma model. We have published a manuscript describing the use of ribosome profiling in normal brain tissue of Camk2a-Ribotag mice and the ability of ribosome profiling to detect a pharmacological perturbation (mTOR inhibition with AZD). We used ribosome profiling to identify translation efficiency alterations in Camk2a-Ribotag glioma brain tissue. From these experiments we identified an upregulation in the translation efficiency of genes associated with DNA methylation and demethylation which suggest that specific genes associated with epigenetics are regulated at the level of translation.

4.2 Results

Ribosome profiling in normal mouse brain suggests cell type specific translational regulation

We performed ribosome profiling and RNA sequencing in the right frontal lobe of normal mouse brain. Ribosome profiling provided ribosome density and RNA sequencing provided the total mRNA abundance. Using this information we calculated the translation efficiency (TE) by dividing ribosome density by the total mRNA abundance. We observed a broad distribution of TEs suggesting that there is a high degree of translational regulation in normal brain (figure 4.1a). In collaboration with the Sims lab, our lab previously showed that glioma cells have a different TE compared to other cells in the brain tumor microenvironment which suggested that there is cell type specific regulation of translation (Gonzalez, Sims et al.

2014). To assess if there is cell type specific translational regulation, we used gene expression profiles from a previous study (Zhang, Chen et al. 2014) to identify cell type specific genes. To perform this analysis we calculated the TEs for cell type specific genes and sorted them from low to high TE, conducted GSEA analysis and obtained an enrichment score for each gene (figure 4.1b). We performed this analysis for neuron, astrocyte, OPC, new oligodendrocyte, myelinating oligodendrocyte, microglia, and endothelial cell type specific genes. These data show that the most neuron specific genes have high and low TEs suggesting that there is a high degree of translational regulation. The most microglial specific genes show low levels of TE which is likely due to the fact that we are sampling healthy brain and thus microglia are not activated . Oligodendrocytes showed a diverse pattern of translation during oligodendrocyte development, OPC specific genes had a high TE whereas myelinating oligodendrocyte specific genes had a low TE. Diverse patterns of TE in cell type specific genes suggested that there is a high degree of translational regulation in normal brain (figure 4.1b).

The Camk2a-Ribotag mouse allows for the enrichment of neuron specific transcripts

The Camk2a-Ribotag mouse allowed us to isolate neuron specific ribosome bound mRNAs (figure 4.1c). We verified the expression of HA-tagged neurons by immunofluorescent staining in normal brain tissue (figure 4.1d). We homogenized brain tissue to obtain a total homogenate lysate, from this lysate we isolated neuron specific ribosome bound mRNAs by immunoprecipitating HA-tagged ribosomes with an HA-antibody. The total homogenate contains ribosome and non-ribosome bound transcripts while the immunoprecipitated (IP) fraction contains HA-tagged ribosomes. Then we isolated ribosome bound transcripts for RNA sequencing. To analyze this data we took the ratio of normalized counts from the IP over the homogenate to obtain an enrichment score (ES) for cell type specific genes (figure 4.1e). Our

data show high enrichment for excitatory neuron specific genes and depletion of genes specific to other cell types (inhibitory neurons, OPCs, oligodendrocytes, astrocytes) supporting our immunofluorescence results that HA expression is restricted to neurons in normal brain tissue.

Ribosome profiling detects inhibition of mTOR with AZD in normal Camk2a-Ribotag mouse brain

mTOR signaling is central in integrating and processing signals to maintain cell homeostasis which is thought to occur via translation through downstream effectors S6K1 and 4EBP1. mTOR activation phosphorylates S6K1 which phosphorylates ribosomal protein S6 (S6) and activates translation. Phosphorylated S6 (pS6) induces the translation of mRNAs with a 5' terminal oligopyrimidine motif (TOP) which includes genes for components of the translational machinery such as ribosomal proteins and elongation factors (Meyuhas 2000, Moschetta, Reale et al. 2014). To identify the effects of mTOR inhibition we treated normal mice with the ATP-competitive mTOR inhibitor AZD8055 (AZD). We delivered AZD (20 mg/kg) by oral gavage and collected the right frontal lobe brain tissue one hour after administration. We used a short treatment so as to minimize the effects of de novo protein synthesis. We determined that pS6 expression decreased in AZD treated brains as demonstrated by immunostaining and western blot (figure 4.2a,d), specifically in HA-tagged cortical neurons (figure 4.2a).

To assess the effects of mTOR inhibition on the TE in normal brain we performed differential gene expression analysis of the TE in AZD treated vs vehicle treated using RiboDiff. These results showed a significant downregulation in the TE of TOP motif containing genes after 1 hour AZD treatment in normal brain (figure 4.2b). We also showed that the decrease in TOP gene expression was undetectable by RNA sequencing alone which supports previous findings

that mRNA levels alone are not concordant with protein expression (Maier, Güell et al. 2009). We show that the alterations in TE were statistically significant, 37 genes were differentially translated, 25 of these were known TOP containing motif genes and the remaining 11 were ribosomal proteins (figure 4.2c). These data show that translational control of gene expression precedes transcriptional control of gene expression in response to mTOR inhibition with AZD. This is in agreement with the fact that stress or pharmacological interventions induce detectable changes in translation prior to transcription (Hsieh, Liu et al. 2012, Thoreen, Chantranupong et al. 2012).

Ribosome profiling reveals an upregulation of DNA methylation and demethylation genes in homogenate Camk2a-Ribotag mouse glioma brain

We performed ribosome profiling on homogenate lysate from Ribotag-Camk2a tumor brains to identify translational alterations. We decided to use ribosome profiling to identify translational alterations in addition to the translational alterations we determined by TRAP methods used in chapter 2 and 3 because ribosome profiling would provide additional information about the ribosome density and TE per mRNA. To assess differential gene expression based on TE in tumor homogenate vs normal brain homogenate we used the RiboDiff algorithm (Zhong, Karaletsos et al. 2015). From this analysis we identified 104 differentially translated genes (table 2, p<0.05). We used Panther to identify the gene ontologies (GO) associated with these 104 genes, for biological processes GOs we identified the DNA methylation or demethylation GO. This GO included Ezh2, Dnmt3a, and Tet1-3 (figure 4.4a-b) as the genes from our data that were enriched in this GO. Similarly, using these 104 genes for molecular function GOs we identified the methylcytosine dioxygenase activity GO, which included Tet1, Tet2, Tet3 genes (figure 3.4a). Ezh2, Dnmt3a, and Tet1-3 were translationally

upregulated (log2foldchange>0) in tumor homogenate tumor relative to normal brain homogenate (table 2). These results show that Ezh2, Dnmt3a, and Tet1-3 are translationally regulated in our glioma model and suggest that a similar mechanism might underlie their expression in human glioma.

We attempted to perform ribosome profiling from IP in tumor brains, however we obtained low yield ribosome footprints. We generated sequencing libraries from IP in tumor brains however we did not sequence them since it was advised by our collaborators that the quality of our sequencing data would be poor because of the low yield in ribosome footprints. We determined that there ribosome footprints had low yield during the size selection by gel electrophoresis step of library generation.

4.3 Discussion

In this chapter I described how we used ribosome profiling to identify translational alterations in mouse brain tissue. I described how we used ribosome profiling in normal brain from Camk2a-Ribotag mice to test the effects of mTOR inhibition with AZD. Ribosome profiling revealed that mTOR inhibition with AZD induced a translational downregulation of TOP motif genes which are canonical mTOR targets. Lastly, we identified that diffusely infiltrating glioma cells induced a translational upregulation of DNA methylation and demethylation genes in our Camk2a-Ribotag mouse glioma model.

We showed that administration of the mTOR inhibitor AZD to normal Camk2a-Ribotag mice, reduced pS6 levels in cortical neurons and translationally downregulated TOP-motif containing genes (Hornstein, Torres et al. 2016). Treatment with AZD lasted for one hour, demonstrating that translational downregulation of TOP-motif genes is an early event after

mTOR inhibition with AZD. From the genes that were translationally downregulated after one hour AZD treatment, we did not identify known cell type specific genes. This could be due to the short duration of mTOR inhibition, suggesting that translational regulation of cell type specific genes might require longer mTOR inhibition to be detectable.

The upregulation of DNA methylation and demethylation genes in our mouse glioma model support previous studies that show upregulation of some of these genes in glioma (Etcheverry, Aubry et al. 2010). DNA methylation is associated with transcriptional repression of tumor suppressor genes in cancer, thereby enabling tumor growth (Maleszewska and Kaminska 2013). Dnmt3a is a methyltransferase that establishes new methylation patterns in unmethylated DNA regions during development. Ezh2 is a histone methyltransferase that promotes transcriptional silencing, particularly of genes associated with lineage specification suggesting that Ezh2 promotes tumor growth by suppressing differentiation (Kim and Roberts 2016). It has been shown that Dnmt3a and Ezh2 are upregulated in GBM which suggests that expression of these epigenetic markers may contribute to glioma growth (Etcheverry, Aubry et al. 2010). Ezh2 was shown to have a higher translation rate in transformed glioma cells relative to normal brain in a different glioma mouse model (PDGFB-p53 retrovirally induced model) that is also used in our lab (Gonzalez, Sims et al. 2014). This suggests that Ezh2 may underlie tumor growth mechanisms that are common in both glioma models.

Several studies have shown that Tet proteins are involved in the reversal of DNA methylation and that depletion of Tet genes are associated with enhanced tumor growth (Bian, Li et al. 2014, Rasmussen and Helin 2016). However, another study showed that there is an upregulation of Tet1 in proneural glioma cell lines compared to other glioma subtypes (Takai, Masuda et al. 2014). Our tumor model is considered a proneural glioma due to the genetic

alterations in PDGFRa and p53 . It is possible that studies that show downregulation of Tet isoforms grouped did not distinguish among glioma subtypes and as a result did not detect Tet1 expression specifically in proneural glioma.

We performed ribosome profiling on tumor homogenate, which includes all cells found in the tumor microenviroment thus we cannot determine the cell type specific contribution of Tet1 upregulation. We can infer that the upregulation in Tet1 is primarily a contributed to by glioma cells since glioma cells compose the majority of cells in tumor homogenate. However, it would be ideal to determine which cell type contributes to the upregulation of these epigenetic alterations by performing ribosome profiling on cell type specific ribosome bound transcripts. It is possible that the upregulation of Tet1 expression is a result of alterations in synaptic plasticity. Overexpression of Tet1 induced an upregulation of synaptic plasticity genes (Santiago, Antunes et al. 2014) which suggests that the upregulation of Tet1 may be a compensatory mechanism that tries to restore the expression of genes involved in synaptic plasticity in our glioma model.

The results described in this chapter show how ribosome profiling can be used to identify translational alterations in response to mTOR inhibition with AZD in mouse brain. We applied ribosome profiling to our Camk2a-Ribotag mouse glioma model and identified a translational upregulation in the expression of epigenetic genes which suggests a mechanism for the expression of these genes. These findings provide the framework for future studies that will assess the translational alterations of specific cell types in glioma tissue using ribosome profiling.
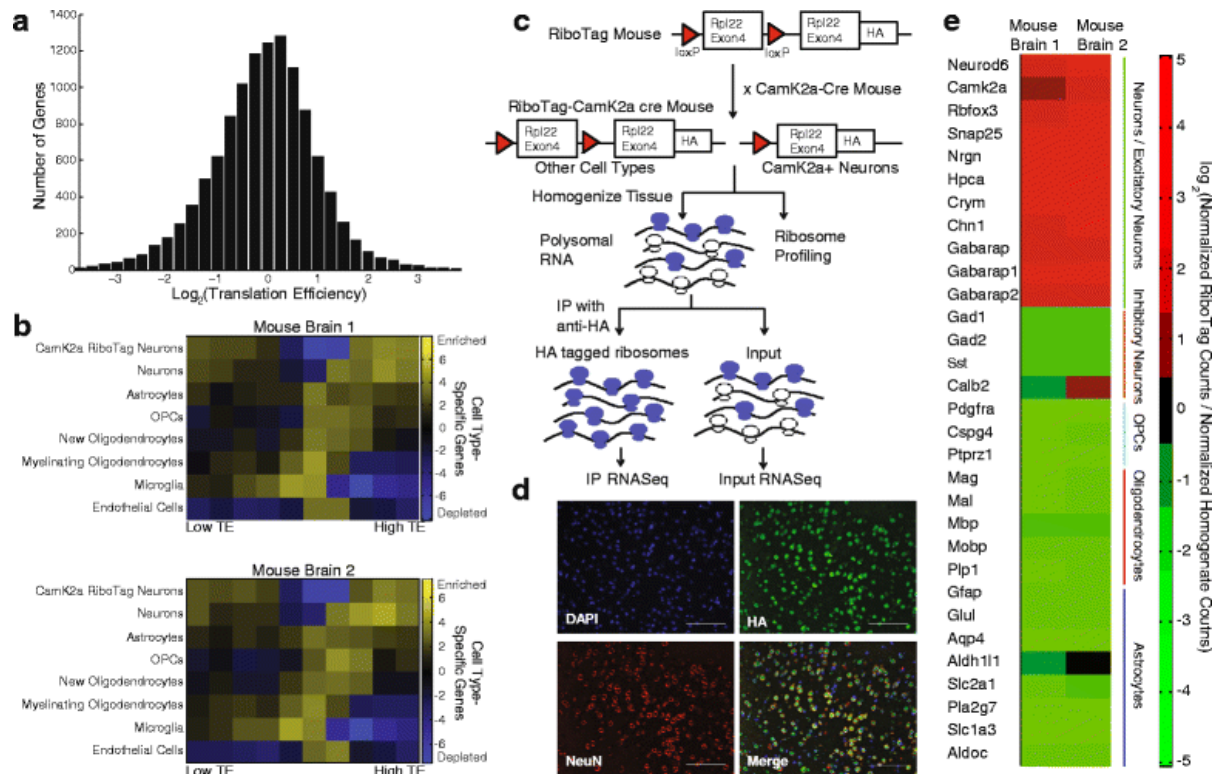
Figure 4.1: Unique patterns in the translation efficiency of cell type-specific genes in normal Camk2a-Ribotag mouse brain. A, The broad range of translation efficiencies (TEs) across genes expressed in normal mouse brain based on ribosome profiling. B, TEs measured in two different normal mouse brains with ribosome profiling were combined with cell type-specific gene expression profiles to associate cell type-specific gene expression and TE. We used gene set enrichment analysis (GSEA) to associate gene sets assembled from genes with similar TEs with a ranked list of all genes ordered by cell type-specificity for each cell type in the brain. The resulting heatmaps show the enrichment of genes with different TEs in cell type-specific genes for each cell type. B, The Ribotag mouse model shows how the Camk2a-Ribotag mouse was generated. This provides an orthogonal means of identifying neuron-specific genes that are actively translated. D, Fluorescence imaging shows that Rpl22-HA (from the Ribotag allele) expression is specific NeuN+ cells (a pan-neuronal marker). D, Heatmap of the Ribotag enrichment scores following immunoprecipitation of polysomes from Camk2a-Ribotag normal mouse brains demonstrates strong enrichment of genes specific to excitatory neurons and depletion of genes specific to other cell types in the brain in two different mouse brains
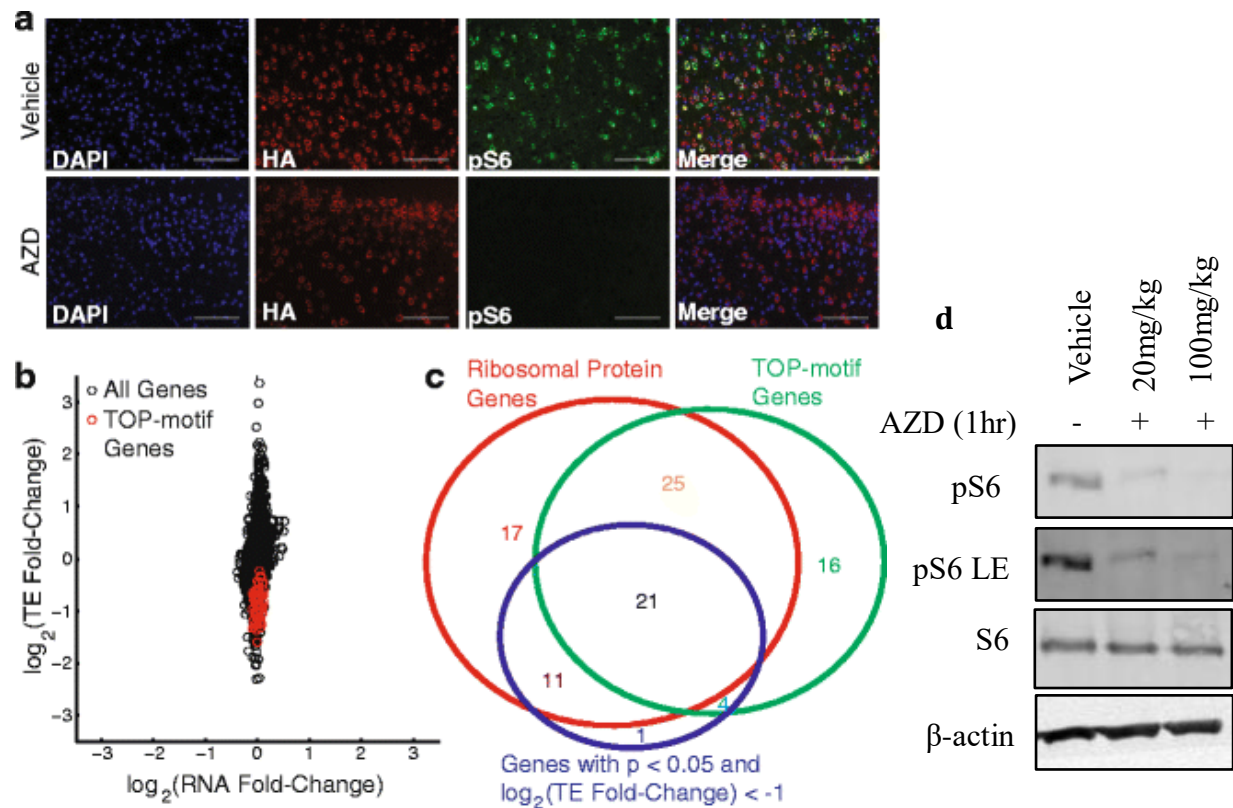
Figure 4.2: mTOR controls TOP motif-containing genes in normal Camk2a-Ribotag mouse brain. A, Treatment for 1 hour with AZD-8055 was sufficient to drastically decrease levels of pS6 in normal mouse brains. HA-staining indicates the presence of HA-tagged Camk2a+ neurons. B, Comparison of RNA and TE fold changes between AZD treated and untreated mice. TE exhibits larger amplitude changes than RNA levels in response to mTOR inhibition in the brain. The TE of TOP motif-containing genes are greatly reduced. C, We used RiboDiff to identify genes with significant differential translation efficiency and DESeq2 to identify genes with significant differential RNA expression in treated versus untreated mice. The Venn diagram shows the overlap between genes with significant translational reduction after AZD treatment, ribosomal proteins, and TOP motif-containing genes. D, western blot of pS6 and S6 expression from right frontal brain lobe of vehicle, AZD 20mg/kg, or AZD 100mg/kg after 1 hour treatment.

Table 2: Differentially translated genes determined by ribosome profiling (p<0.05) in homogenate Camk2a-Ribotag glioma mouse brain

gene	P-value	log2(Tumor /Normal)	gene	P-value	log2(Tumor /Normal)	gene	P-value	log2(Tumor /Normal)
Nup93	0.000E+00	1.350	Adamts10	2.712E-03	3.658	Leng8	1.755E-02	0.784
Agrn	0.000E+00	1.165	Ascc2	3.069E-03	0.934	Fbxo5	1.805E-02	3.161
Col5a1	5.290E-13	3.132	Ccnb2	3.776E-03	3.286	Cpsf4	1.969E-02	1.370
Ezh2	2.010E-10	2.637	Igsf9b	4.351E-03	1.861	0610030E	2.252E-02	2.151
Flnb	1.160E-09	1.564	Hmgb1	4.703E-03	-1.407	Smarca1	2.348E-02	0.699
Srsf9	1.970E-09	1.982	Fbn2	4.828E-03	3.278	Dnahc2	2.399E-02	1.854
Prr22	1.460E-07	6.712	Darc	4.971E-03	6.186	Arhgap22	2.481E-02	1.725
Dnmt3a	1.710E-07	1.417	Brwd3	4.971E-03	1.159	Rbm4	2.489E-02	1.034
Pkd1	1.920E-07	1.516	Mmp16	4.971E-03	0.695	Akap13	2.748E-02	0.762
Clasrp	1.920E-07	1.519	Gas2	5.405E-03	1.590	Wdr90	2.748E-02	1.331
Ctnnal1	1.950E-06	1.714	Dennd1b	5.453E-03	1.343	Chd7	2.748E-02	1.296
Snrnp70	2.060E-06	0.828	Paxbp1	6.749E-03	0.914	Atg16l2	2.819E-02	1.385
Col20a1	8.140E-06	3.526	Mdn1	7.366E-03	0.810	Asun	2.886E-02	0.668
Tet2	3.350E-05	2.041	Rpl37	7.366E-03	1.506	Lrch3	3.219E-02	0.832
Arpc1a	3.810E-05	-1.109	Bub1b	7.662E-03	1.680	Ube2r2	3.219E-02	-0.496
Myo9b	6.930E-05	1.698	Obsll	7.815E-03	0.919	Nvl	3.267E-02	0.827
Fam173a	6.930E-05	-1.199	Tet1	8.253E-03	1.855	Nbeal2	3.612E-02	1.601
Pcdhb3	7.790E-05	-2.925	Cdyl	8.949E-03	1.258	Trpm4	3.627E-02	1.404
Pstpip2	1.480E-04	1.787	Pask	8.949E-03	2.195	Gatm	3.769E-02	0.556
Col11a1	2.290E-04	2.647	Pdia5	8.949E-03	1.938	Ttc28	4.140E-02	0.850
Tacc3	3.040E-04	1.932	Gm17296	8.949E-03	1.270	Ankrd28	4.140E-02	-0.725
Wsb1	3.810E-04	1.155	Ppp4r1	8.949E-03	0.939	Usp40	4.435E-02	1.035
Dcx	3.810E-04	1.895	Col6a1	8.949E-03	1.047	Pagr1a	4.517E-02	0.746
Flna	4.020E-04	1.013	Dynlt1b	9.079E-03	3.526	Casp2	4.580E-02	0.947
Rgl2	4.470E-04	1.498	Mroh8	9.398E-03	2.933	Ltbp4	4.580E-02	0.596
Apex2	4.760E-04	1.514	Pcdh15	9.492E-03	0.790	Klhdc4	4.580E-02	1.014
Xylt1	1.130E-03	0.838	Pcdhgb8	1.014E-02	2.172	Rpap1	4.796E-02	0.628
Tet3	1.130E-03	1.718	Ugdh	1.108E-02	1.240			
Dot1l	1.130E-03	1.623	Gpr183	1.112E-02	-2.702			
Pcbp4	1.130E-03	0.732	Tmem181a	1.421E-02	1.161			
Sbf2	1.130E-03	0.906	Cryab	1.447E-02	-0.993			
Kif21b	1.201E-03	0.873	Nup160	1.447E-02	0.796			
Sec24a	2.322E-03	1.139	Tnpo1	1.453E-02	0.812			
Mpzl1	2.404E-03	1.666	Smpdl3a	1.560E-02	-0.797			
Lepre1	2.411E-03	1.668	Dusp11	1.560E-02	1.133			
Dnahc8	2.411E-03	2.233	Nup188	1.587E-02	0.882			
Spag5	2.484E-03	1.329	Cep112	1.632E-02	1.827			
Stk38	2.712E-03	1.220	Megf6	1.632E-02	2.224			

A

GO biological process	# of genes in this GO (reference list)	# of genes from our list found in this GO	fold Enrichment	P-value
DNA methylation or demethylation (GO:0044728)	55	5	20.65	4.44E-02

GO molecular function	# of genes in this GO (reference list)	# of genes from our list found in this GO	fold Enrichment	P-value
Methylcytosine dioxygenase activity	4	3	>100	2.69E-03

B   DNA methylation or demethylation GO

	p-value	log2(TE-fold change)
Ezh2	2.01E-10	2.64
Dnmt3a	1.71E-07	1.42
Tet2	3.35E-05	2.04
Tet3	1.13E-03	1.72
Tet1	8.25E-03	1.86

Figure 4.4: Gene ontologies for differentially translated genes in homogenate glioma mouse brains. A, Gene ontologies of 104 significantly translated genes from total homogenate of 3 tumor brains for GO biological process and GO molecular function. B, table of genes found in the DNA methylation or demethylation GO with corresponding adjusted p-value and log2 (translation efficiency fold change) from RiboDiff analysis, Tet1-3 are the 3 genes from our list found in the methylcytosine dioxygenase activity GO.

CHAPTER 5

Conclusions and future directions

Conclusions

In this thesis we used the Camk2a-Ribotag mouse glioma model to identify translational alterations specifically in neurons found in the glioma infiltrated cortex. In chapter 2 we use TRAP methods to show that there is a downregulation in the translation of synaptic genes in glioma tissue which is likely correlated with the decrease in dendritic spine density we discovered using diolistic imaging. Using TRAP we also show that there is an increase in the translation of actin binding genes associated with dendritic morphology and plasticity which overall suggest that there is a compensatory mechanism taking place in our glioma model. In chapter 3 we also use TRAP methods to show that mTOR inhibition with AZD reversed several of the neuron specific translational alterations induced by the tumor. In chapter 4 we used ribosome profiling to identify translational alterations after mTOR inhibition with AZD in normal brain and we show how we applied ribosome profiling to identify the translational upregulation of genes associated with DNA methylation and demethylation in our glioma model. Overall these findings show how our mouse glioma model can be used to identify cell type specific translational alterations in the brain tumor microenvironment.

A new diffusely infiltrating glioma mouse model reveals neuronal alterations in the brain tumor microenvironment

The Camk2a-Ribotag mouse glioma model we developed proved to be an essential tool for identifying neuronal alterations in the brain tumor microenvironment. Our mouse model histologically depicts the intermingling of neurons and glioma cells, a characteristic that is prominent in human glioma (Wesseling, Kros et al. 2011). Using translational ribosome affinity purification (TRAP) (Doyle, Dougherty et al. 2008, Heiman, Kulicke et al. 2014) our system allowed us to identify translational alterations specifically in neurons that had not been identified before. Neuronal alterations in glioma have likely been undetected because of a few issues 1) there is a variably lower abundance of neurons within the tumor compared to normal brain 2) alterations in cellular composition obscure cell type specific alterations in bulk tumor 3) the harsh methods needed to dissociate brain tissue makes it difficult to isolate neurons (Poulin, Tasic et al. 2016). Our Camk2a-Ribotag mouse glioma model overcomes these issues by allowing us to tag ribosomes and selectively isolate ribosome bound neuronal transcripts from glioma infiltrated cortex. Using TRAP, we discovered that there is a downregulation in the translation of synaptic genes and an increase in the translation of dendritic spine genes in our glioma model. We also show that there is increased expression of drebrin, an actin binding protein in dendritic spines, in the synaptosomal fraction of tumor brains. We also demonstrate that dendritic spine density is decreased from Camk2a+ neurons. Together, these data suggest that there are alterations in the synaptic component of glioma brains, and that these alterations may be a result of ongoing reactive plasticity in glioma.

The effects of mTOR inhibition with AZD in the Camk2a-Ribotag mouse glioma model

In our studies we detected an upregulation of mTOR activity in mouse glioma tumor tissue and showed that inhibition of mTOR with AZD decreased mTOR activity particularly in neurons. This led us to conclude that AZD effectively targets mTOR in brain tumor tissue. Using TRAP methods we demonstrate that many of the neuron specific signatures, including genes associated with synapses and actin binding genes, were reversed after a 6 hour treatment with AZD. This shows that mTOR can regulate the translation of many neuron specific genes including dendritic spine and synaptic genes in our glioma model as was determined by TRAP. The observation that AZD can reverse the alterations in synaptic and dendritic spine genes suggests that mTOR signaling is a potential mechanism underlying neuronal alterations in glioma infiltrated cortex.

Ribosome profiling reveals translational alterations in the Camk2a-Ribotag mouse glioma model

Ribosome profiling provides a measure of translation by measuring the number of ribosomes per transcript and the location of ribosomes in each transcript (Ingolia, Ghaemmaghami et al. 2009, Ingolia 2016). This method provides a quantitative measure of translation, which is not provided by TRAP, and one that allows for determining how efficiently a gene is translated (Kapeli and Yeo 2012). Using ribosome profiling we showed that cell type specific genes have varying translation efficiencies which suggests that they are under tight translational control in normal brain (Hornstein, Torres et al. 2016). We also show that mTOR inhibition with AZD resulted in a downregulation of canonical mTOR targets (TOP genes) in normal brain (Hornstein, Torres et al. 2016). These findings provided the framework for the ribosome profiling experiments we performed in glioma brain tissue. Using ribosome profiling

we identified alterations in the translation of genes associated with DNA methylation and demethylation in homogenate glioma brain tissue. This data provides evidence for the translational regulation of specific genes associated with epigenetic alterations.

Future directions

We identified a downregulation in the translation of several synaptic mRNAs specifically in neurons from glioma infiltrated cortex. Diolistic imaging also revealed that there were fewer dendritic spines in neurons from glioma infiltrated cortex, these findings suggest that there are fewer synapses or that the existing synapses are not functional within glioma tissue. To determine if synaptic mRNAs are translated into protein future studies could assess the expression of these synaptic transcripts at the protein level either by western blot analysis of the synaptosomal fraction and immunofluorescence analysis of glioma infiltrated cortex. Dendritic spines are dynamic structures that can alter their properties in response to synaptic stimuli (Hlushchenko, Koskinen et al. 2016). It would also be important to assess dendritic spine morphology, since different dendritic spine morphologies can indicate synaptic maturity which could help us understand if they are functional synapses (Lai and Ip 2013, Maiti, Manna et al. 2015).

The actin binding genes we identified as upregulated in neurons within glioma infiltrated brain tissue are also associated with genes enriched in neuronal RNA granules (El Fatimy, Davidovic et al. 2016). RNA granules carry specific mRNAs to be locally translated in subcellular neuronal compartments such as dendritic spines. Our findings suggest that the translation of locally regulated mRNAs is altered in neurons from glioma infiltrated cortex. One way to determine the translation efficiency is to perform ribosome profiling. All of our neuron

specific data has been obtained using TRAP methods in order to identify neuron specific ribosome bound transcripts, however this approach can only tell us whether a transcript has a ribosome on it, it does not distinguish transcripts that have one or more ribosomes bound. Ribosome profiling is able to tell us ribosome density in addition to providing data about the location of ribosomes on a transcript. Mapping the location and density of ribosomes on transcripts can provide mechanistic insights into the regulation of translation, for example increased levels of ribosome occupancy at specific sites provide evidence for ribosome pausing. Future experiments could include performing ribosome profiling on neuron specific ribosome bound transcripts to provide additional insight into how efficiently these transcripts are being translated.

Our findings showed that mTOR inhibition reversed many of the alterations determined by TRAP methods, future experiments could characterize the functional consequences of mTOR inhibition on neuron specific alterations. This could include assessing protein levels of dendritic spine genes and synaptic genes after mTOR inhibition by western blot analysis of the synaptosomal fraction and by immunofluorescence analysis of glioma infiltrated cortex. Analyzing the effects of mTOR inhibition on dendritic spine density using diolistic imaging could also provide further evidence of the consequences of mTOR inhibition on dendritic spine dynamics within the glioma infiltrated cortex. Additionally, it would be important to characterize how dendritic spine morphology is affected by mTOR inhibition to better assess synaptic maturity. Ultimately it would be ideal to characterize the functional consequences of mTOR inhibition using our glioma model by measuring synaptic strength or performing electrophysiological measurements of neuronal activity. It will also be important to assess the effects of mTOR inhibition on the neurological symptoms observed in our mouse glioma model,

including seizures using video EEG or cognitive impairments using behavioral tests. These experiments could provide data regarding the effects of mTOR inhibition in a mouse model that resembles the histological and behavioral characteristics in low grade glioma, and suggest the use of mTOR inhibitors to target neurological dysfunction in low grade glioma.

Ribosome profiling allowed us to determine translational alterations in DNA methylation and demethylation genes from bulk glioma tissue. It would be critical to further analyze these existing data to determine the location of ribosomes on these transcripts. This could inform us whether ribosomes are stalled or not and in what specific region of the transcript they are primarily found. Our results were obtained from homogenate glioma tissue, which contains tumor cells as well as many other cells found in the tumor microenvironment thus we cannot determine the cell type specificity. It would be useful to perform ribosome profiling on the neuron specific transcripts obtained from the IP fraction in Camk2a-Ribotag glioma brain tissue in order to identify the neuron specific translational alterations in glioma infiltrated cortex.

The mouse glioma model we developed provides a useful tool for studying cell type specific alterations in glioma and could be used to identify alterations in other brain cell populations including astrocytes, microglia, endothelial cells and inhibitory neurons. This could provide a better understanding of how infiltrating glioma cells alter the brain tumor microenvironment. Overall, the work described in this thesis showed that there are alterations in dendritic spines and synaptic genes and that mTOR is a possible mechanism underlying these changes. Hopefully the findings obtained from this work will contribute to a better understanding of the mechanisms underlying neurological symptoms in glioma.

CHAPTER 6

Methods

6.1 Mouse models and tissue processing

Camk2a-Ribotag mice

Camk2a-Cre mice (JAX ID 005359) have the mouse calcium/calmodulin-dependent protein kinase II alpha (*Camk2a*) promoter driving Cre recombinase expression in the forebrain, specifically in principal excitatory neurons. Camk2a-Cre mice were crossed to Ribotag mice (JAX ID 011029) which contain a conditional knock-in allele where exon 4 of the ribosomal protein (Rpl22) is flanked by loxP sites, followed by an identical exon tagged with three repeated hemagglutinin epitope coding sequences (HA-tag). The resulting Camk2a-Ribotag cross expresses the HA-tagged Rpl22 protein in principal excitatory neurons. Camk2a-Cre heterozygotes were crossed to homozygous Ribotag mice and genotyped with primers for Cre (GCG GTC TGG CAG TAA AAA CTA TC (transgene), GTG AAA CAG CAT TGC TGT CAC TT (transgene), CTA GGC CAC AGA ATT GAA AGA TCT (internal positive control forward), GTA GGT GGA AAT TCT AGC ATC ATC C (internal positive control reverse)) and for Ribotag (GGG AGG CTT GCT GGA TAT G (forward), TTT CCA GAC ACA GGC TAA GTA CAC (reverse)).

Previous reports have shown that recombination with the Camk2a promoter-driven cre begins during the third postnatal week and is completed by the fourth postnatal week (Tsien, Chen et al.

1996); therefore for experiments using normal brain, we chose to use mice that were 12-13 weeks old.

Stereotactic retroviral injection

Transgenic C57BL/6 mice carrying loxP recognition sites at exon 7 of Trp53 were crossed with a reporter transgenic mouse containing a mCherry-luciferase fusion gene floxed by loxP sites. These mice were bred to homozygosity and gliomas were induced by stereotactic injection of a retrovirus expressing PDGFA and Cre recombinase into the subcortical white matter of the right frontal lobe in P4 neonates. PDGFA-IRES-Cre was tittered to 10^6 in Ribotag-Astrocytes. To target the subcortical white matter in neonates, we used coordinates of 1mm lateral, 1mm rostral and 1mm deep with bregma as the reference point. 1uL of retrovirus was injected using the coordinates described above and tumor growth was monitored by bioluminescent imaging as described previously (Lei, Sonabend et al. 2011).

Glioma cell isolation from PDGFA induced tumor

Tumor cells were isolated from a PDGFA retrovirally induced tumors (52 days post injection)for subsequent stereotactic injection in Camk2a-Ribotag adult mice. The right frontal lobe of a PDGFA-p53 tumor bearing brain was dissected and washed in PBS. Tissue was minced and enzymatically dissociated with TrypLE at 37°C in a shaking water bath for 5 minutes. Tissue was triturated by passing through a 18G and 21G needle, filtered through a 70um mesh filter and neutralized with 50% FBS. Cells were collected by centrifugation and resuspended in cell culture media. Media was composed of DMEM, 10 ng/mL PDGF-AA (Peprotech), 10 ng/mL bFGF (Peprotech), N2 supplement (Gibco), antibiotic/antimycotic, 0.5% FBS. Cells were

cultured and passaged in poly-l-lysine coated plates. As a result of the breeding cross, isolated cells express mCherry reporter which was visualized by fluorescent microscopy.

Glioma cell injection into Camk2a-Ribotag mice

Isolated glioma cells were stereotactically injected in adult (10-12 weeks old) Camk2a-Ribotag mice. 50,000 cells were resuspended in 2uL OptiMEM and were stereotactically injected to the subcortical white matter in the right frontal lobe of adult mice. To target the subcortical white matter in adults, we used coordinates of 2mm lateral, 2mm rostral and 2mm deep with bregma as the reference point. Tumor progression was monitored by bioluminescent imaging as previously described (Lei, Sonabend et al. 2011).

Camk2a-Ribotag tumor bearing mice were sacrificed 5 weeks post injection (15-17 weeks old) for all experiments described. We chose this time period because starting at 4 weeks post-injection mice begin to show signs of tumor morbidity. Mice were sacrificed by cervical dislocation and their brain was dissected and fixed in PFA for immunostaining and snap frozen in liquid nitrogen for RNA extraction and western blotting.

Given the fact that I am using glioma cells derived from a retroviral induced glioma model to inject into the Camk2a-Ribotag mice I explored the differences among these two models. I compared the retrovirally induced model to the cell induced model using differential gene expression (DESeq) calculated for each tumor model. I determined that the many of the genes (83%) differentially expressed in the homogenate of the retrovirally induced model are also differentially expressed in the cell induced model suggesting that both models are similar I assessed the GO of the similar genes and identified GOs that are associated with tumor cells

which suggests that both retroviral and cell induced models share similar genes that drive tumor growth.

Luciferase imaging

Bioluminescent imaging began 14 days post-injection in Camk2a-Ribotag mice, mice were imaged every week after that until they displayed signs of tumor morbidity. Mice were anesthetized with ketamine (100mg/kg) and given 100ul of luciferin substrate by IP injection. Bioluminescent imaging was performed 10 minutes after luciferin injection in the IVIS Spectrum Bioluminescence and Fluorescence Optical Imaging System at the Irving Cancer Research Center in Columbia University.

Tissue processing and immunostaining

Brains were collected for staining 5 weeks post injection (wpi) in adult Camk2a-Ribotag mice. At 5wpi brains were fixed in 4%PFA for 48h. For fluorescent staining, brains were cryoprotected in 10-30% sucrose for 2 days and embedded in OCT. Cryosections (12um) were fixed in 4%PFA for 15 minutes at room temperature, permeabilized with 0.5% Triton for 10 minutes, blocked with 5% goat serum for 1 hour and incubated with primary antibodies overnight at 4°C. Next day, sections were incubated with AlexaFluor conjugated secondary antibodies for 1 hour at room temperature and counter-stained with DAPI.

For peroxidase staining, brains were embedded in paraffin, sections (5um) were immersed in xylene then rehydrated by incubation in 100%, 95%, and 75% ethanol. Antigen retrieval was performed in 10mM citrate buffer (pH 6.0) in a pressure cooker for 10 minutes. Slides were immersed in 3% hydrogen peroxide for 10 minutes to block endogenous peroxidases. Sections were blocked with 5% goat serum for 1 hour at room temperature and primary antibody

incubation was left overnight at 4°C. Next day, sections were incubated with biotin conjugated secondary antibodies for 1 hour at room temperature. ABC mixture was added to sections for 30 minutes, followed by incubation with DAB chromogen until staining was observed. Sections were washed in water and counterstained with hematoxylin, dehydrated with 75%, 95% and 100% ethanol and mounted with Permount. Sections were visualized with either a fluorescent or a light microscope and processed with Image J software.

Tissue processing for RNA extraction

Snap frozen tissue samples (5 mg) were homogenized at 4 °C with a Dounce homogenizer in 1 mL of polysome lysis buffer (20 mM Tris-HCl pH 7.5, 250 mM NaCl, 15 mM MgCl$_2$,1 mM DTT, 0.5 % Triton X-100, 0.024 U/ml TurboDNase, 0.48 U/mL RNasin, and 0.1 mg/ml cycloheximide). Homogenates were centrifuged for 10 minutes at 4 °C, 14,000 × g. The supernatant was removed and used for the isolation of ribosome footprints and total RNA. SUPERase-In (0.24U/mL) was added to the lysate used for total RNA to prevent RNA degradation.

Drug delivery

AZD-8055 (Selleckchem) was dissolved in Captisol and diluted to a final Captisol concentration of 30 % (w/v). A single dose of AZD-8055 was administered by oral gavage (20mg/kg) and delivered to normal Camk2a-Ribotag adult mice (12-13 weeks old). Vehicle consisted of 30 % captisol and was also delivered by oral gavage. Normal Camk2a-Ribotag mice were sacrificed 1 hour after AZD-8055 or vehicle administration; two mice were used per condition. Cervical dislocation was performed and the right frontal lobe of the brain was collected and snap-frozen in liquid nitrogen prior to polysome extraction. The remaining brain lobes were fixed in 4 %

paraformaldehyde for 48 h and embedded in paraffin for histological analysis. The same protocol was followed for AZD time course experiments, except that mice were sacrificed between 1-24 hours after AZD delivery and there were 2 doses of AZD delivered (20mg/kg or 100 mg/kg). For one mouse, AZD was delivered twice, the second dose was 1 hour before sacrificing for western blot analysis (25 hours AZD).

AZD was delivered (100 mg/kg) by oral gavage to tumor bearing Camk2a-Ribotag mice (5 weeks post glioma cell injection). Mice were sacrificed 6 hours after a single dose of AZD by cervical dislocation (treatment length determined based on previous experiments). Brains were dissected and the right frontal lobe was snap frozen in liquid nitrogen for RNA extraction, the rest of the brain was fixed in 4% PFA for immunohistochemistry.

Western blotting

Tissue was collected 1-25 hours after vehicle or AZD-8055 administration (20 mg/kg or 100 mg/kg AZD-8055). The right frontal brain lobe was lysed from male mice that were 12-15 weeks old. Tissue was lysed in 1 mL cell extraction buffer (Invitrogen #FNN10011) supplemented with protease (Sigma #P7626) and phosphatase inhibitors (Sigma#P5726, #P0044) with a Dounce homogenizer. Lysate was centrifuged and the supernatant was collected for total protein quantification. Total protein (30 μg) was loaded to a NuPAGE 4-12 % Bis-Tris gel and subject to gel electrophoresis according to the manufacturer's instructions (Invitrogen #NP0321BOX). Bands were detected by fluorescent imaging using the Typhoon imaging system. Licor and HRP secondary antibodies were also used for western blotting.

Antibodies

The following primary antibodies were used for immunofluorescence and western blotting: mouse monoclonal anti-HA.11 ascites (1:500, Biolegend #901515), rabbit anti-pS6 S240/244 (1:500, Cell Signaling #2215), rabbit anti-NeuN (1:500, Cell Signaling #12943), rabbit anti-pS6 S235/236 (1:1000, Cell Signaling #2211), rabbit anti-S6 (1:1000, Cell Signaling #2217), rabbit anti-β-actin (1:1000, Cell Signaling #4970S). The following secondary antibodies were used for immunofluorescence and western blotting: goat anti-rabbit Alexa 488 (1:1000, Invitrogen #A11008) and goat anti-mouse Alexa 568 (1:1000, Invitrogen #A11031).

Antibodies used for immuhistochemistry staining include rabbit anti-Olig2 (1:100, Millipore AB9610), mouse anti-HA (1:500, Biolegend #901515), mouse anti-NeuN (1:100, Millipore MAB 377), rabbit anti-Ki67 (1:500, Cell signaling 9129). The mouse anti-HA antibody was used for normal brain immunoprecipitations, and the rabbit polyclonal anti-HA (Abcam 9110) was used for tumor brain and treated tumor brain immunoprecipitations, we discovered that the rabbit antibody gave better RNA quality and yield.

6.2 Molecular biology for generating sequencing libraries

Immunoprecipitation

100 uL of lysate was used as input (total homogenate RNA) from which RNA was extracted using the RNeasy Mini kit (Qiagen). The remaining lysate was used for indirect immunoprecipitation (IP) of polysomes, we coupled 15uL of rabbit polyclonal anti-HA (abcam) to lysate with rotation at 4C for 4 hours. We used 150uL of protein G Dynabeads (30mg/mL, Life Technologies) and washed them with 600 uL polysome buffer. The conjugated lysate was then added to protein G-coated dynabeads and incubated with rotation at 4C overnight. Beads

were then washed with polysome buffer. RNA was extracted using the RNeasy Mini Kit and RNA integrity was assessed by Bioanalyzer (Agilent).

RNA sequencing libraries

RNA samples from Camk2a-Ribotag normal brain tissue were provided to the Columbia Sulzberger Genome Center for poly(A)-selection and RNA-Seq using the Illumina TruSeq kit. A total of four RNASeq libraries were generated for AZD-treated and vehicle normal mice. RNASeq libraries were generated from matched samples used in ligation-free ribosome profiling experiments. Four additional libraries were sequenced from non-ribosome profiling matched samples; two total input samples and two matched IP samples.

RNA samples from Camk2a-Ribotag tumor bearing tissue were depleted of ribosomal RNA using Ribo-Zero rRNA Removal Kit (MRZH11124) according to the manufacturer's protocol prior to library generation. Libraries were generated using the NEBNext Ultra Directional RNA Library Prep Kit for Illumina from New England Biolabs (E7420S) according to the manufacturer's protocol. Three RNASeq libraries were generated from total RNA from different three tumor brains. Three additional RNASeq libraries were generated from the polysome IP of the same three tumor brains.

Ribosome profiling libraries

Ribosome profiling libraries were generated from the same six total RNA samples described above, three tumor brains and three normal brains, using the SMARTer smRNA-Seq Kit for Illumina from Clontech laboratories (635029) as described previously (Hornstein, Torres et al. 2016). Briefly, ribosome footprints were isolated with a sucrose gradient, size selected and dephosphorylated. Ribosome footprints were polyadenylated, reverse transcribed, depleted of

ribosomal RNA using complimentary oligos, amplified by PCR and validated with bioanalyzer prior to sequencing.

6.3 Analysis of dendritic spine genes and dendritic spine density

Synaptosome isolation

The right frontal lobe from 5 tumor and 5 non-tumor bearing Camk2a-Ribotag mice was used for synaptosome isolation. I followed a synaptosome isolation protocol that has been previously described with a few modifications (Smalheiser and Lugli 2014). The tissue was flash frozen in liquid nitrogen and stored in liquid nitrogen until lysed. Tissue was lysed in 1mL homogenization buffer (50mM Hepes, 125mM NaCl, 100mM sucrose, 1:100 protease cocktail inhibitor) using a Dounce homogenizer on ice. 75uL of this lysate was saved for total homogenate, the rest was centrifuged at a low speed (1000g) for 10 minutes at 4 degrees, the pellet contained nuclear components and was saved. The supernatant was centrifuged (15000g) for 15 minutes at 4 degrees, the pellet contained crude synaptic membranes and was first washed then resuspended in 75uL cell extraction buffer (described above). The supernatant contained cytoplasmic components and was saved. The total, cytoplasmic and synaptic fractions were used for protein quantification using the BioRad DC Protein assay then used for western blot analysis as described above.

Diolistic labelling of brain sections and image analysis

DiI-coated tungsten particle preparation, delivery and tissue labeling were performed as described in (Staffend and Meisel 2011) with minor modifications. Mice were anaesthetized using a mixture of ketamine and xylaxine (100/10 mg/kg) and perfused with 10 mL PBS followed by 20 mL of a 2% PFA solution at a rate of 5 mL/min. Brains were removed, post-fixed

97

for 10 minutes in 2% PFA and transferred to PBS. 200 μm-thick coronal sections were acquired on a vibratome (Leica). Sections were labelled by delivery of DiI-coated tungsten beads using a Helios gene gun (Biorad) at 120 psi. DiI was allowed to diffuse for 24 hours at 4°C followed by post-fixation with 4% PFA for 1 hour at room temperature.

For antibody staining of DiI-labelled tissue, sections were permeabilized for 15 minutes in 0.1% Triton-X 100 in PBS and blocked in 0.01% Triton-X 100, 10% normal goat serum in PBS for 30 minutes at room temperature. Primary antibody (anti-HA; HA11 Covance) incubation was performed overnight at room temperature, followed by counterstain with secondary antibody and DAPI for 1 hour at room temperature. Sections were mounted on glass slides and imaged on an inverted Zeiss LSM 800 confocal microscope using a 63X/1.4 NA or a 40X/1.3 NA oil immersion objective. Images of whole labelled neurons were acquired at 1 μm steps. Z-stacks of dendritic spines were acquired at a frame size of 50.71×50.71μm (1024×1024 pixels) and a step size of 0.2 μm. Dendritic spine number was counted manually with the help of FIJI software (NIH).

6.4 Bioinformatics analysis

Mapping RNA sequencing libraries

The RNA-Seq data were aligned to the mm10 genome and RefSeq transcriptome annotation using the STAR aligner (Dobin, Davis et al. 2013) and quantified using the featureCounts program in the subread package (Liao, Smyth et al. 2014).

Enrichment score

Enrichment scores were derived from three normal brain IP experiments and the corresponding homogenates. The enrichment score was determined for each gene by first normalizing counts in

the IP and homogenate by size factors generated from DESeq2. Following normalization, the enrichment scores were calculated by dividing normalized IP counts by normalized homogenate counts as previously described (Hornstein, Torres et al. 2016). This analysis was also performed for 3 tumor brain IP experiments and their corresponding homogenates and 3 AZD treated tumor brain IPs and their corresponding homogenate. For the experiments described in chapter 2 and 3 we used an enrichment score cutoff of 1.5, genes with and ES>1.5 were considered enriched.

Differential gene expression

Differential expression analysis was accomplished using DESeq2 (Love, Huber et al. 2014). Differential gene expression analysis for RNA sequencing counts was performed using DESeq2 for 3 tumor brains vs 3 normal brains and for 3 AZD treated tumor brains vs 3 untreated tumor brains. This analysis was performed for tumor vs normal brain homogenate, tumor IP vs normal brain IP, AZD treated tumor homogenate vs untreated tumor homogenate, AZD treated tumor IP vs untreated tumor IP. From these analysis, only genes with p<0.05 were considered differentially expressed genes. This analysis also revealed whether differentially expressed genes were upregulated (log2 fold change>0) or downregulated (log2 fold change<0).

Gene ontology

Gene ontology analysis was performed using the panther classification system (Thomas, Campbell et al. 2003). Gene ontology enrichment analysis was performed for molecular function and only the top 2-5 gene ontologies are shown in our figures. We also used DAVID gene ontology analysis for experiments described in chapter 3 (Huang, Sherman et al. 2008, Huang, Sherman et al. 2009). Gene ontology analysis for chapter 4 was performed as described previously (Hornstein, Torres et al. 2016).

Translation efficiency

To calculate translation efficiency and analyze differential translation efficiency we used the RiboDiff algorithm as described before (Zhong, Karaletsos et al. 2015, Hornstein, Torres et al. 2016). This analysis was performed for differential translation efficiency between normal brain vs AZD treated normal brain and tumor homogenate vs normal brain homogenate.

Gene set enrichment analysis (GSEA)

GSEA was performed as described for the published experiments in chapter 4. The results were used to define which genes were most associated with specific cell types. GSEA was performed for normal brain and tumor brains using the list of neuron specific genes from a previous study (Zhang, Chen et al. 2014). GSEA was also performed for the homogenate and IP tumor data using the list of genes enriched in RNA granules from a previous study (El Fatimy, Davidovic et al. 2016). Gene set enrichment analysis was done using the GSEA Java program from the Broad Institute in "pre-ranked/classic" mode after removing all genes in the annotation that do not encode proteins (Subramanian, Tamayo et al. 2005). Genes were ranked either by their RiboTag enrichment scores or by their -/+log (p adj) from differential expression analysis.

REFERENCES

1. Chiu IM, Morimoto ET, Goodarzi H, Liao JT, O'Keeffe S, Phatnani HP, Muratet M, Carroll MC, Levy S, Tavazoie S, et al. A neurodegeneration-specific gene-expression signature of acutely isolated microglia from an amyotrophic lateral sclerosis mouse model. Cell Rep. 2013;4(2):385–401.

2. Akhavan, D., T. F. Cloughesy and P. S. Mischel (2010). "mTOR signaling in glioblastoma: lessons learned from bench to bedside." Neuro-Oncology.

3. Allen, N. J. and B. A. Barres (2009). "Glia — more than just brain glue." Nature **457**: 675.

4. Assanah, M., R. Lochhead, A. Ogden, J. Bruce, J. Goldman and P. Canoll (2006). "Glial Progenitors in Adult White Matter Are Driven to Form Malignant Gliomas by Platelet-Derived Growth Factor-Expressing Retroviruses." The Journal of Neuroscience **26**(25): 6781-6790.

5. Bai, F. and F. A. Witzmann (2007). "Synaptosome Proteomics." Sub-cellular biochemistry **43**: 77-98.

6. Bergo, E., G. Lombardi, I. Guglieri, E. Capovilla, A. Pambuku and V. Zagonel (2015). "Neurocognitive functions and health-related quality of life in glioblastoma patients: a concise review of the literature." European Journal of Cancer Care: n/a-n/a.

7. Bergo, E., G. Lombardi, A. Pambuku, A. Della Puppa, L. Bellu, #x, D. Avella and V. Zagonel (2016). "Cognitive Rehabilitation in Patients with Gliomas and Other Brain Tumors: State of the Art." BioMed Research International **2016**: 11.

8. Bhat, M., N. Robichaud, L. Hulea, N. Sonenberg, J. Pelletier and I. Topisirovic (2015). "Targeting the translation machinery in cancer." Nature Reviews Drug Discovery **14**: 261.

9. Bian, E.-B., J. Li, X.-J. He, G. Zong, T. Jiang, J. Li and B. Zhao (2014). "Epigenetic modification in gliomas: role of the histone methyltransferase EZH2." Expert Opinion on Therapeutic Targets **18**(10): 1197-1206.

10. Bockaert, J. and P. Marin (2015). "mTOR in Brain Physiology and Pathologies." Physiological Reviews **95**(4): 1157-1187.

11. Bosma, I., M. J. Vos, J. J. Heimans, M. J. B. Taphoorn, N. K. Aaronson, T. J. Postma, H. M. van der Ploeg, M. Muller, W. P. Vandertop, B. J. Slotman and M. Klein (2007). "The course of neurocognitive functioning in high-grade glioma patients." Neuro-Oncology **9**(1): 53-62.

12. Brar, G. A. and J. S. Weissman (2015). "Ribosome profiling reveals the what, when, where, and how of protein synthesis." Nature reviews. Molecular cell biology **16**(11): 651-664.

13. Brennan, C. W., R. G. W. Verhaak, A. McKenna, B. Campos, H. Noushmehr, S. R. Salama, S. Zheng, D. Chakravarty, J. Z. Sanborn, S. H. Berman, R. Beroukhim, B. Bernard, C.-J. Wu,

G. Genovese, I. Shmulevich, J. Barnholtz-Sloan, L. Zou, R. Vegesna, S. A. Shukla, G. Ciriello, W. K. Yung, W. Zhang, C. Sougnez, T. Mikkelsen, K. Aldape, D. D. Bigner, E. G. Van Meir, M. Prados, A. Sloan, K. L. Black, J. Eschbacher, G. Finocchiaro, W. Friedman, D. W. Andrews, A. Guha, M. Iacocca, B. P. O'Neill, G. Foltz, J. Myers, D. J. Weisenberger, R. Penny, R. Kucherlapati, C. M. Perou, D. N. Hayes, R. Gibbs, M. Marra, G. B. Mills, E. Lander, P. Spellman, R. Wilson, C. Sander, J. Weinstein, M. Meyerson, S. Gabriel, P. W. Laird, D. Haussler, G. Getz and L. Chin (2013). "The Somatic Genomic Landscape of Glioblastoma." <u>Cell</u> **155**(2): 462-477.

14. Buckingham, S. C., S. L. Campbell, B. R. Haas, V. Montana, S. Robel, T. Ogunrinu and H. Sontheimer (2011). "Glutamate release by primary brain tumors induces epileptic activity." <u>Nat Med</u> **17**(10): 1269-1274.

15. Buffo, A., I. Rite, P. Tripathi, A. Lepier, D. Colak, A.-P. Horn, T. Mori and M. Götz (2008). "Origin and progeny of reactive gliosis: A source of multipotent cells in the injured brain." <u>Proceedings of the National Academy of Sciences of the United States of America</u> **105**(9): 3581-3586.

16. Cahoy, J. D., B. Emery, A. Kaushal, L. C. Foo, J. L. Zamanian, K. S. Christopherson, Y. Xing, J. L. Lubischer, P. A. Krieg, S. A. Krupenko, W. J. Thompson and B. A. Barres (2008). "A Transcriptome Database for Astrocytes, Neurons, and Oligodendrocytes: A New Resource for Understanding Brain Development and Function." <u>The Journal of Neuroscience</u> **28**(1): 264-278.

17. Campbell, S. L., S. C. Buckingham and H. Sontheimer (2012). "Human glioma cells induce hyperexcitability in cortical networks." <u>Epilepsia</u> **53**(8): 1360-1370.

18. Chresta, C. M., B. R. Davies, I. Hickson, T. Harding, S. Cosulich, S. E. Critchlow, J. P. Vincent, R. Ellston, D. Jones, P. Sini, D. James, Z. Howard, P. Dudley, G. Hughes, L. Smith, S. Maguire, M. Hummersone, K. Malagu, K. Menear, R. Jenkins, M. Jacobsen, G. C. Smith, S. Guichard and M. Pass (2010). "AZD8055 is a potent, selective, and orally bioavailable ATP-competitive mammalian target of rapamycin kinase inhibitor with in vitro and in vivo antitumor activity." <u>Cancer Res</u> **70**(1): 288-298.

19. Citraro, R., A. Leo, A. Constanti, E. Russo and G. De Sarro (2016). "mTOR pathway inhibition as a new therapeutic strategy in epilepsy and epileptogenesis." <u>Pharmacological Research</u> **107**: 333-343.

20. Claes, A., A. J. Idema and P. Wesseling (2007). "Diffuse glioma growth: a guerilla war." <u>Acta Neuropathologica</u> **114**(5): 443-458.

21. Coniglio, S. J. and J. E. Segall (2013). "Review: Molecular mechanism of microglia stimulated glioblastoma invasion." <u>Matrix Biology</u> **32**(7): 372-380.

22. Crino, P. B. (2011). "mTOR: A pathogenic signaling pathway in developmental brain malformations." <u>Trends in Molecular Medicine</u> **17**(12): 734-742.

23. Cuddapah, V. A., S. Robel, S. Watkins and H. Sontheimer (2014). "A neurocentric perspective on glioma invasion." Nature Reviews Neuroscience **15**: 455.

24. Cuevas-Diaz Duran, R., H. Wei and J. Q. Wu (2017). "Single-cell RNA-sequencing of the brain." Clinical and Translational Medicine **6**: 20.

25. Curatolo, P. and R. Moavero (2013). "mTOR inhibitors as a new therapeutic option for epilepsy." Expert Review of Neurotherapeutics **13**(6): 627-638.

26. Darmanis, S., S. A. Sloan, D. Croote, M. Mignardi, S. Chernikova, P. Samghababi, Y. Zhang, N. Neff, M. Kowarsky, C. Caneda, G. Li, S. D. Chang, I. D. Connolly, Y. Li, B. A. Barres, M. H. Gephart and S. R. Quake (2017). "Single-Cell RNA-Seq Analysis of Infiltrating Neoplastic Cells at the Migrating Front of Human Glioblastoma." Cell Reports **21**(5): 1399-1410.

27. Davis, M. E. (2016). "Glioblastoma: Overview of Disease and Treatment." Clinical journal of oncology nursing **20**(5): S2-S8.

28. de Groot, J. and H. Sontheimer (2011). "Glutamate and the Biology of Gliomas." Glia **59**(8): 1181-1189.

29. Delgado-López, P. D., E. M. Corrales-García, J. Martino, E. Lastra-Aras and M. T. Dueñas-Polo (2017). "Diffuse low-grade glioma: a review on the new molecular classification, natural history and current management strategies." Clinical and Translational Oncology **19**(8): 931-944.

30. Desmurget, M., F. Bonnetblanc and H. Duffau (2007). "Contrasting acute and slow-growing lesions: a new door to brain plasticity." Brain **130**(4): 898-914.

31. Di Liegro, C. M., G. Schiera and I. Di Liegro (2014). "Regulation of mRNA transport, localization and translation in the nervous system of mammals (Review)." International Journal of Molecular Medicine **33**(4): 747-762.

32. Dobin, A., C. A. Davis, F. Schlesinger, J. Drenkow, C. Zaleski, S. Jha, P. Batut, M. Chaisson and T. R. Gingeras (2013). "STAR: ultrafast universal RNA-seq aligner." Bioinformatics **29**(1): 15-21.

33. Dougherty, J. D., E. F. Schmidt, M. Nakajima and N. Heintz (2010). "Analytical approaches to RNA profiling data for the identification of genes enriched in specific cells." Nucleic Acids Research **38**(13): 4218-4230.

34. Doyle, J. P., J. D. Dougherty, M. Heiman, E. F. Schmidt, T. R. Stevens, G. Ma, S. Bupp, P. Shrestha, R. D. Shah, M. L. Doughty, S. Gong, P. Greengard and N. Heintz (2008). "Application of a Translational Profiling Approach for the Comparative Analysis of CNS Cell Types." Cell **135**(4): 749-762.

35. Doyle, M. and M. A. Kiebler (2011). "Mechanisms of dendritic mRNA transport and its role in synaptic tagging." The EMBO Journal **30**(17): 3540-3552.

36. Dragatsis, I. and S. Zeitlin (2000). "CaMKIIα-cre transgene expression and recombination patterns in the mouse brain." genesis **26**(2): 133-135.

37. Duffau, H. (2014). "Diffuse low-grade gliomas and neuroplasticity." Diagnostic and Interventional Imaging **95**(10): 945-955.

38. Efeyan, A. and D. M. Sabatini (2010). "mTOR and cancer: many loops in one pathway." Curr Opin Cell Biol **22**(2): 169-176.

39. El Fatimy, R., L. Davidovic, S. Tremblay, X. Jaglin, A. Dury, C. Robert, P. De Koninck and E. W. Khandjian (2016). "Tracking the Fragile X Mental Retardation Protein in a Highly Ordered Neuronal RiboNucleoParticles Population: A Link between Stalled Polyribosomes and RNA Granules." PLOS Genetics **12**(7): e1006192.

40. Etcheverry, A., M. Aubry, M. de Tayrac, E. Vauleon, R. Boniface, F. Guenot, S. Saikali, A. Hamlat, L. Riffaud, P. Menei, V. Quillien and J. Mosser (2010). "DNA methylation in glioblastoma: impact on gene expression and clinical outcome." BMC Genomics **11**: 701-701.

41. Fan, Q.-W. and W. A. Weiss (2012). "Inhibition of PI3K-Akt-mTOR Signaling in Glioblastoma by mTORC1/2 Inhibitors." Methods in Molecular Biology (Clifton, N.j.) **821**: 349-359.

42. Feldman, M. E., B. Apsel, A. Uotila, R. Loewith, Z. A. Knight, D. Ruggero and K. M. Shokat (2009). "Active-site inhibitors of mTOR target rapamycin-resistant outputs of mTORC1 and mTORC2." PLoS Biol **7**(2): e38.

43. Földy, C., S. Darmanis, J. Aoto, R. C. Malenka, S. R. Quake and T. C. Südhof (2016). "Single-cell RNAseq reveals cell adhesion molecule profiles in electrophysiologically defined neurons." Proceedings of the National Academy of Sciences of the United States of America **113**(35): E5222-E5231.

44. Freije, W. A., F. E. Castro-Vargas, Z. Fang, S. Horvath, T. Cloughesy, L. M. Liau, P. S. Mischel and S. F. Nelson (2004). "Gene Expression Profiling of Gliomas Strongly Predicts Survival." Cancer Research **64**(18): 6503.

45. French, J. A., J. A. Lawson, Z. Yapici, H. Ikeda, T. Polster, R. Nabbout, P. Curatolo, P. J. de Vries, D. J. Dlugos, N. Berkowitz, M. Voi, S. Peyrard, D. Pelov and D. N. Franz (2016). "Adjunctive everolimus therapy for treatment-resistant focal-onset seizures associated with tuberous sclerosis (EXIST-3): a phase 3, randomised, double-blind, placebo-controlled study." The Lancet **388**(10056): 2153-2163.

46. Gal-Ben-Ari, S., J. W. Kenney, H. Ounalla-Saad, E. Taha, O. David, D. Levitan, I. Gildish, D. Panja, B. Pai, K. Wibrand, T. I. Simpson, C. G. Proud, C. R. Bramham, J. D. Armstrong and K. Rosenblum (2012). "Consolidation and translation regulation." Learning & Memory **19**(9): 410-422.

47. Garrido-Gil, P., P. Fernandez-Rodríguez, J. Rodríguez-Pallares and J. L. Labandeira-Garcia (2017). "Laser capture microdissection protocol for gene expression analysis in the brain." Histochemistry and Cell Biology **148**(3): 299-311.

48. Gill, B. J., D. J. Pisapia, H. R. Malone, H. Goldstein, L. Lei, A. Sonabend, J. Yun, J. Samanamud, J. S. Sims, M. Banu, A. Dovas, A. F. Teich, S. A. Sheth, G. M. McKhann, M. B. Sisti, J. N. Bruce, P. A. Sims and P. Canoll (2014). "MRI-localized biopsies reveal subtype-specific differences in molecular and cellular composition at the margins of glioblastoma." Proceedings of the National Academy of Sciences of the United States of America **111**(34): 12550-12555.

49. Goel, S., S. B. Wharton, L. P. Brett and I. R. Whittle (2003). "Morphological changes and stress responses in neurons in cerebral cortex infiltrated by diffuse astrocytoma." Neuropathology **23**(4): 262-270.

50. Goellner, B. A., Hermann (2011). "The synaptic cytoskeleton in development and disease." Developmental Neurobiology **72**(1): 111-125.

51. Gonzalez, C., J. S. Sims, N. Hornstein, A. Mela, F. Garcia, L. Lei, D. A. Gass, B. Amendolara, J. N. Bruce, P. Canoll and P. A. Sims (2014). "Ribosome Profiling Reveals a Cell-Type-Specific Translational Landscape in Brain Tumors." The Journal of Neuroscience **34**(33): 10924-10936.

52. Guan, X., M. N. Hasan, S. Maniar, W. Jia and D. Sun (2018). "Reactive Astrocytes in Glioblastoma Multiforme." Molecular Neurobiology.

53. Guertin, D. A. and D. M. Sabatini (2009). "The Pharmacology of mTOR Inhibition." Science Signaling **2**(67): pe24-pe24.

54. Guo, D., L. Zeng, D. L. Brody and M. Wong (2013). "Rapamycin Attenuates the Development of Posttraumatic Epilepsy in a Mouse Model of Traumatic Brain Injury." PLoS ONE **8**(5): e64078.

55. Gutmann, D. H. (2015). "Microglia in the tumor microenvironment: taking their TOLL on glioma biology." Neuro-Oncology **17**(2): 171-173.

56. Hambardzumyan, D., D. H. Gutmann and H. Kettenmann (2015). "The role of microglia and macrophages in glioma maintenance and progression." Nature Neuroscience **19**: 20.

57. Hawrylycz, M. J., E. S. Lein, A. L. Guillozet-Bongaarts, E. H. Shen, L. Ng, J. A. Miller, L. N. van de Lagemaat, K. A. Smith, A. Ebbert, Z. L. Riley, C. Abajian, C. F. Beckmann, A. Bernard, D. Bertagnolli, A. F. Boe, P. M. Cartagena, M. M. Chakravarty, M. Chapin, J. Chong, R. A. Dalley, B. D. Daly, C. Dang, S. Datta, N. Dee, T. A. Dolbeare, V. Faber, D. Feng, D. R. Fowler, J. Goldy, B. W. Gregor, Z. Haradon, D. R. Haynor, J. G. Hohmann, S. Horvath, R. E. Howard, A. Jeromin, J. M. Jochim, M. Kinnunen, C. Lau, E. T. Lazarz, C. Lee, T. A. Lemon, L. Li, Y. Li, J. A. Morris, C. C. Overly, P. D. Parker, S. E. Parry, M. Reding, J. J. Royall, J. Schulkin, P. A. Sequeira, C. R. Slaughterbeck, S. C. Smith, A. J. Sodt, S. M. Sunkin, B. E. Swanson, M. P. Vawter, D. Williams, P. Wohnoutka, H. R. Zielke, D. H.

Geschwind, P. R. Hof, S. M. Smith, C. Koch, S. G. N. Grant and A. R. Jones (2012). "An anatomically comprehensive atlas of the adult human brain transcriptome." <u>Nature</u> **489**: 391.

58. Haydon, P. G. and M. Nedergaard (2015). "How Do Astrocytes Participate in Neural Plasticity?" <u>Cold Spring Harbor Perspectives in Biology</u> **7**(3): a020438.

59. Heiman, M., R. Kulicke, R. J. Fenster, P. Greengard and N. Heintz (2014). "Cell-Type-Specific mRNA Purification by Translating Ribosome Affinity Purification (TRAP)." <u>Nature protocols</u> **9**(6): 1282-1291.

60. Heiman, M., A. Schaefer, S. Gong, J. D. Peterson, M. Day, K. E. Ramsey, M. Suárez-Fariñas, C. Schwarz, D. A. Stephan, D. J. Surmeier, P. Greengard and N. Heintz (2008). "A Translational Profiling Approach for the Molecular Characterization of CNS Cell Types." <u>Cell</u> **135**(4): 738-748.

61. Helmy, K., J. Halliday, E. Fomchenko, M. Setty, K. Pitter, C. Hafemeister and E. C. Holland (2012). "Identification of Global Alteration of Translational Regulation in Glioma In Vivo." <u>PLOS ONE</u> **7**(10): e46965.

62. Herms, J. and M. M. Dorostkar (2016). "Dendritic Spine Pathology in Neurodegenerative Diseases." <u>Annual Review of Pathology: Mechanisms of Disease</u> **11**(1): 221-250.

63. Hershey, J. W. B., N. Sonenberg and M. B. Mathews (2012). "Principles of Translational Control: An Overview." <u>Cold Spring Harbor Perspectives in Biology</u> **4**(12): a011528.

64. Hlushchenko, I., M. Koskinen and P. Hotulainen (2016). "Dendritic spine actin dynamics in neuronal maturation and synaptic plasticity." <u>Cytoskeleton</u> **73**(9): 435-441.

65. Hoeffer, C. A. and E. Klann (2010). "mTOR Signaling: At the Crossroads of Plasticity, Memory, and Disease." <u>Trends in neurosciences</u> **33**(2): 67.

66. Hornstein, N., D. Torres, S. Das Sharma, G. Tang, P. Canoll and P. A. Sims (2016). "Ligation-free ribosome profiling of cell type-specific translation in the brain." <u>Genome Biology</u> **17**(1): 149.

67. Hsieh, A. C., Y. Liu, M. P. Edlind, N. T. Ingolia, M. R. Janes, A. Sher, E. Y. Shi, C. R. Stumpf, C. Christensen, M. J. Bonham, S. Wang, P. Ren, M. Martin, K. Jessen, M. E. Feldman, J. S. Weissman, K. M. Shokat, C. Rommel and D. Ruggero (2012). "The translational landscape of mTOR signalling steers cancer initiation and metastasis." <u>Nature</u> **485**(7396): 55-61.

68. Huang, D. W., B. T. Sherman and R. A. Lempicki (2008). "Systematic and integrative analysis of large gene lists using DAVID bioinformatics resources." <u>Nature Protocols</u> **4**: 44.

69. Huang, D. W., B. T. Sherman and R. A. Lempicki (2009). "Bioinformatics enrichment tools: paths toward the comprehensive functional analysis of large gene lists." <u>Nucleic Acids Research</u> **37**(1): 1-13.

70. Huang, X., H. Zhang, J. Yang, J. Wu, J. McMahon, Y. Lin, Z. Cao, M. Gruenthal and Y. Huang (2010). "Pharmacological inhibition of the mammalian target of rapamycin pathway suppresses acquired epilepsy." Neurobiology of disease **40**(1): 193-199.

71. Huberfeld, G. and C. J. Vecht (2016). "Seizures and gliomas — towards a single therapeutic approach." Nature Reviews Neurology **12**: 204.

72. Huberfeld, G. and C. J. Vecht (2016). "Seizures and gliomas [mdash] towards a single therapeutic approach." Nat Rev Neurol **12**(4): 204-216.

73. Hunt, C., L. Schenker and M. Kennedy (1996). "PSD-95 is associated with the postsynaptic density and not with the presynaptic membrane at forebrain synapses." The Journal of Neuroscience **16**(4): 1380-1388.

74. Huszthy, P. C., I. Daphu, S. P. Niclou, D. Stieber, J. M. Nigro, P. Ø. Sakariassen, H. Miletic, F. Thorsen and R. Bjerkvig (2012). "In vivo models of primary brain tumors: pitfalls and perspectives." Neuro-Oncology **14**(8): 979-993.

75. Ingolia, N. T. (2016). "Ribosome Footprint Profiling of Translation throughout the Genome." Cell **165**(1): 22-33.

76. Ingolia, N. T., S. Ghaemmaghami, J. R. Newman and J. S. Weissman (2009). "Genome-wide analysis in vivo of translation with nucleotide resolution using ribosome profiling." Science **324**.

77. Ivanov, A., M. Esclapez and L. Ferhat (2009). "Role of drebrin A in dendritic spine plasticity and synaptic function: Implications in neurological disorders." Communicative & Integrative Biology **2**(3): 268-270.

78. Jaworski, J., S. Spangler, D. P. Seeburg, C. C. Hoogenraad and M. Sheng (2005). "Control of Dendritic Arborization by the Phosphoinositide-3′-Kinase–Akt–Mammalian Target of Rapamycin Pathway." The Journal of Neuroscience **25**(49): 11300-11312.

79. Johung, T. and M. Monje (2017). "Neuronal activity in the glioma microenvironment." Current Opinion in Neurobiology **47**: 156-161.

80. Kapeli, K. and G. W. Yeo (2012). "Genome-Wide Approaches to Dissect the Roles of RNA Binding Proteins in Translational Control: Implications for Neurological Diseases." Frontiers in Neuroscience **6**: 144.

81. Katz, A. M., N. M. Amankulor, K. Pitter, K. Helmy, M. Squatrito and E. C. Holland (2012). "Astrocyte-Specific Expression Patterns Associated with the PDGF-Induced Glioma Microenvironment." PLOS ONE **7**(2): e32453.

82. Kiebler, M. A. and G. J. Bassell (2006). "Neuronal RNA Granules: Movers and Makers." Neuron **51**(6): 685-690.

83. Kim, K. H. and C. W. M. Roberts (2016). "Targeting EZH2 in cancer." Nature Medicine **22**: 128.

84. King, H. A. and A. P. Gerber (2016). "Translatome profiling: methods for genome-scale analysis of mRNA translation." Briefings in Functional Genomics **15**(1): 22-31.

85. Kong, N. W., W. R. Gibb and M. C. Tate (2016). "Neuroplasticity: Insights from Patients Harboring Gliomas." Neural Plasticity **2016**: 12.

86. Kreis, P., R. Hendricusdottir, L. Kay, I. E. Papageorgiou, M. van Diepen, T. Mack, J. Ryves, A. Harwood, N. R. Leslie, O. Kann, M. Parsons and B. J. Eickholt (2013). "Phosphorylation of the Actin Binding Protein Drebrin at S647 Is Regulated by Neuronal Activity and PTEN." PLOS ONE **8**(8): e71957.

87. Krueger , D. A., M. M. Care , K. Holland , K. Agricola , C. Tudor , P. Mangeshkar , K. A. Wilson , A. Byars , T. Sahmoud and D. N. Franz (2010). "Everolimus for Subependymal Giant-Cell Astrocytomas in Tuberous Sclerosis." New England Journal of Medicine **363**(19): 1801-1811.

88. Krueger Darcy, A., A. Wilfong Angus, K. Holland-Bouley, E. Anderson Anne, K. Agricola, C. Tudor, M. Mays, M. Lopez Christina, M. O. Kim and N. Franz David (2013). "Everolimus treatment of refractory epilepsy in tuberous sclerosis complex." Annals of Neurology **74**(5): 679-687.

89. La Manno, G., D. Gyllborg, S. Codeluppi, K. Nishimura, C. Salto, A. Zeisel, Lars E. Borm, Simon R. Stott, Enrique M. Toledo, J C. Villaescusa, P. Lönnerberg, J. Ryge, Roger A. Barker, E. Arenas and S. Linnarsson (2016). "Molecular Diversity of Midbrain Development in Mouse, Human, and Stem Cells." Cell **167**(2): 566-580.e519.

90. Lai, K.-O. and N. Y. Ip (2013). "Structural plasticity of dendritic spines: The underlying mechanisms and its dysregulation in brain disorders." Biochimica et Biophysica Acta (BBA) - Molecular Basis of Disease **1832**(12): 2257-2263.

91. Laplante, M. and D. M. Sabatini (2009). "mTOR signaling at a glance." Journal of Cell Science **122**(20): 3589-3594.

92. Lei, L., A. M. Sonabend, P. Guarnieri, C. Soderquist, T. Ludwig, S. Rosenfeld, J. N. Bruce and P. Canoll (2011). "Glioblastoma Models Reveal the Connection between Adult Glial Progenitors and the Proneural Phenotype." PLOS ONE **6**(5): e20041.

93. Lein, E. S., M. J. Hawrylycz, N. Ao, M. Ayres, A. Bensinger, A. Bernard, A. F. Boe, M. S. Boguski, K. S. Brockway, E. J. Byrnes, L. Chen, L. Chen, T.-M. Chen, M. Chi Chin, J. Chong, B. E. Crook, A. Czaplinska, C. N. Dang, S. Datta, N. R. Dee, A. L. Desaki, T. Desta, E. Diep, T. A. Dolbeare, M. J. Donelan, H.-W. Dong, J. G. Dougherty, B. J. Duncan, A. J. Ebbert, G. Eichele, L. K. Estin, C. Faber, B. A. Facer, R. Fields, S. R. Fischer, T. P. Fliss, C. Frensley, S. N. Gates, K. J. Glattfelder, K. R. Halverson, M. R. Hart, J. G. Hohmann, M. P. Howell, D. P. Jeung, R. A. Johnson, P. T. Karr, R. Kawal, J. M. Kidney, R. H. Knapik, C. L. Kuan, J. H. Lake, A. R. Laramee, K. D. Larsen, C. Lau, T. A. Lemon, A. J. Liang, Y. Liu, L.

T. Luong, J. Michaels, J. J. Morgan, R. J. Morgan, M. T. Mortrud, N. F. Mosqueda, L. L. Ng, R. Ng, G. J. Orta, C. C. Overly, T. H. Pak, S. E. Parry, S. D. Pathak, O. C. Pearson, R. B. Puchalski, Z. L. Riley, H. R. Rockett, S. A. Rowland, J. J. Royall, M. J. Ruiz, N. R. Sarno, K. Schaffnit, N. V. Shapovalova, T. Sivisay, C. R. Slaughterbeck, S. C. Smith, K. A. Smith, B. I. Smith, A. J. Sodt, N. N. Stewart, K.-R. Stumpf, S. M. Sunkin, M. Sutram, A. Tam, C. D. Teemer, C. Thaller, C. L. Thompson, L. R. Varnam, A. Visel, R. M. Whitlock, P. E. Wohnoutka, C. K. Wolkey, V. Y. Wong, M. Wood, M. B. Yaylaoglu, R. C. Young, B. L. Youngstrom, X. Feng Yuan, B. Zhang, T. A. Zwingman and A. R. Jones (2007). "Genome-wide atlas of gene expression in the adult mouse brain." <u>Nature</u> **445**(7124): 168-176.

94. Lepeta, K., M. V. Lourenco, B. C. Schweitzer, P. V. M. Adami, P. Banerjee, S. Catuara-Solarz, M. L. F. Revenga, A. M. Guillem, M. Haidar, O. M. Ijomone, B. Nadorp, L. Qi, N. D. Perera, L. K. Refsgaard, K. M. Reid, M. Sabbar, A. Sahoo, N. Schaefer, R. K. Sheean, A. Suska, R. Verma, C. Vicidomini, D. Wright, X. D. Zhang and C. Seidenbecher (2016). "Synaptopathies: synaptic dysfunction in neurological disorders – A review from students to students." <u>Journal of Neurochemistry</u> **138**(6): 785-805.

95. Liao, Y., G. K. Smyth and W. Shi (2014). "featureCounts: an efficient general purpose program for assigning sequence reads to genomic features." <u>Bioinformatics</u> **30**(7): 923-930.

96. Liddelow, S. A. and B. A. Barres "Reactive Astrocytes: Production, Function, and Therapeutic Potential." <u>Immunity</u> **46**(6): 957-967.

97. Lin, W.-H. and D. J. Webb (2009). "Actin and Actin-Binding Proteins: Masters of Dendritic Spine Formation, Morphology, and Function." <u>The open neuroscience journal</u> **3**: 54-66.

98. Lipton, J. O. and M. Sahin (2014). "The Neurology of mTOR." <u>Neuron</u> **84**(2): 275-291.

99. Louis, D. N., A. Perry, G. Reifenberger, A. von Deimling, D. Figarella-Branger, W. K. Cavenee, H. Ohgaki, O. D. Wiestler, P. Kleihues and D. W. Ellison (2016). "The 2016 World Health Organization Classification of Tumors of the Central Nervous System: a summary." <u>Acta Neuropathologica</u> **131**(6): 803-820.

100. Love, M. I., W. Huber and S. Anders (2014). "Moderated estimation of fold change and dispersion for RNA-seq data with DESeq2." <u>Genome Biology</u> **15**(12): 550.

101. Lu, F., Y. Chen, C. Zhao, H. Wang, D. He, L. Xu, J. Wang, X. He, Y. Deng, E. E. Lu, X. Liu, R. Verma, H. Bu, R. Drissi, M. Fouladi, A. O. Stemmer-Rachamimov, D. Burns, M. Xin, J. B. Rubin, E. M. Bahassi, P. Canoll, E. C. Holland and Q. R. Lu (2016). "Olig2-Dependent Reciprocal Shift in PDGF and EGF Receptor Signaling Regulates Tumor Phenotype and Mitotic Growth in Malignant Glioma." <u>Cancer cell</u> **29**(5): 669-683.

102. Maier, T., M. Güell and L. Serrano (2009). "Correlation of mRNA and protein in complex biological samples." <u>FEBS Letters</u> **583**(24): 3966-3973.

103. Maiti, P., J. Manna, G. Ilavazhagan, J. Rossignol and G. L. Dunbar (2015). "Molecular regulation of dendritic spine dynamics and their potential impact on synaptic plasticity and neurological diseases." <u>Neuroscience & Biobehavioral Reviews</u> **59**: 208-237.

104.   Maleszewska, M. and B. Kaminska (2013). "Is Glioblastoma an Epigenetic Malignancy?" Cancers **5**(3): 1120-1139.

105.   Mašek, T., L. Valášek and M. Pospíšek (2011). Polysome Analysis and RNA Purification from Sucrose Gradients. RNA: Methods and Protocols. H. Nielsen. Totowa, NJ, Humana Press**:** 293-309.

106.   Masui, K., P. S. Mischel and G. Reifenberger (2016). Chapter 6 - Molecular classification of gliomas. Handbook of Clinical Neurology. M. S. Berger and M. Weller, Elsevier. **134:** 97-120.

107.   Mayer, C. and I. Grummt (2006). "Ribosome biogenesis and cell growth: mTOR coordinates transcription by all three classes of nuclear RNA polymerases." Oncogene **25**: 6384.

108.   Meikle, L., D. M. Talos, H. Onda, K. Pollizzi, A. Rotenberg, M. Sahin, F. E. Jensen and D. J. Kwiatkowski (2007). "A Mouse Model of Tuberous Sclerosis: Neuronal Loss of Tsc1 Causes Dysplastic and Ectopic Neurons, Reduced Myelination, Seizure Activity, and Limited Survival." The Journal of Neuroscience **27**(21): 5546-5558.

109.   Meyers, C. A., & Kayl, A.E. (2002). Neurocognitive Function. Cancer in the nervous system. Oxford, Oxford University Press**:** 557-571.

110.   Meyuhas, O. (2000). "Synthesis of the translational apparatus is regulated at the translational level." Eur J Biochem **267**.

111.   Miotto, E. C., A. Silva Junior, C. C. Silva, H. N. Cabrera, M. A. R. Machado, G. R. G. Benute, M. C. S. Lucia, M. Scaff and M. J. Teixeira (2011). "Cognitive impairments in patients with low grade gliomas and high grade gliomas." Arquivos de Neuro-Psiquiatria **69**: 596-601.

112.   Mizui, T., H. Takahashi, Y. Sekino and T. Shirao (2005). "Overexpression of drebrin A in immature neurons induces the accumulation of F-actin and PSD-95 into dendritic filopodia, and the formation of large abnormal protrusions." Molecular and Cellular Neuroscience **30**(1): 149-157.

113.   Moschetta, M., A. Reale, C. Marasco, A. Vacca and M. R. Carratù (2014). "Therapeutic targeting of the mTOR-signalling pathway in cancer: benefits and limitations." British Journal of Pharmacology **171**(16): 3801-3813.

114.   Naing, A., C. Aghajanian, E. Raymond, D. Olmos, G. Schwartz, E. Oelmann, L. Grinsted, W. Burke, R. Taylor, S. Kaye, R. Kurzrock and U. Banerji (2012). "Safety, tolerability, pharmacokinetics and pharmacodynamics of AZD8055 in advanced solid tumours and lymphoma." British Journal of Cancer **107**(7): 1093-1099.

115.   Noebels, J. (2015). "Pathway-driven discovery of epilepsy genes." **18**: 344.

116.   Nudo, R. J. (2013). "Recovery after brain injury: mechanisms and principles." <u>Frontiers in Human Neuroscience</u> **7**: 887.

117.   Nutt, C. L., D. R. Mani, R. A. Betensky, P. Tamayo, J. G. Cairncross, C. Ladd, U. Pohl, C. Hartmann, M. E. McLaughlin, T. T. Batchelor, P. M. Black, A. von Deimling, S. L. Pomeroy, T. R. Golub and D. N. Louis (2003). "Gene Expression-based Classification of Malignant Gliomas Correlates Better with Survival than Histological Classification." <u>Cancer Research</u> **63**(7): 1602.

118.   O'Brien, E. R., C. Howarth and N. R. Sibson (2013). "The role of astrocytes in CNS tumors: pre-clinical models and novel imaging approaches." <u>Frontiers in Cellular Neuroscience</u> **7**: 40.

119.   Oh, W. J. and E. Jacinto (2011). "mTOR complex 2 signaling and functions." <u>Cell Cycle</u> **10**(14): 2305-2316.

120.   Olah, M., E. Patrick, A.-C. Villani, J. Xu, C. C. White, K. J. Ryan, P. Piehowski, A. Kapasi, P. Nejad, M. Cimpean, S. Connor, C. J. Yung, M. Frangieh, A. McHenry, W. Elyaman, V. Petyuk, J. A. Schneider, D. A. Bennett, P. L. De Jager and E. M. Bradshaw (2018). "A transcriptomic atlas of aged human microglia." <u>Nature Communications</u> **9**(1): 539.

121.   Ota, Y., A. T. Zanetti and R. M. Hallock (2013). "The Role of Astrocytes in the Regulation of Synaptic Plasticity and Memory Formation." <u>Neural Plasticity</u> **2013**: 185463.

122.   Parsons, D. W., S. Jones, X. Zhang, J. C.-H. Lin, R. J. Leary, P. Angenendt, P. Mankoo, H. Carter, I. M. Siu, G. L. Gallia, A. Olivi, R. McLendon, B. A. Rasheed, S. Keir, T. Nikolskaya, Y. Nikolsky, D. A. Busam, H. Tekleab, L. A. Diaz, J. Hartigan, D. R. Smith, R. L. Strausberg, S. K. N. Marie, S. M. O. Shinjo, H. Yan, G. J. Riggins, D. D. Bigner, R. Karchin, N. Papadopoulos, G. Parmigiani, B. Vogelstein, V. E. Velculescu and K. W. Kinzler (2008). "An Integrated Genomic Analysis of Human Glioblastoma Multiforme." <u>Science (New York, N.Y.)</u> **321**(5897): 1807.

123.   Patel, A. P., I. Tirosh, J. J. Trombetta, A. K. Shalek, S. M. Gillespie, H. Wakimoto, D. P. Cahill, B. V. Nahed, W. T. Curry, R. L. Martuza, D. N. Louis, O. Rozenblatt-Rosen, M. L. Suvà, A. Regev and B. E. Bernstein (2014). "Single-cell RNA-seq highlights intratumoral heterogeneity in primary glioblastoma." <u>Science (New York, N.Y.)</u> **344**(6190): 1396-1401.

124.   Pekna, M. and M. Pekny (2012). "The Neurobiology of Brain Injury." <u>Cerebrum: the Dana Forum on Brain Science</u> **2012**: 9.

125.   Pfrieger, F. W. (2010). "Role of glial cells in the formation and maintenance of synapses." <u>Brain Research Reviews</u> **63**(1): 39-46.

126.   Phillips, H. S., S. Kharbanda, R. Chen, W. F. Forrest, R. H. Soriano, T. D. Wu, A. Misra, J. M. Nigro, H. Colman, L. Soroceanu, P. M. Williams, Z. Modrusan, B. G. Feuerstein and K. Aldape (2006). "Molecular subclasses of high-grade glioma predict prognosis, delineate a

pattern of disease progression, and resemble stages in neurogenesis." <u>Cancer Cell</u> **9**(3): 157-173.

127.   Picardi, E., D. S. Horner and G. Pesole (2017). "Single-cell transcriptomics reveals specific RNA editing signatures in the human brain." <u>RNA</u> **23**(6): 860-865.

128.   Placone, A. L., A. Quiñones-Hinojosa and P. C. Searson (2016). "The role of astrocytes in the progression of brain cancer: complicating the picture of the tumor microenvironment." <u>Tumor Biology</u> **37**(1): 61-69.

129.   Poulin, J.-F., B. Tasic, J. Hjerling-Leffler, J. M. Trimarchi and R. Awatramani (2016). "Disentangling neural cell diversity using single-cell transcriptomics." **19**: 1131.

130.   Rasmussen, K. D. and K. Helin (2016). "Role of TET enzymes in DNA methylation, development, and cancer." <u>Genes & Development</u> **30**(7): 733-750.

131.   Rosborough, B. R., D. Raïch-Regué, Q. Liu, R. Venkataramanan, H. R. Turnquist and A. W. Thomson (2014). "Adenosine triphosphate-competitive mTOR inhibitors: a new class of immunosuppressive agents that inhibit allograft rejection." <u>American journal of transplantation : official journal of the American Society of Transplantation and the American Society of Transplant Surgeons</u> **14**(9): 2173-2180.

132.   Ruggero, D. (2013). "Translational Control in Cancer Etiology." <u>Cold Spring Harbor Perspectives in Biology</u> **5**(2): a012336.

133.   Santiago, M., C. Antunes, M. Guedes, N. Sousa and C. J. Marques (2014). "TET enzymes and DNA hydroxymethylation in neural development and function — How critical are they?" <u>Genomics</u> **104**(5): 334-340.

134.   Sanz, E., R. Evanoff, A. Quintana, E. Evans, J. A. Miller, C. Ko, P. S. Amieux, M. D. Griswold and G. S. McKnight (2013). "RiboTag Analysis of Actively Translated mRNAs in Sertoli and Leydig Cells In Vivo." <u>PLOS ONE</u> **8**(6): e66179.

135.   Sanz, E., L. Yang, T. Su, D. R. Morris, G. S. McKnight and P. S. Amieux (2009). "Cell-type-specific isolation of ribosome-associated mRNA from complex tissues." <u>Proc Natl Acad Sci U S A</u> **106**.

136.   Sarnat, H. B. and L. Flores-Sarnat (2013). Chapter 44 - Neuropathology of pediatric epilepsy. <u>Handbook of Clinical Neurology</u>. O. Dulac, M. Lassonde and H. B. Sarnat, Elsevier. **111:** 399-416.

137.   Sato, A. (2016). "mTOR, a Potential Target to Treat Autism Spectrum Disorder." <u>CNS & Neurological Disorders Drug Targets</u> **15**(5): 533-543.

138.   Savaskan, N. E., Z. Fan, T. Broggini, M. Buchfelder and I. Y. Eyüpoglu (2015). "Neurodegeneration in the Brain Tumor Microenvironment: Glutamate in the Limelight." <u>Current Neuropharmacology</u> **13**(2): 258-265.

139.   Sbai, O., M. Khrestchatisky, M. Esclapez and L. Ferhat (2012). "Drebrin A expression is altered after pilocarpine-induced seizures: Time course of changes is consistent for a role in the integrity and stability of dendritic spines of hippocampal granule cells." Hippocampus **22**(3): 477-493.

140.   Shai, R., T. Shi, T. J. Kremen, S. Horvath, L. M. Liau, T. F. Cloughesy, P. S. Mischel and S. F. Nelson (2003). "Gene expression profiling identifies molecular subtypes of gliomas." Oncogene **22**: 4918.

141.   Sharma, A., C. A. Hoeffer, Y. Takayasu, T. Miyawaki, S. M. McBride, E. Klann and R. S. Zukin (2010). "Dysregulation of mTOR Signaling in Fragile X Syndrome." The Journal of Neuroscience **30**(2): 694-702.

142.   Shigeoka, T., J. Jung, C. E. Holt and H. Jung (2018). Axon-TRAP-RiboTag: Affinity Purification of Translated mRNAs from Neuronal Axons in Mouse In Vivo. RNA Detection: Methods and Protocols. I. Gaspar. New York, NY, Springer New York**:** 85-94.

143.   Showkat, M., M. A. Beigh and K. I. Andrabi (2014). "mTOR Signaling in Protein Translation Regulation: Implications in Cancer Genesis and Therapeutic Interventions." Molecular Biology International **2014**: 14.

144.   Silvera, D., S. C. Formenti and R. J. Schneider (2010). "Translational control in cancer." Nature Reviews Cancer **10**: 254.

145.   Smalheiser, N. R. and G. Lugli (2014). "Preparation of Synaptosomes from Postmortem Human Prefrontal Cortex." bioRxiv.

146.   Soden, M. E., S. M. Miller, L. M. Burgeno, P. E. M. Phillips, T. S. Hnasko and L. S. Zweifel (2016). "Genetic Isolation of Hypothalamic Neurons that Regulate Context-Specific Male Social Behavior." Cell Reports **16**(2): 304-313.

147.   Sonabend, A. M., M. Bansal, P. Guarnieri, L. Lei, B. Amendolara, C. Soderquist, R. Leung, J. Yun, B. Kennedy, J. Sisti, S. Bruce, R. Bruce, R. Shakya, T. Ludwig, S. Rosenfeld, P. A. Sims, J. N. Bruce, A. Califano and P. Canoll (2014). "The Transcriptional Regulatory Network of Proneural Glioma Determines the Genetic Alterations Selected During Tumor Progression." Cancer research **74**(5): 1440-1451.

148.   Sonenberg, N. and A. G. Hinnebusch (2009). "Regulation of Translation Initiation in Eukaryotes: Mechanisms and Biological Targets." Cell **136**(4): 731-745.

149.   Sontheimer, H. (2008). "A role for glutamate in growth and invasion of primary brain tumors." Journal of neurochemistry **105**(2): 287-295.

150.   Sottoriva, A., I. Spiteri, S. G. M. Piccirillo, A. Touloumis, V. P. Collins, J. C. Marioni, C. Curtis, C. Watts and S. Tavaré (2013). "Intratumor heterogeneity in human glioblastoma reflects cancer evolutionary dynamics." Proceedings of the National Academy of Sciences **110**(10): 4009-4014.

151.   Špaček, J. and M. Hartmann (1983). "Three-Dimensional analysis of dendritic spines." Anatomy and Embryology **167**(2): 289-310.

152.   Staffend, N. A. and R. L. Meisel (2011). "DiOlistic labeling in fixed brain slices: phenotype, morphology and dendritic spines." Current protocols in neuroscience / editorial board, Jacqueline N. Crawley ... [et al.] **CHAPTER**: Unit2.13-Unit12.13.

153.   Stupp , R., W. P. Mason , M. J. van den Bent , M. Weller , B. Fisher , M. J. B. Taphoorn , K. Belanger , A. A. Brandes , C. Marosi , U. Bogdahn , J. Curschmann , R. C. Janzer , S. K. Ludwin , T. Gorlia , A. Allgeier , D. Lacombe , J. G. Cairncross , E. Eisenhauer and R. O. Mirimanoff (2005). "Radiotherapy plus Concomitant and Adjuvant Temozolomide for Glioblastoma." New England Journal of Medicine **352**(10): 987-996.

154.   Subramanian, A., P. Tamayo, V. K. Mootha, S. Mukherjee, B. L. Ebert, M. A. Gillette, A. Paulovich, S. L. Pomeroy, T. R. Golub, E. S. Lander and J. P. Mesirov (2005). "Gene set enrichment analysis: A knowledge-based approach for interpreting genome-wide expression profiles." Proceedings of the National Academy of Sciences of the United States of America **102**(43): 15545-15550.

155.   Takai, H., K. Masuda, T. Sato, Y. Sakaguchi, T. Suzuki, T. Suzuki, R. Koyama-Nasu, Y. Nasu-Nishimura, Y. Katou, H. Ogawa, Y. Morishita, H. Kozuka-Hata, M. Oyama, T. Todo, Y. Ino, A. Mukasa, N. Saito, C. Toyoshima, K. Shirahige and T. Akiyama (2014). "5-Hydroxymethylcytosine Plays a Critical Role in Glioblastomagenesis by Recruiting the CHTOP-Methylosome Complex." Cell Reports **9**(1): 48-60.

156.   Takano, T., J. H. C. Lin, G. Arcuino, Q. Gao, J. Yang and M. Nedergaard (2001). "Glutamate release promotes growth of malignant gliomas." Nat Med **7**(9): 1010-1015.

157.   Takei, N. and H. Nawa (2014). "mTOR signaling and its roles in normal and abnormal brain development." Frontiers in Molecular Neuroscience **7**: 28.

158.   Tang, G., K. Gudsnuk, S.-H. Kuo, M. L. Cotrina, G. Rosoklija, A. Sosunov, M. S. Sonders, E. Kanter, C. Castagna, A. Yamamoto, Z. Yue, O. Arancio, B. S. Peterson, F. Champagne, A. J. Dwork, J. Goldman and D. Sulzer (2014). "Loss of mTOR-dependent macroautophagy causes autistic-like synaptic pruning deficits." Neuron **83**(5): 1131-1143.

159.   Taphoorn, M. J. B. and M. Klein (2004). "Cognitive deficits in adult patients with brain tumours." The Lancet Neurology **3**(3): 159-168.

160.   Tasic, B., V. Menon, T. N. Nguyen, T. K. Kim, T. Jarsky, Z. Yao, B. Levi, L. T. Gray, S. A. Sorensen, T. Dolbeare, D. Bertagnolli, J. Goldy, N. Shapovalova, S. Parry, C. Lee, K. Smith, A. Bernard, L. Madisen, S. M. Sunkin, M. Hawrylycz, C. Koch and H. Zeng (2016). "Adult mouse cortical cell taxonomy revealed by single cell transcriptomics." Nat Neurosci **19**(2): 335-346.

161.   The Cancer Genome Atlas Research, N. (2008). "Comprehensive genomic characterization defines human glioblastoma genes and core pathways." Nature **455**(7216): 1061-1068.

162.   Thomas, P. D., M. J. Campbell, A. Kejariwal, H. Mi, B. Karlak, R. Daverman, K. Diemer, A. Muruganujan and A. Narechania (2003). "PANTHER: A Library of Protein Families and Subfamilies Indexed by Function." Genome Research **13**(9): 2129-2141.

163.   Thoreen, C. C., L. Chantranupong, H. R. Keys, T. Wang, N. S. Gray and D. M. Sabatini (2012). "A unifying model for mTORC1-mediated regulation of mRNA translation." Nature **485**.

164.   Thoreen, C. C., S. A. Kang, J. W. Chang, Q. Liu, J. Zhang, Y. Gao, L. J. Reichling, T. Sim, D. M. Sabatini and N. S. Gray (2009). "An ATP-competitive mammalian target of rapamycin inhibitor reveals rapamycin-resistant functions of mTORC1." J Biol Chem **284**(12): 8023-8032.

165.   Tirosh, I. and M. L. Suvà (2017). "Dissecting human gliomas by single-cell RNA sequencing." Neuro-Oncology: nox126-nox126.

166.   Tsien, J. Z., D. F. Chen, D. Gerber, C. Tom, E. H. Mercer, D. J. Anderson, M. Mayford, E. R. Kandel and S. Tonegawa (1996). "Subregion- and Cell Type–Restricted Gene Knockout in Mouse Brain." Cell **87**(7): 1317-1326.

167.   van den Bent, M. J., T. J. Snijders and J. E. C. Bromberg (2012). "Current treatment of low grade gliomas." Memo **5**(3): 223-227.

168.   Vecht, C. J., M. Kerkhof and A. Duran-Pena (2014). "Seizure Prognosis in Brain Tumors: New Insights and Evidence-Based Management." The Oncologist **19**(7): 751-759.

169.   Venkatesh, Humsa S., Tessa B. Johung, V. Caretti, A. Noll, Y. Tang, S. Nagaraja, Erin M. Gibson, Christopher W. Mount, J. Polepalli, Siddhartha S. Mitra, Pamelyn J. Woo, Robert C. Malenka, H. Vogel, M. Bredel, P. Mallick and M. Monje (2015). "Neuronal Activity Promotes Glioma Growth through Neuroligin-3 Secretion." Cell **161**(4): 803-816.

170.   Venkatesh, H. S., L. T. Tam, P. J. Woo, J. Lennon, S. Nagaraja, S. M. Gillespie, J. Ni, D. Y. Duveau, P. J. Morris, J. J. Zhao, C. J. Thomas and M. Monje (2017). "Targeting neuronal activity-regulated neuroligin-3 dependency in high-grade glioma." Nature **549**(7673): 533-537.

171.   Verhaak, R. G. W., K. A. Hoadley, E. Purdom, V. Wang, Y. Qi, M. D. Wilkerson, C. R. Miller, L. Ding, T. Golub, J. P. Mesirov, G. Alexe, M. Lawrence, M. O'Kelly, P. Tamayo, B. A. Weir, S. Gabrie, W. Winckler, S. Gupta, L. Jakkula, H. S. Feiler, J. G. Hodgson, C. D. James, J. N. Sarkaria, C. Brennan, A. Kahn, P. T. Spellman, R. K. Wilson, T. P. Speed, J. W. Gray, M. Meyerson, G. Getz, C. M. Perou, D. N. Hayes and N. The Cancer Genome Atlas Research (2010). "An integrated genomic analysis identifies clinically relevant subtypes of glioblastoma characterized by abnormalities in PDGFRA, IDH1, EGFR and NF1." Cancer cell **17**(1): 98.

172.   Verkhratsky, A. and M. Nedergaard (2017). "Physiology of Astroglia." Physiological Reviews **98**(1): 239-389.

173.   Wei, J., K. Gabrusiewicz and A. Heimberger (2013). "The Controversial Role of Microglia in Malignant Gliomas." Clinical and Developmental Immunology **2013**: 12.

174.   Weller, M., W. Wick, K. Aldape, M. Brada, M. Berger, S. M. Pfister, R. Nishikawa, M. Rosenthal, P. Y. Wen, R. Stupp and G. Reifenberger (2015). "Glioma." Nature Reviews Disease Primers **1**: 15017.

175.   Wesseling, P., J. M. Kros and J. W. M. Jeuken (2011). "The pathological diagnosis of diffuse gliomas: towards a smart synthesis of microscopic and molecular information in a multidisciplinary context." Diagnostic Histopathology **17**(11): 486-494.

176.   Wong, M. (2013). "Mammalian target of rapamycin (mTOR) pathways in neurological diseases." Biomed J **36**.

177.   Yuste, R. and T. Bonhoeffer (2001). "Morphological Changes in Dendritic Spines Associated with Long-Term Synaptic Plasticity." Annual Review of Neuroscience **24**(1): 1071-1089.

178.   Zalfa, F., S. Adinolfi, I. Napoli, E. Kühn-Hölsken, H. Urlaub, T. Achsel, A. Pastore and C. Bagni (2005). "Fragile X Mental Retardation Protein (FMRP) Binds Specifically to the Brain Cytoplasmic RNAs BC1/BC200 via a Novel RNA-binding Motif." Journal of Biological Chemistry **280**(39): 33403-33410.

179.   Zeisel, A., A. B. Muñoz-Manchado, S. Codeluppi, P. Lönnerberg, G. La Manno, A. Juréus, S. Marques, H. Munguba, L. He, C. Betsholtz, C. Rolny, G. Castelo-Branco, J. Hjerling-Leffler and S. Linnarsson (2015). "Cell types in the mouse cortex and hippocampus revealed by single-cell RNA-seq." Science **347**(6226): 1138-1142.

180.   Zeng, L.-H., L. Xu, D. H. Gutmann and M. Wong (2008). "Rapamycin Prevents Epilepsy in a Mouse Model of Tuberous Sclerosis Complex." Annals of neurology **63**(4): 444-453.

181.   Zhang, F.-X., Q.-J. Sun, X.-Y. Zheng, Y.-T. Lin, W. Shang, A.-H. Wang, R.-S. Duan and Z.-F. Chi (2014). "Abnormal Expression of Synaptophysin, SNAP-25, and Synaptotagmin 1 in the Hippocampus of Kainic Acid-Exposed Rats with Behavioral Deficits." Cellular and Molecular Neurobiology **34**(6): 813-824.

182.   Zhang, Y., K. Chen, S. A. Sloan, M. L. Bennett, A. R. Scholze, S. O'Keeffe, H. P. Phatnani, P. Guarnieri, C. Caneda, N. Ruderisch, S. Deng, S. A. Liddelow, C. Zhang, R. Daneman, T. Maniatis, B. A. Barres and J. Q. Wu (2014). "An RNA-Sequencing Transcriptome and Splicing Database of Glia, Neurons, and Vascular Cells of the Cerebral Cortex." The Journal of Neuroscience **34**(36): 11929-11947.

183.   Zhong, Y., T. Karaletsos, P. Drewe, V. T. T Sreedharan, K. Singh, H.-G. Wendel and G. Rätsch (2015). "RiboDiff: Detecting Changes of Translation Efficiency from Ribosome Footprints." bioRxiv.

184.   Zong, H., R. G. W. Verhaak and P. Canoll (2012). "The cellular origin for malignant glioma and prospects for clinical advancements." <u>Expert Review of Molecular Diagnostics</u> **12**(4): 383-394.